Efforts Towards Bifunctional PZM21 Analogues as Potential Novel Analgesics

By

Julia Mandato

A thesis submitted in partial fulfillment of the requirements for the

Masters degree in science

University of Ottawa

Candidate	**Supervisor**
Julia Mandato	**Dr. André M. Beauchemin**

Abstract

Complex pharmacological problems such as chronic pain require creative drug design that goes beyond single point binding and polypharmacology approaches. Current MOR agonists used for pain relief, notably opioid drugs, have negative side effects from activation of the β-arrestin recruitment pathway limiting their use. Pain relief through Na_v channel blockers is not successful due to dangerous side effects attributed to nonselective binding. Literature evidence suggests that combined therapy of MOR biased agonists and selective $Na_v1.7$ VSD4 blockers, either independently or as a bifunctional drug, can result in potent analgesia with limited side effects due to selective activation of secondary pathways and highly specific binding. Synergy of the two pharmacophores can additionally lead to higher potency and lower doses of less addictive pain relief drugs.

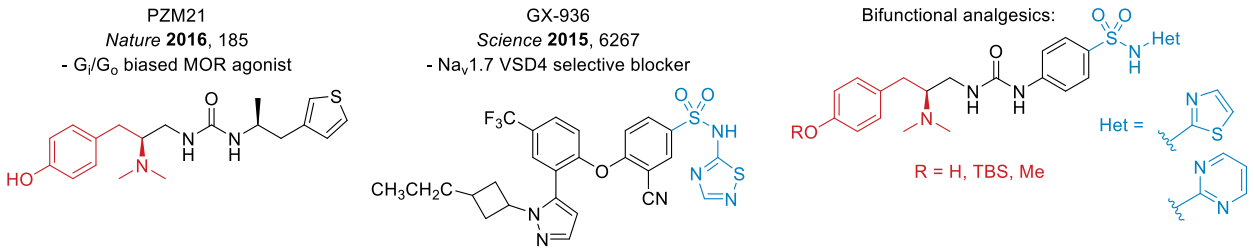

This work presents efforts toward bifunctional compounds to target these *two components* in the pain network with *one molecule*. Compounds containing pharmacophores inspired by the MOR biased agonist PZM21 and aryl sulfonamide $Na_v1.7$ VSD4 selective blockers were designed, synthesized, and tested for analgesic activity. Through three generations of SAR, 21 compounds were tested for agonist activity at MOR and 12 compounds were tested for VSD4 blocking at $Na_v1.7$. Two compounds, **7a** and **7b** showed activity similar to know VSD4 blockers and two compounds **23a** and **24a** showed MOR agonist activity with selectivity and activation similar to PZM21. Major insight has been gained regarding the requirements of binding at each receptor

including pharmacophore functionalities, flexibility, and overall orientation of the compound driven by a required conformation to bind at each receptor. The results reported in this thesis provided essential information for current work toward a bifunctional compound.

Acknowledgements

I want to thank Dr. André Beauchemin for his support over the past 2 years and for leading such a wonderful group. I knew as soon as I met with André that I wanted to join his group. Chemistry is challenging enough, but having a supervisor who helps not only with chemical reactions but with navigating graduate school made my time at uOttawa special and safe. I will always be so proud and grateful to have been a member of the Beauchemin lab. Dr. Monica Gill quickly became a mentor, role model and friend to me when she joined our lab. Monica helped me so much navigating my project (and my life as I planned to leave grad school), and I am so grateful for her support and seemingly never-ending confidence in me. Thank you, Sherif and Will, for being with me on "Team Med-Chem," and Dr. Patrick Giguère for believing in the three of us.

Coming to sit in an office full of friends makes failing a column a lot easier. Bhavana, who has been by my side since the very first day, and I cannot imagine doing this without you. Every work week ending with her, Max, Rosemary, and Braeden on my couch for girls night made my heart happy. Grad school is filled with you girls - in the lab and on Saturday nights, always with endless laughter. Daniel always made the morning shift easier to come in for, Fred's endless supply of side eyes and his usually perfect advice; and Huy, Alshimaa, Mira, Kaitlyn, Leah, Eryn and Etienne were all a pleasure to work with and know.

I also want to thank my Mom, Dad, Luke and my best friends Sarah and Hannah for always listening to me over the phone and supporting me all the way in Ottawa. You always knew what to say.

This was the longest lab report of my life, and it wasn't easy. Strength found me in places and times I didn't know it would, and I am so proud of myself for that. When in doubt, un dernier p'tit coup de cœur.

Statement of Contributions

The synthetic work presented in this thesis was done in collaboration with PhD candidate Mr Sherif Meshref and MSc candidate Mr William Gagné-Monfette. Their work had been credited where applicable throughout this document. As part of the project, I synthesized 12 compounds for biological testing (out of 21 completed over the course of the project) and contributed to the synthesis of key building blocks. Biological testing was conducted by MSc candidate Shivani Patel and Dr. Geneviève Laroche.

Dr. Andre Beauchemin and Dr. Monica Gill were consulted bi-weekly throughout the course of the project, providing input and ideas. Dr. Patrick Giguère was also consulted bi-weekly and played an integral role in compound design.

All text, figures, schemes, and tables are original content. No artificial intelligence software was used to assist in the production or writing of this thesis.

Table of Contents

List of Schemes

List of Figures

List of Tables

Abbreviations

^{13}C	Carbon 13
^{1}H	proton
Å	angstrom (10^{-10} meters)
ADE	Adverse Drug Effect
ADME	Absorption, Distribution, Metabolism, Excretion
Arg	Arginine
Asp	Aspartate
cAMP	Cyclic adenosine monophosphate
CIP	Congenital insensitivity to pain
CNS	Central nervons system
cryoEM	Cryogenic Electron Microscopy
CYP450	Cytochrome P450
D	Aspartate
d	Deuterium (in NMR solvents)
DCM	Dichloromethane
DDI	Drug-Drug Interaction
DMF	Dimethyl formamide
DMSO	Dimethyl sulfoxide
DOR	δ opioid receptor
Equiv	Equivalent
Et	Ethyl
GI	Gastrointestinal
GPCR	G-Protein Coupled Receptor
h	Hours
HATU	Hexafluorophosphate Azabenzotriazole Tetramethyl Uronium
HBD	Hydrogen bond donor
Het	Heterocycle
Hz	Hertz
ICM-VLS	Virtual Ligand Screening
J	Coupling constant
kcal	kilocalorie
KOR	κ opioid receptor
L	litre
LAH	Lithium Aluminum Hydride
LG	Generic leaving group
LiHMDS	Lithium bis(trimethylsilyl)amide
Me	Methyl
mg	milligram(s)
min	minutes

mL	millilitre(s)
MOR	μ opioid receptor
N	Asparagine
NMR	Nuclear Magnetic Resonance
ºC	degrees Celsius
PDB	Protein data bank
PNS	Peripheral nervous system
Q	Glutamine
R	Arginine
Rf	Retention factor
rt	Room temperature
SAR	Structure Activity Relationship
sat	Saturated
SEM	Standard error of the mean
TBAF	tertabutylammonium fluoride
TBS	2,2,2-trifluoroethanol
Temp	Temperature
TFA	Trifloroacetic acid
TFE	*tert*-butyldimethyl silyl
THF	tertahydrofuran
TLC	Thin layer chromatography
VGSC	Voltage-gated Sodium channel
VSD4	Voltage Sensing Domain IV
W	Tryptophan
Y	Tyrosine
δ	Chemical shift in parts per million
μL	microlitre

Chapter 1: Introduction

1.1 Introduction to Structure-Based Design in Medicinal Chemistry

Structure-based drug design is a common and very successful strategy in medicinal chemistry, where drugs are designed based on the functionalities, shapes, sizes, and orientations that will best fit and bind to a target receptor and elicit a pharmacological response.[1] This strategy is a go-to in the medicinal chemistry community and many promising small molecules have gone onto clinical trials beginning with this med chem approach.[2] It continues to be a reliable method for the design, synthesis, and application of biologically active small molecules. Structure based drug design, also called rational drug design, is an interdisciplinary type of research. It requires input from synthetic chemists and structural biologists in order to successfully design small molecules and properly synthesize and characterize them before they reach clinical trials and become marketable drugs. While this drug design approach can be highly effective, it is not an easy task. Being able to design compounds that bind receptors with selectivity and in turn provide a desired pharmacological response is complicated. The body is complex – composed of proteins and enzymes, communication pathways involving overlapping second messenger systems, countless small molecules – and predicting the behaviour and effect of an exogenous compound like a drug is very challenging. Many factors in the design of a drug must be carefully considered. These factors range from the overall shape and size of the molecule to minor adjustments to the orientation, electrostatics, and other physiochemical properties.[1]

The ideal outcome of rationally designed drug would be to form a biologically active small molecule that could bind to a selected target (or targets) with high specificity, have limited off-target activity and related adverse drug effects (ADEs), and a successful pharmacokinetic and pharmacodynamic profile in the body. The challenge medicinal chemists face is finding molecules

that can accomplish all these roles, while still maintaining a potent pharmacological effect. In many cases not all these goals can be accomplished with just one drug, and a single-point binding approach is not sufficient for the pharmacological effect desired. This prompts new strategies for compound design that go beyond single point binding. One example of this is applying a polypharmacology approach.

It is difficult to define polypharmacology because it can encompass several goals and describes a complex approach to treatment.[3] In general, it refers to a pharmacological strategy where a patient is prescribed more than one medication at the same time to treat an illness. One example where this therapeutic strategy is used is in pain relief. Patients taking opioids for pain relief are often prescribed additional drugs, either to aid in analgesia or to ease side effects and complications associated with opioid treatment. A recent study reported that over 20% of opioid users are taking more than ten concurrent medications.[4] When there are many drug substances in the body, there is potential for them to interact with each other, either directly or indirectly though secondary effects leading to drug-drug interactions (DDIs). Problematic side effects can arise from DDIs, referred to as adverse drug events (ADEs) and can be very serious.

The pharmacokinetic and pharmacodynamic profiles of all drugs including their absorption, distribution, metabolism, and elimination (ADME) must be considered when a patient is prescribed a medication. When multiple drugs are prescribed, each drug substance will have a unique ADME profile, and each must be considered independently, as well as where and how they overlap. Overlapping ADME profiles can promote or inhibit each other at any step in the process, and this is often the case with a polypharamcology therapeutic approach. One example is in the case of prodrugs. Prodrugs require structural modification upon entering the body which is generally carried out via metabolism of the prodrug. The metabolites are the active drug. Only then

can the active metabolite cause a pharmacologic effect.[5] A major issue with opioid prodrugs like *codeine* and *oxycodone* that require metabolism by the CYP450 family of enzymes is inhibition or competition of the target enzyme. Codeine is metabolized by the CYP2D6 enzyme and has a relatively weak binding affinity. This means that it can easily be outcompeted by other drugs a patient is taking that also are metabolised by this enzyme. This often results in the requirement for higher or more frequent dosing, leading to tolerance, dependence and missuse.[4]

Polypharmacology can be successful when medications are prescribed correctly and ADME profiles are complementary, but this is often difficult and sometimes the challenges outweigh the benefits. Instead of introducing *multiple drugs* that bind to *multiple targets* it can be favourable to design *one drug* that is capable of binding to *multiple targets*, that can accomplish the same thing. This alternative to pharmacology is designing drugs that are dual binding or bifunctional. These drugs would be able to bind to more than one receptor and cause more than one pharmacological effect.[6] The drug is designed to target two separate binding sites. This can help to reduce the number of medications and/or the dose of medications a patient may require. The fewer drugs a patient is prescribed, the reduced risk of DDI and associated ADE.[2] Dual binding can be a powerful strategy medicinal chemists use to design drugs to better solve challenging pharmacological problems in the body, such as chronic pain. Binding at a single receptor is often not sufficiently specific or potent to achieve the desired pharmacological response, especially in the case of complex medical problems. There are many components in the pain network and pain is a highly complex experience, so a drug that is more complex is needed to solve this issue. In recent years, medicinal chemists are focusing on the design of dual binding drugs to treat chronic pain.[7,8,9]

Dual binding requires merging two unique pharmacophores into one molecule. Different strategies can be used to join functionally distinct pharmacophores. One way to do this is by identifying highly integrated pharmacophores, which are usually only discovered through high throughput screening of libraries of thousands to millions of small molecules. A more practical strategy is using rational drug design to design compounds that are dual binding containing unique pharmacophores which can be joined directly or through a non-functional linker. Both of these cases require a carefully considered design requiring knowledge of the electronics, size and shape of the binding site.[6] Compounds that engage in dual binding can be further classified into bitopic or bifunctional ligands.

Bitopic ligands are a *single compound* that can engage *two binding sites on the same receptor*.[10,11] An example of this would be a compound with two pharmacophores that target both the allosteric and the orthosteric binding sites of the same GPCR.[12] Bitopic ligands are often highly selective because they bind at two points on the same receptor. They allow simultaneous targeting of two sites at once and need to be very well fitted to their respective binding pockets and locations. This can be achieved through a number of binding modes (Figure 1.1).

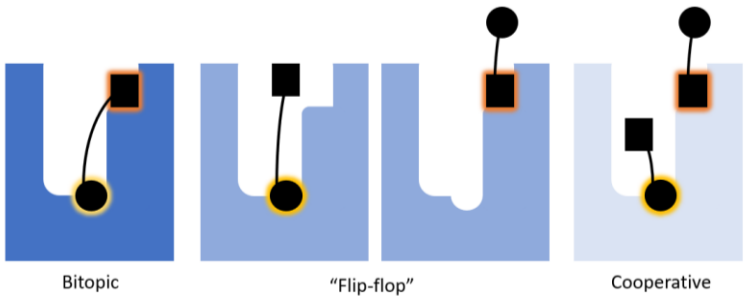

Figure 1.1: Potential modes of bitopic binding

The ligand can bind both locations on the receptor at the same site as shown in the cooperative mode, or separately as seen in the "flip-flop" method. Either way, it is one compound targeting *two* locations at the *same* receptor.[10] One disadvantage of this strategy is that is relies heavily on detailed knowledge of the binding site. This includes all relevant information such as shape of the pocket and the pocket surface, electrostatics of the binding site and size of the binding site, often as specific as Å-level measurements. The orientation of a molecule when it resides in the binding site will determine the location of the key components of the pharmacophore. These functionalities are what interact with specific amino acids in the binding pocket, so they must be perfectly placed in order to achieve contact. This is all required to correctly design the pharmacophores and linker between them if one is required. The design process becomes less challenging when additional structural data, such as X-ray crystallographic structures or cryoEM imaging, are available, that demonstrate the binding of the ligand to the receptor.[10]

Another way to achieve dual binding is through bifunctional ligands. A bifunctional ligand still contains *two unique pharmacophores* joined by a linker, but the targets are *two different receptors* (Figure 1.2), in contrast to targeting two locations on the same receptor.[11] Similar to bitopic binding, this strategy also requires extensive knowledge of the binding sites but additionally is often limited to systems where related receptors are located in close proximity to each other. This is required because the compound must have access to both receptors in order to bind.

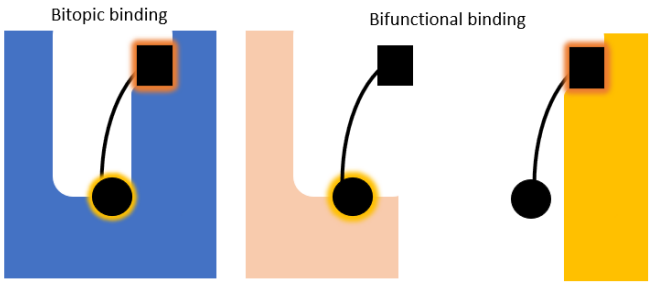

Figure 1.2: Comparison of bitopic and bifunctional binding

Bitopic ligands can accomplish a synergistic pharmacological effect through increased binding affinity at the receptor location, but a bifunctional ligand can also achieve synergy through downstream effects in the body, such as secondary messenger systems or triggering neurotransmitter release. This can be very positive in terms of efficacy, but medicinal chemists must tread lightly. It cannot be assumed that once the pharmacophores are joined in a bitopic or bifunctional ligand that they act in the same was as they do independently. As an example, an antagonistic pharmacophore may adopt partial agonist activity when joined with another completely unrelated pharmacophore.[6] As previously discussed, binding pockets are very sensitive to the orientation and size of ligands, and binding of one ligand could alter the shape of the entire protein.[13] This has the potential to change the shape of binding pockets and prevent contact with one of the pharmacophores in the molecule. A dual-binding strategy is high risk, but with careful SAR decisions, detailed information about receptor structure and binding, it can also be high reward (Figure 1.3).[2,14]

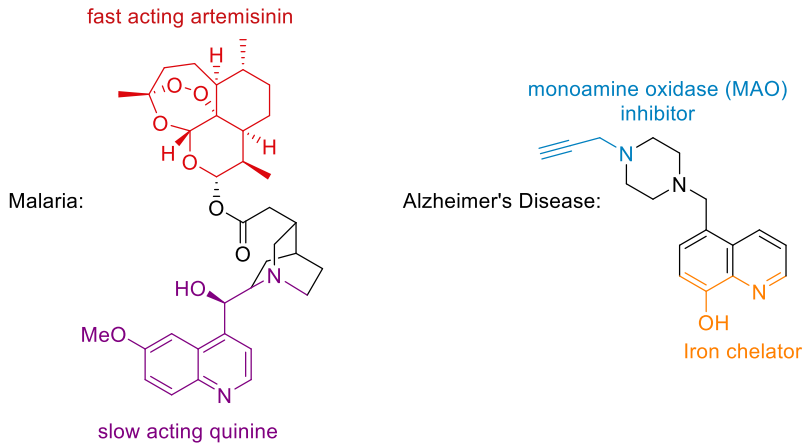

Figure 1.3: Examples of dual binding drug candidates

Examples of dual binding drugs are shown in Figure 1.3. The compound on the left is an antimalarial agent that contains two unique pharmacophores. Shown in purple is a quinine that acts slowly on the malaria purine nucleoside phosphorylase enzyme. In red is a much faster acting arteminisin, that effects the heme detoxification pathway of the malaria parasite. Both quinine and artemisinin exist as independent drugs, but combining these different pharmacokinetic properties into one drug increases the efficacy.[2] Both bitopic and bifunctionally designed drugs are advantageous over a polypharmacology strategy because they limit the number of exogenous drugs a patient will require. This can limit DDI and improve patient compliance. From a practical perspective, this is advantageous as well because the time spent on pharmacokinetic and pharmacodynamic studies is reduced with fewer drugs.[6] The extra advantage of a bifunctionally designed molecule is the potential for a synergistic pharmacologic response, which could limit dose. Dual-binding approaches like these allow medicinal chemists to design molecules strategically and can help solve challenging, complex problems involving many components and receptors, such as chronic pain. [8,9]

1.2 Existing Strategies for Opioid Mediated Pain Relief

Pain is one of the most complex pharmacological problems. One in five Canadians live with chronic pain and require medication or treatment.[15] Pain is also involved in many diseases and is a part of surgical recovery. Opioids are often prescribed to people experiencing chronic or intense pain, but they are also a drug of abuse and there is an ongoing opioid crisis in Canada. According to Health Canada, since 2016 there have been over 34,000 opioid toxicity related deaths in Canada, 81% were caused by fentanyl use.[15] Opioids remain one of the most dangerous drugs of abuse because they are highly addictive, and patients taking opioids for pain relief often develop tolerance and dependence.

Opioids do produce analgesia, but they can have effects of euphoria as well. Euphoria comes from neurochemical release by effecting GABAergic neurons in the midbrain. This triggers the release of dopamine, the body's "happy chemical" and a surge of happiness and euphoric feelings follow. The euphoric feeling leads to cravings for the drug. Activation of the β-arrestin pathways cause tolerance, making people crave higher doses. Together this leads to prescription opioids being taken at high doses to achieve euphoria.[4,16] It becomes easy for individuals to become addicted to taking opioids, resulting in hospitalizations, overdoses, and deaths.

Despite these concerns and the startling number of opioid related deaths in recent years, opioid analgesics remain the preferred therapeutic method for pain treatment.[17] They are incredibly powerful and effective at analgesia, both for chronic and neuropathic pain.[18] Despite widespread use of drugs such as *morphine* and their success in pain relief, they also pose a major threat as they have many negative side effects. In addition to dependence and addiction, major side effects include respiratory depression and GI symptoms such as constipation. These are caused by activation of the β-arrestin pathway.[19,20] Creating biased agonists that only interact at one subtype

of opioid receptors and activate a specific pathway, inducing analgesia without negative side effects and addictive qualities would allow the development of safer pain therapeutics.[17]

1.12 Mu Opioid Receptor Biased Agonists – PZM21 and Single-Point Binding

Opioid receptors are a type of G-protein coupled receptor, or GPCR. GPCRs are the largest family of membrane proteins and through connections to a diverse system of secondary messengers they are responsible for mediating many of the body's responses. Through opioid binding, one of these responses is inducing analgesia.[21] All GPCRs, including opioid receptors, are composed of seven transmembrane domains separated by alternating intracellular and extracellular loops.[21] Opioid receptors are a type of GPCR, a member of the subfamily called rhodopsin receptors.[22] They are G_i/G_o-coupled receptors and involved in signal transduction,[22] and like many GPCRs their effects are induced through downstream signalling pathways.

There are three types of opioid receptors in humans, μ-opioid receptor, δ-opioid receptor and κ-opioid receptor, denoted MOR, DOR and KOR respectively. KOR agonists act as potent analgesics but are not favourable for treatment due to their strong sedative and psychomimetic side effects.[23] DOR agonists are not as widely studied, as many early developed compounds did not proceed to clinical trials due to convulsions and seizures in animal studies as well as a lack of potent analgesic activity.[23] Most opioids target the MOR.[24,25]

MOR agonists are potent therapeutics and the best treatment available for analgesia. MOR are located throughout the CNS, but receptors located in the midbrain are the most activated areas for analgesia.[26] Analgesia begins when an agonist binds the receptor. There are two binding locations on MOR, the orthosteric and allosteric binding sites. Activation through agonist binding at the orthosteric site, causes phosphorylation of the protein subunits (Scheme 1.1).[22] This causes the separation of the G_i subunit and activates a second messenger system that inhibits adenyl cyclase

and activates G-protein linked inwardly rectifying K^+ channels (GIRKS).[22] The influx of K^+ into the cell hyperpolarizes the membrane, in turn decreases activation of sodium and calcium channels and reduces excitation of the cell.[22] This reduction of neuronal excitability is what causes analgesia.[19]

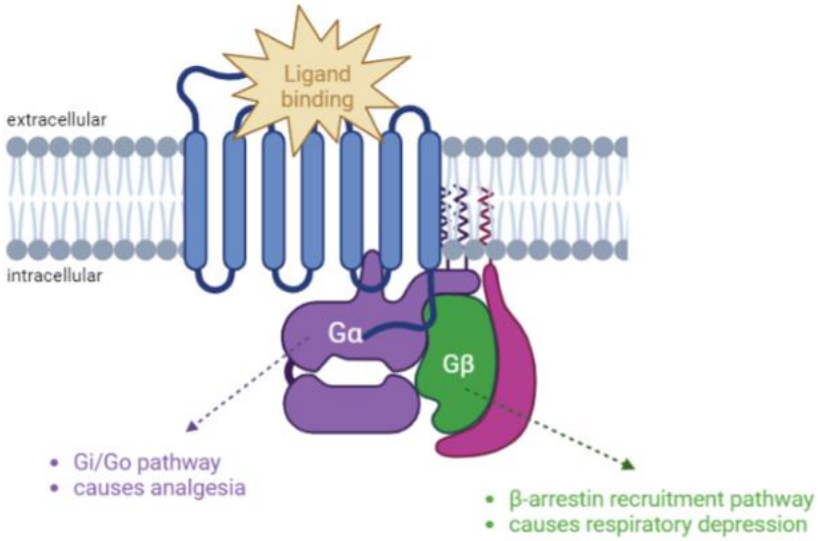

Scheme 1.1: MOR agonist binding and potential pathways

Despite success as analgesics, there are drawbacks of opioids. The negative side effects of opioids including respiratory depression and gastrointestinal issues are thought to be mediated through a different second messenger system called the β-arrestin recruitment pathway (Scheme 1.1).[19] Studies performed in β-arrestin 2 knockout mice suggest that this pathway is what mediated the negative side effects, independent of the analgesic activity associated with MOR agonist binding.[17] A drug that could stimulate the MOR analgesic pathway while limiting β-arrestin recruitment could be an ideal drug for pain relief with reduced side effects.[19]

Drugs available as MOR agonists range in structure and pharmacophore (Figure 1.4), but all contain some similarities. The natural ligand, *morphine*, is a recognizable example. The mu in

MOR originates from morphine. The common opioid pharmacophore (highlighted in red) for receptor activation includes a basic amine that becomes protonated at physiological pH, separated by a two to three carbon linker to an aromatic ring.[27]

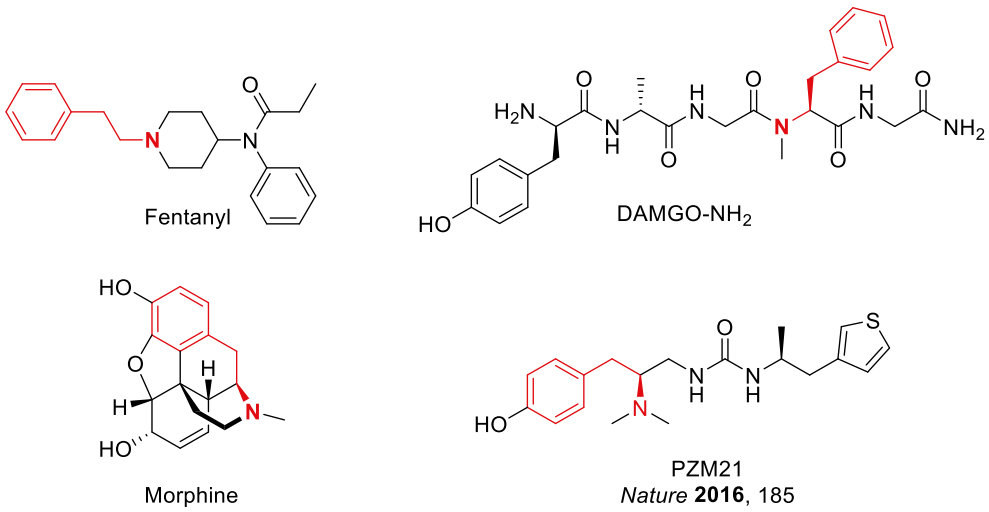

Figure 1.4: Examples of MOR selective agonists containing common pharmacophore

Fentanyl is highly lipophilic, contributing to membrane anchoring and extremely potent at MOR. Morphine is an alkaloid, while DAMGO-NH_2 is an enkephalin-like peptide. Despite these differences, they all contain the common pharmacophore. This amine interacts through a strong cationic interaction with a negatively charged Asp147 residue in the orthosteric binding pocket of MOR, inducing analgesia through the previously described G_i/G_o pathway.[19] A recent publication from Manglik *et al.* demonstrates a compound that is a biased agonist for MOR.[28] The compound titled PZM21 is selective for binding at the MOR over the DOR and KOR, and also preferentially stimulates G_i/G_o activation over β-recruitment, resulting in decreased side effects while still maintaining potent analgesia. Most notably, PZM21 contains the basic amine pharmacophore, the same as other known MOR agonists (Figure 1.4).

There are few examples in the literature similar to PZM21 of biased opioid agonists that activate MOR with limited β-arrestin recruitment. Another publication from Wang *et al.* discusses

TRV-130 (Figure 1.5) a compound with similar MOR activation pathways as PZM21.[1929] Both structures contain the basic amine and a thiophene moiety. These discoveries, notably PZM21, inspired the idea of using a biased agonist that is successful at stimulating selective pathways of GPCRs for pain relief.[17,19]

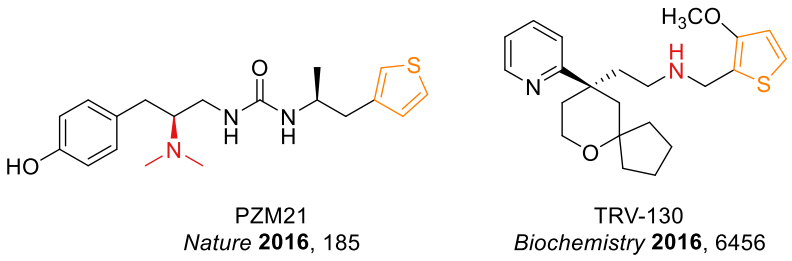

Figure 1.5: Structures of PZM21 and TRV-130, examples of MOR G_i/G_o biased ligands

1.2 Ion Channels in the Pain Network – $Na_v1.7$ VSD4 Blocking Drugs

All perception of stimuli in the body, including pain, relies on signalling through the nervous system. The nervous system is the way the body communicates stimulus to feelings, and a major component of how humans perceive pain relies on propagating the pain signal in response to a painful stimulus. This signal propagation relies on ion channels in neurons that control the flow of positively charged ions in and out of the cell. This changes the electrochemical gradient, triggering action potentials and propagating a neuronal signal.[30] A major player in this network are voltage gated-sodium ion channels known as VGSCs. VGSCs are responsible for generation and transmission of neuronal signals in both the peripheral and central nervous system.[31] There are nine isoforms of human VGSC's denoted $Na_v1.1$-1.9 that each play different roles in neuronal signalling depending on their location in the body. $Na_v1.1$, 1.2, 1.3 and 1.7 are the most closely related and all located in the nervous system, and function to propagate the neuronal signal response to stimuli such as pain.[32,33]

$Na_v1.7$ and other VGSCs work as part of a system to conduct the action potential (Figure 1.6). This works in several steps, starting with an initial stimulus, whether that is physical or a biochemical response in the body. As the name suggests, VGSCs are channels, and open and close to allow ions to pass through the cell membrane based on membrane potential. They are composed on an α-pore subunit and an auxiliary stabilizing β-subunit. The pore is composed of four intracellular domains, and four corresponding peripherally located voltage sensing domains.[31,34] Importantly, VGSCs are closed at resting membrane potential of -70 mV. Depolarization is caused by a stimulus and is detected by the voltage sensing domains and causes the channels to open, allowing Na^+ ions to rush into the cell further depolarizing it to +30 mV. This rapidly reverses the membrane potential from resting (from -70 mV to +30 mV). When it reaches this threshold, the VGSCs close, stopping Na^+ influx. This change in the electrochemical gradient opens a different type of ion channel, potassium gated channels, repolarizing the cell back to -70 mV by K^+ flowing out of the cell.[30]

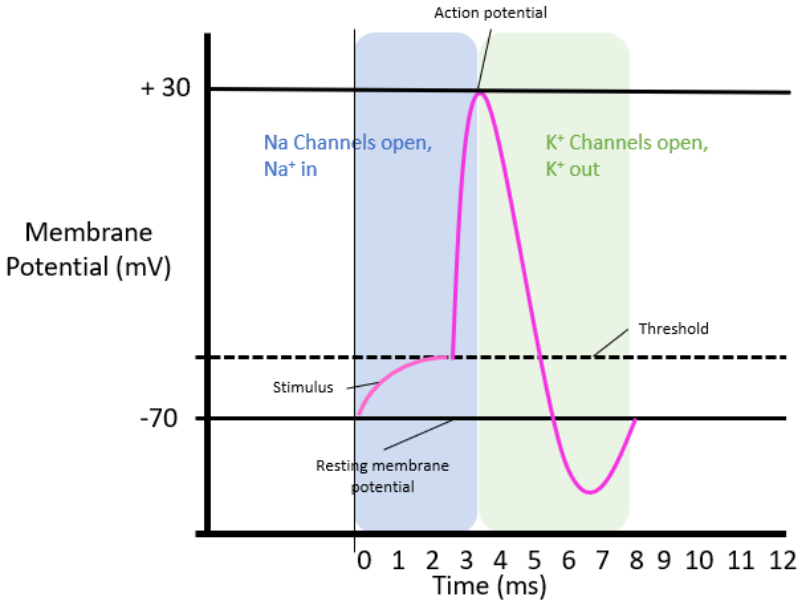

Figure 1.6: Action potential propagation facilitated by VGSCs

This movement of ions and subsequent changes in cell membrane potential cause action potentials that propagate signals throughout the body. This process repeats from neuron to neuron and allows responses to stimulus to reach the CNS in milliseconds, and the body can response accordingly.[30] Preventing the opening or closing of these ion channels would interrupt this cycle of action potential propagation, effectively preventing the CNS to perceive any indication of a painful stimulus. One strategy to prevent channel opening/closing is using compounds that can halt the influx of Na^+ ions by physically blocking the channel and locking it in a closed position. If Na^+ cannot enter the cell, the whole system will be stopped and the electrochemical gradient cannot cycle from -70 mV to +30 mV, preventing action potential propagation.

General Na_v blockers have been used clinically for decades to do this through treating CNS problems, such as anticonvulsants *car-bamazepin* and *phenytoin* for epilepsy (Figure 1.7). Pain has also been treated with general Na_v blockers like *lidocaine* and *bupivacaine* which are topical anaesthetics.[35] However, these drugs are nonselective and target several isoforms of Na_v. A challenge of designing small molecules to interact with VGSCs selectively is the high sequence homology among the nine isoforms. Na_v isoforms contain over 50% amino acid similarity, therefore selectively activating one isoform over another is a challenge and relies on parts of the sequence that are non-homologous.[34]

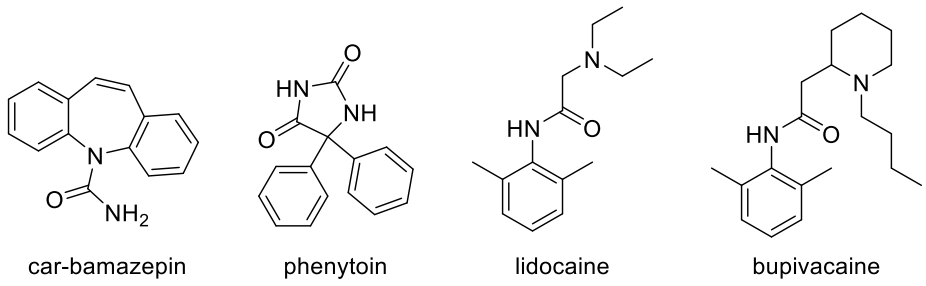

Figure 1.7: Structures of examples of general Na_v blocking drugs

This results in blocking Na_v isoforms not responsible for pain perception, causing adverse and potentially very dangerous side effects, $Na_v1.5$ and 1.6 are excellent examples of this. $Na_v1.5$ is expressed in cardiac myocytes, if this isoform is blocked it can result in problems with cardiac function and cause arrhythmic side effects, such as QT syndrome. $Na_v1.6$ is present in skeletal muscle, if it is blocked symptoms of epilepsy and related adverse effects arise.[31] Additionally, general Na_v blockers are not state dependent and can bind to any Na_v isoform at any state in the cycle, open, closed or resting.

As discussed previously, $Na_v1.7$ has been identified as crucial in pain signalling and pain perception. $Na_v1.7$ is primarily located in dorsal root ganglia cells, particularly in peripheral pain sensing neurons called nociceptive neurons. These include olfactory neurons, epithelium, and sympathetic ganglion. The role of $Na_v1.7$ is to conduct pain signals by propagating Na^+ currents in response to cellular depolarization.[31] There is significant genetic evidence supporting this role in pain perception. Studies show that mice lacking the $Na_v1.7$ gene are totally insensitive to pain.[36] There is also human evidence that individuals who have point mutations in the SCN9A gene that encodes $Na_v1.7$. Gain of function mutations to SCN9A result in spontaneous pain syndromes and extreme pain disorders, whereas loss of function mutations causes individuals to experience no pain through a rare genetic condition known as CIP.[36] Both the location of $Na_v1.7$ in the body and these genetic results points towards $Na_v1.7$ playing a key role in pain perception and make it an ideal target for pain medications. Voltage sensing domains (VSD) I-IV are key in regulating channel opening and closing as described. VSD-III is responsible for opening the channel in response to membrane depolarization from external stimulus. The location of these domains relative to the pore of the protein are illustrated (Figure 1.8).[34]

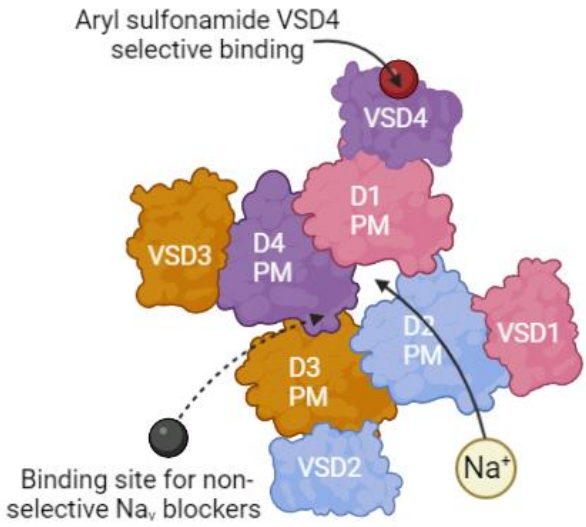

Figure 1.8: Nav 1.7 schematic showing the location and binding of non-selective Nav blockers (black) and aryl sulfonamide VSD4 selective binding (red)

VSD4 is unique in its role of termination Na^+ influx by initiating fast inactivation and quickly closing the channel shut when the membrane potential is reached.[34] By locking the channel in the closed state, pharmacophores that act here can stop Na^+ influx and subsequent signalling, halting an action potential without physically blocking the pore. In this way, a $Na_v1.7$ VSD4 selective inhibitor would be capable of stopping electrical signals in response to pain before they reach the CNS and are perceived.

It is a challenge to design Na_v selective compounds, as they rely on specific sequence positions that are not homologous, but several $Na_v1.7$ VSD4 selective pharmacophores have been identified and show evidence of achieving mild analgesia with limited off target effects.[32] Notable compounds (Figure 1.9) show the crucial functionalities. The aryl sulfonamide pharmacophore interacts through an anionic contact with positively charged Arg1602 and Arg1608 in the VSD4 of the receptor.[37] As described previously, general Na_v blockers bind by blocking the pore of the channel and physically preventing ion movement across the membrane, but newer research like

these $Na_v1.7$ selective compounds target specific portions of the protein that control the opening and closing of the channel.[34,38]

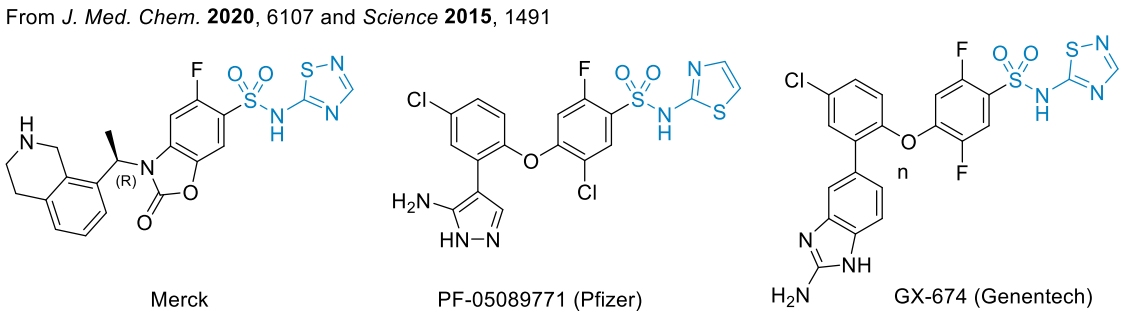

Figure 1.9: Structures of $Na_v1.7$ VSD4 selective pharmacophores in the literature

This exciting area of research has attracted the interest from many major pharmaceutical companies to develop $Na_v1.7$ selective and state-dependent drugs for pain management. Despite selectivity achieved by targeting non-homologous sequences in VSD4, these compounds still display some partial activation to the other Na_v isoforms and do not induce analgesia as strongly or as successfully as typical opioid pharmacophores.[32]

1.3 Solving the Pain Problem- Advantages of Bitopic and Bifunctionally Designed Drugs

MOR selective drugs are not enough to solve the pain problem due to their negative side effects. Despite selectivity for MOR over DOR and KOR, opioid therapy often requires patients to take several medications and mitigate DDIs. General Na_v blockers are not sufficient either due to their off-target activity.[37] $Na_v1.7$ selective drugs are very promising, but still are not a complete solution, as they do not fully eliminate off target binding and have weak analgesic effect on their own.[32] Drug candidates like those shown in Figure 1.9 also exhibit poor ADME properties. Most notably CYP450 metabolism complications cause them to have unfavourable pharmacokinetic properties preventing them from making it through clinical trials.

A recent publication from Minett *et al.* suggests that a combinational therapy of opioids and $Na_v1.7$ antagonists could be an excellent solution to the described challenges with current available pain relief strategies.[36] $Na_v1.7$ blockers alone may not be sufficient for pain relief, but combined with a low dose of opioid, they could achieve potent analgesia. Instead of two separate drugs, a bifunctional ligand could achieve this same effect (Figure 1.2). Designing *one* compound that could interact at *two receptors* in this way would be ideal and overcome issues associated with multidrug pharmacological strategies of opioids and $Na_v1.7$ blockers. A bitopic compound like this could also have additive binding effects and enhance selectivity through increased binding affinity at the receptors. A bifunctional compound could provide a synergistic pharmacological effect downstream in the body by activating additional pathways such as second messenger systems. A publication from Mueller *et al.* describes synergistic analgesia accomplished from combined therapy of μ-theraphotoxin-Pn3a, a complex peptide, and potent and selective $Na_v1.7$ inhibitor with MOR agonist oxycodone.[39]

This bifunctional approach inspired Dr. Patrick Giguère. It presents an opportunity to overcome many of the issues present with current available opioid therapeutics.[19,40] This resulted in the opportunity for a collaboration. Dr. Giguère hypothesized that targeting two components in the pain network could be a strategy to produce potent, selective analgesics with reduced side effects. This project developed in a highly collaborative and interdisciplinary way, as is often the case with medicinal chemistry outside of academia.

More recently, a publication from Gao *et al.* showcases a bifunctional compound that had analgesic potential through dual targeting of the pain network and is a major proof of concept for this approach.[9] The title bifunctional compound combined a MOR agonist pharmacophore from the fentanyl scaffold with that of a known TRPV1 ion channel antagonist (Scheme 1.2). TRPV1

is a cation channel that is responsible for Ca^{2+} ion influx and is involved in modulation of pain and temperature.[41] Although this bifunctional ligand did not display significant enough analgesia to become a drug-like candidate, it is a rare example of bifunctional targeting of *two receptors* in the pain network with *one molecule*.[9]

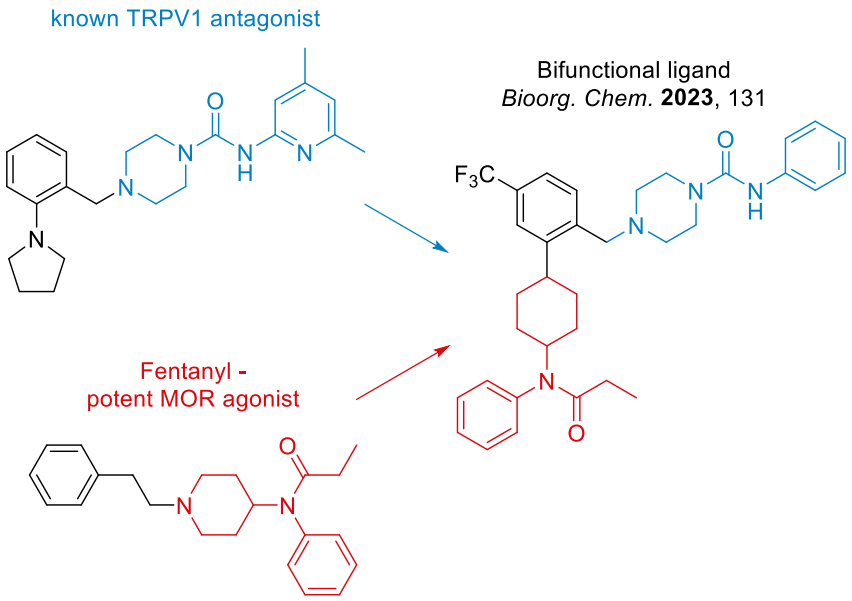

Scheme 1.2: MOR and TRV1 fused bifunctional ligand

1.4 Goals of the Project

Safer analgesics that use alternative and more complex drug design approaches could treat chronic pain effectively by reducing the dangerous side effects and other drawbacks of opioid use. Polypharmacology is a good strategy, but designing bitopic or bifunctional drugs that avoid the practical aspects and ADME challenges of multidrug therapies are even more promising. The goal of this project is to target two components in the pain network – the MOR and $Na_v1.7$ – using a bifunctional drug.

The first step was to identify pharmacophores for each receptor and design a first generation of compounds. This was done with the help of our collaborators in the Giguère group

and lead by MSc Candidate Shivani Patel. Research in the Giguère group focuses on the GPCR opioid system and uses a combination of biochemical, pharmacological and, most notably, a structural approach to better understand functional selectivity in the opioid system. MSc Candidate Shivani Patel screened ligands with ICM-VLS bioinformatics, selecting pharmacophores that would interact with MOR and $Na_v1.7$. Initially, known MOR agonists and $Na_v1.7$ blockers were compared and superimposed, but no pharmacophores shared enough functional similarity. The binding requirements at each receptor were too different, so instead Dr. Giguère investigated compounds that joined both pharmacophores with a short linker. Millions of compounds were computationally and experimentally screened. These bifunctional compounds with two unique pharmacophores appeared to be the best way to achieve binding at both receptors. One pharmacophore would target MOR to activate the G_i/G_o pathway. The other would target VSD4 of $Na_v1.7$ to prevent the channel from opening and allowing Na^+ influx and neuronal signal propagation.

Herein, the goals of designing new bifunctional ligands to target two components of the pain network, MOR and $Na_v1.7$, by linking two unique pharmacophores, is presented. Due to the major differences and binding requirements between the MOR orthosteric binding site and the VSD4 of $Na_v1.7$, a bifunctional approach was chosen over a bitopic approach. As previously discussed, multi-target drugs require extensive knowledge of the binding pocket and orientation of the ligands bound to receptors. Thankfully, many useful crystal structures and cryoEM images were available, or published over the course of this project,[19] which influenced the choice of compound design.

It was proposed that to create a bifunctional ligand, compounds would be designed to contain two unique pharmacophores linked closely through a urea bond similar to that in PZM21.

The core scaffold for MOR binding was selected based on PZM21 as there was crystal structure of MOR bound to PZM21 (PBD: 7SBF) and literature evidence on its bias for the G_i/G_o pathway already.[19] The most important binding contacts for activating MOR, notably the basic amine and phenol oxygen, are shown in Figure 1.10.[19] It was shown by Mangalik *et al.* that modifying the right side of PZM21 derivatives did not affect the potency as the key functionalities in the pharmacophore are only on the left-hand side,[19] so it was hypothesized that the right side could be edited and still maintain MOR selectivity and activity overall. The right side would be modified through the urea bond, thereby introducing new functionality. The urea has minor binding contacts in the MOR pocket,[19] and the Beauchemin lab specializes in strategies to form new C-N bonds. For these reasons, this position was a natural choice to include in the scaffold of compounds to be designed.

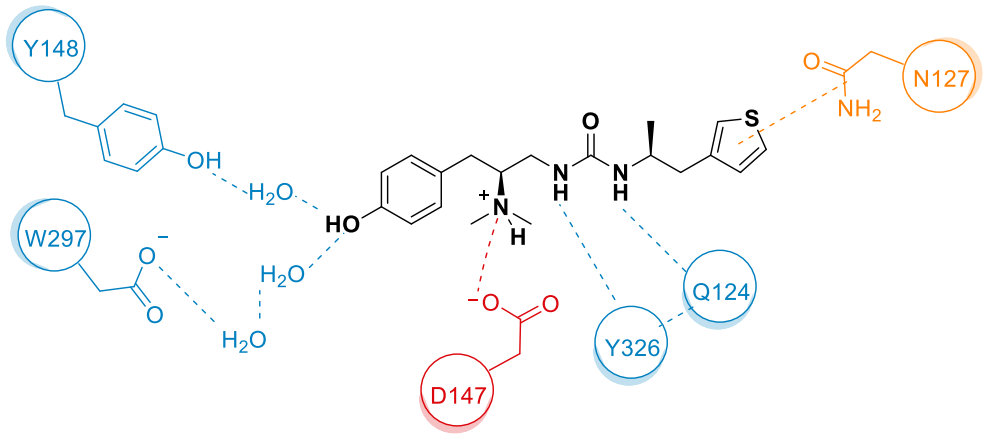

Figure 1.10: Key functionalities and amino acid contacts for PZM21. Crucial contacts are shown in red, intermediate contacts shown in blue, and minimally important contacts shown in orange

The new pharmacophore introduced that would target $Na_v1.7$ was selected based on GX-936 and related structures (Figure 1.11).[34] There is also a crystal structure available of GX-936 bound to the VSD4 of $Na_v1.7$ (PDB: 5EKO) confirming its binding orientation and location on the $Na_v1.7$ receptor. Literature evidence suggests that aryl sulfonamide functionalities are crucial for

$Na_v1.7$ VSD4 interactions, through an anionic contact at Arg residues in the receptor (Figure 1.11).[32,37] Acyl sulfonamide functionalities have also been investigated but shown to be less potent than aryl varieties.[42]

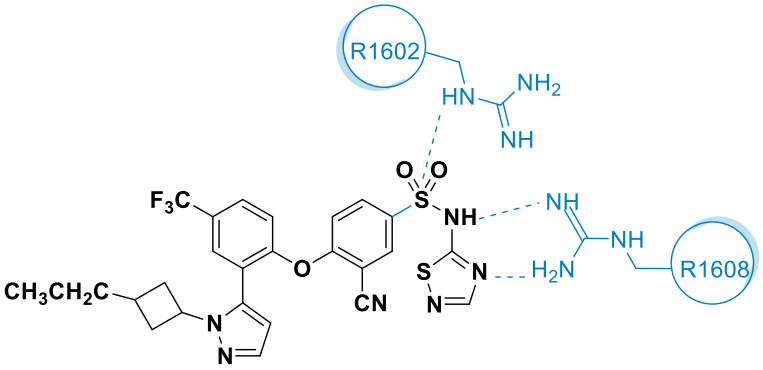

Figure 1.11: GX-936 bound to $Na_v1.7$, showing key amino acid contacts

For the first generation of compounds, two heterocyclic aryl sulfonamide pharmacophores were selected, an aryl sulfonamide bearing a pyrimidine and a thiazole (Figure 1.12). Some aryl sulfonamide heterocycles are highly susceptible to CYP450 metabolism, so two different heterocycles were selected were to mitigate this. By selecting two different pharmacophores early in the project, it was hoped to test $Na_v1.7$ binding against PF-771 as a control and validate a warhead for future SAR rounds.

Figure 1.12: Thiazole (left) and pyrimidine (right) heterocycle targets

It was hypothesized, based on literature compounds, (Figure 1.9) that a high amount of variability could be tolerated on the left side of $Na_v1.7$ binding compounds while still maintaining VSD4 antagonist activity, making this scaffold an excellent choice to combine with PZM21. Three compounds were selected as the first targets, shown in Figure 1.13.

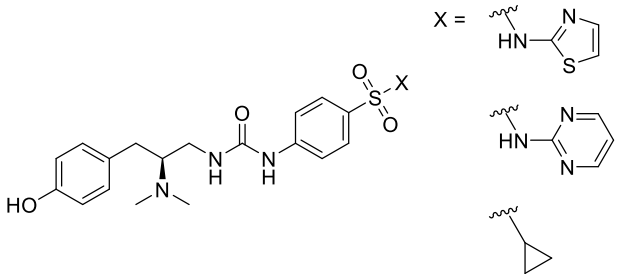

Figure 1.13: Initial targeted compounds

With In summary, the compounds designed were MOR agonists merged with $Na_v1.7$ VSD4 selective blockers. The compounds aimed to both 1) Activate the G_i/G_o pathway by interacting as an agonist at the orthosteric site of MOR, and 2) prevent the opening of $Na_v1.7$ channels by blocking the VSD4. the pharmacophores selected and base scaffold to work with, synthesis began with the first generation of compounds.

Chapter 2: Generation I and Insight to Nav1.7 Binding

2.1 Urea Linked Aryl Sulfonamide Compounds – Generation I

A general structure for the first generation of compounds is shown (Scheme 2.1). These compounds are based greatly off the scaffold of PZM21, containing a rigid urea linker and the pharmacophore for $Na_v1.7$ introduced on the right side.

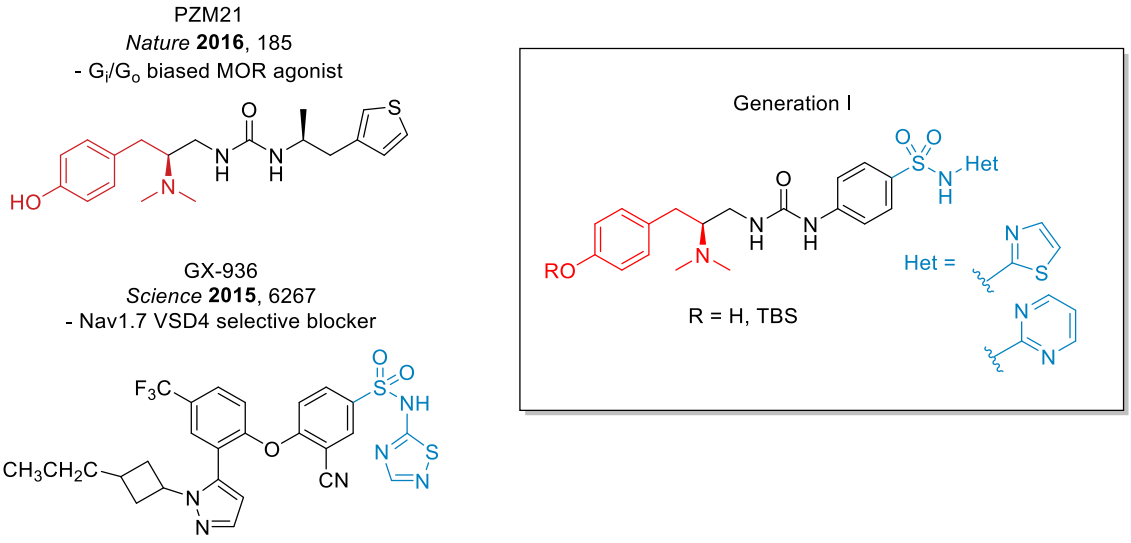

Scheme 2.1: General structure of first generation of compounds. MOR (red) and $Na_v1.7$ (blue) pharmacophores are shown, based of off PZM21 and GX-936 respectively

For the MOR pharmacophore, it was decided to maintain most of the PZM21 scaffold, as it had high selectivity for MOR and was already biased for the G_i/G_o pathway. Compounds were expected to remain potent regardless of changes to the right side, as all the crucial binding functionalities for MOR were included in the west fragment of the compounds.[19]

It was decided to target two related but different $Na_v1.7$ pharmacophores at the same time based on heterocycles present in literature compounds.[32] Fragments bearing the thiazole and pyrimidine heterocycle could be synthesized in tandem allowing two unique ligands to be tested. For the $Na_v1.7$ pharmacophore, in addition to the thiazole and pyrimidine heterocyclic sulfonamides, a sulfone compound was selected. Testing all three pharmacophores would probe if

the electronegative sulfone was sufficient or if a sulfonamide was required to facilitate the anionic interaction with Arg1602 and Arg1608 in VSD4 (Figure 1.11).[37] Inspiration for the Nav1.7 pharmacophores for the target compounds is shown in Figure 2.1.

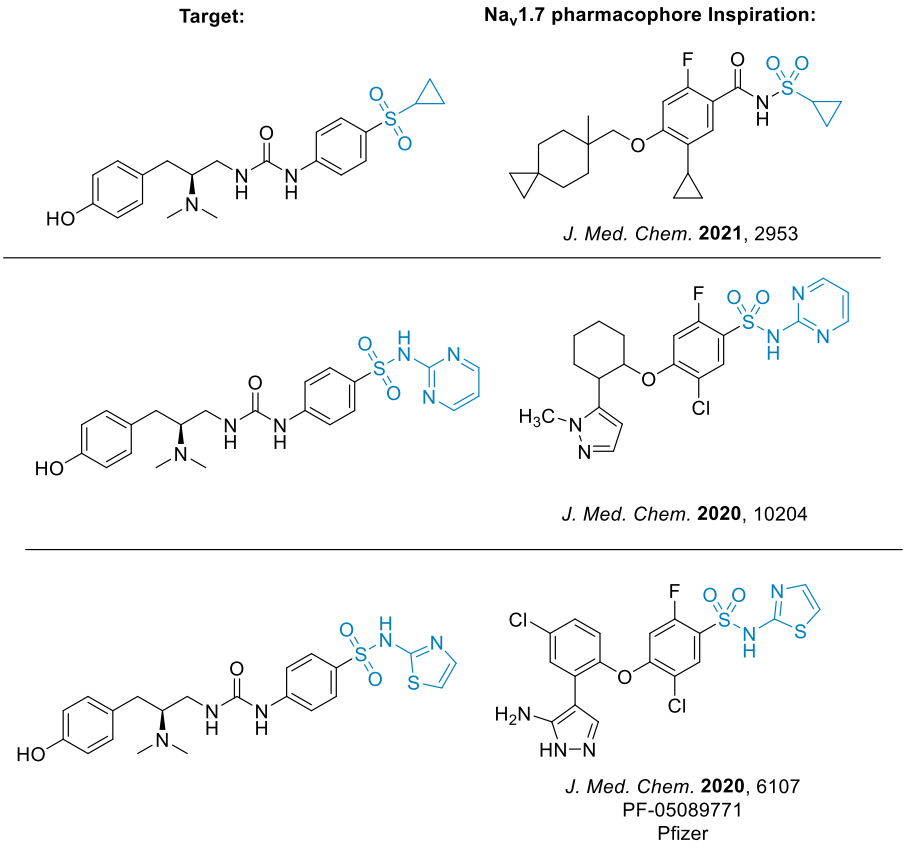

Figure 2.1: Inspiration for Na$_v$1.7 pharmacophores

2.2 Synthesis of Urea Linked Aryl Sulfonamide Compounds – Generation I

A convergent synthetic approach was used for generation I compounds, as it would be most logical to form left and right-side fragments and then connect the two pharmacophores. The proposed synthetic strategy utilized formation of the central urea to accomplish this (Scheme 2.2). This strategy requires the two coupling partners, the dimethylamine MOR pharmacophore (Fragment A) and the heterocyclic sulfonamide Na$_v$1.7 pharmacophore (Fragment B), to be synthesized separately.

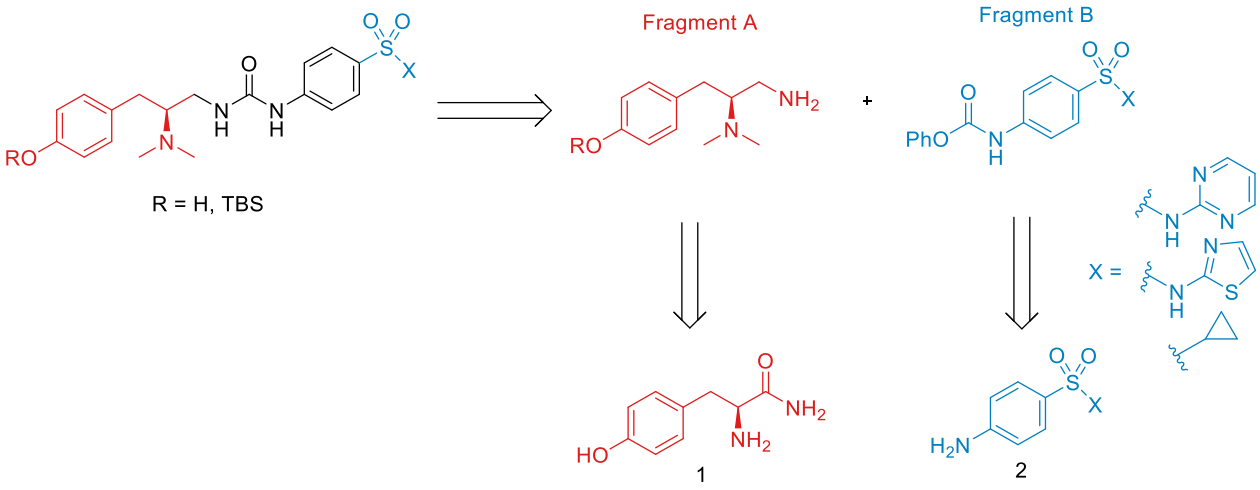

Scheme 2.2: Retrosynthesis for Generation I compounds

Fragment A was modeled very closely after PZM21, with the goal of obtaining a MOR selective interaction to stimulate the G_i/G_o pathway. A quick assembly was expected following literature procedure from recent publications on PZM21.[28] Several analogues of this building block have been patented and published, [28,43,44] so experimental procedures were available. However, challenges were still encountered, attributed to the small size and high heteroatom count of this building block. Purification was particularly challenging. To ease purification, the phenol subunit was protected using a *tert*-butyl-dimethyl silyl protecting group (TBS) at an early stage of the synthesis. The TBS group was selected based on its moderate size and intermediate lability. The formation of this building block was key to the project, and required a robust and reliable route; the diamine moiety would be present in all compounds prepared and tested that would target MOR.

Control of stereochemistry was established at a very early stage in the synthesis by starting with enantiopure amino amide **1**. This stereocenter would become the location of the crucial cationic dimethyl-ammonium group (at physiological pH) and locking the *S* conformation from the beginning would prevent issues with a mixture of enantiomers at later steps in the synthesis. The first step of the synthesis was protecting the phenol of L-tyrosine amide **1** using TBSCl and

imidazole (Scheme 2.3).[45] This reaction was originally performed by heating at 60 °C overnight through oil bath heating. It was optimized to be completed in 40 minutes heating to 80 °C with the Anton Parr Monowave 400R Microwave, a faster and more efficient route.

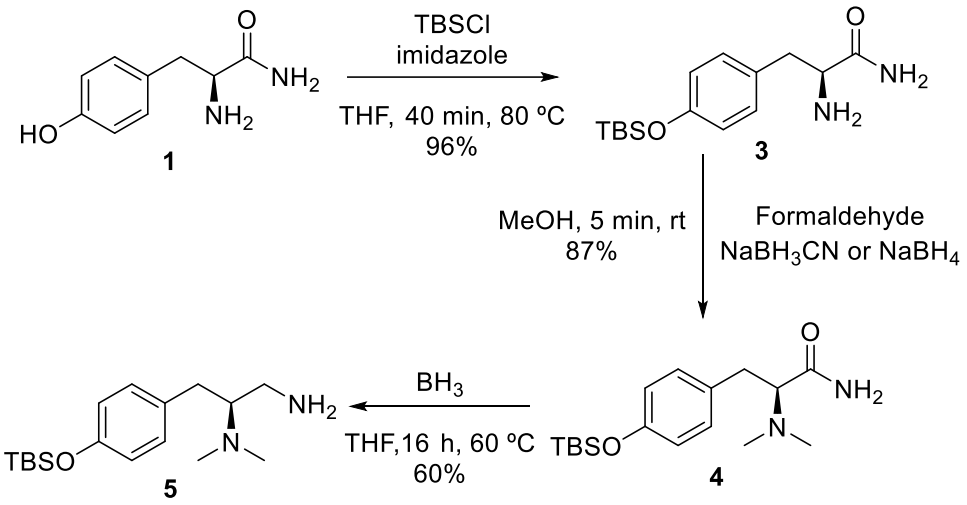

Scheme 2.3: Synthesis of fragment A

The next step was the dimethylation of the amide **3** through reductive amination with formaldehyde (Scheme 2.3).[43] This step was initially quite challenging, a major consideration was how to include formaldehyde as a reagent, which is a gas. The formaldehyde used was added as a solution of 37% w/w solution in water, which contained 8-10% MeOH as an impurity indicated on the bottle. Through quantitative inspection with ^{1}H NMR, it was found that the formaldehyde contained much less than 37% w/w, in the worst cases of older bottles and unreliable manufacturers, less than 10% formaldehyde was in solution. To combat this, the equivalents of formaldehyde was increased dramatically, and a reliable supplier was used for purchasing. To complete the reductive amination, $NaB(OAc)_3H$ or $NaBH_3CN$ were both evaluated as reductants (Table 2.1). Gratifyingly, both were successful with yields of 87% and 92% respectively, achieving

formation of the dimethyl amino amide **4**. The reaction proceeded to completion quickly, and mono methylation was not a concern and not often encountered as a major by-product.

*Table 2.1: Dimethylation Conditions for Compound **4***

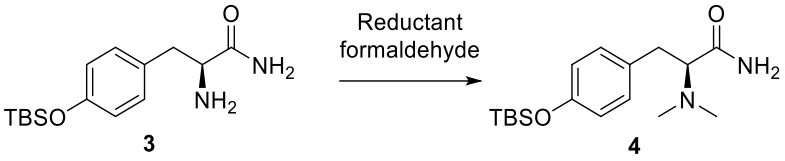

Entry	**Reductant**	**Solvent**	**Time**	**Yield**
1[a]	$NaBH_4$, AcOH ($NaBH(OAc)_3$ formed *in situ*)	DCM	15 min	87 %
2[b]	$NaBH_3CN$	MeOH	5 min	92 %

*a. Conditions: $NaBH_4$ (9.25 equiv) and AcOH (27.1 equiv) in 10 mL of DCM, 1 h, 0 ℃ to rt. Concentrate in vacuo followed by addition of amine **3** (1 equiv) and formaldehyde (14.4 equiv) in 6.3 mL ACN/0.7 mL H_2O, 15 min, rt. b. Conditions: Amine **3** (1 equiv), $NaCNBH_3$ (1.5 equiv), formaldehyde (13 equiv) 0.25M in MeOH, 5 min, rt.*

The final step was reduction of the dimethyl amide **4** to form the dimethyl amine **5**. This was achieved through a BH_3 mediated reduction (Scheme 2.3).[43] A $LiAlH_4$ reduction was attempted as well but resulted in a mixture of TBS-protected and deprotected product, causing separation challenges (Scheme 2.4). BH_3•THF (1.0M) remained the reagent of choice for the reaction. The resulting TBS-protected dimethyl amine was secured over three steps and ready to undergo coupling with fragment B.

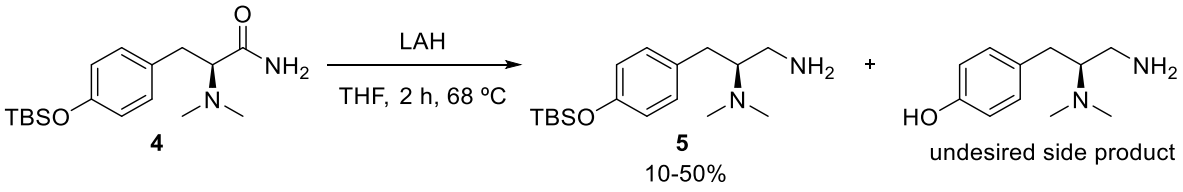

Scheme 2.4: Mixture of products resulting from LAH reduction

Fragment B was formed through a masked isocyanate. The Beauchemin group has extensive knowledge of isocyanate chemistry and using masked isocyanates to form ureas through nucleophilic addition with amines. Isocyanates extremely reactive on their own and polymerize,

often making them difficult reagents to work with directly.[46] A common strategy to control their reactive potential is to mask them with blocking groups to form stable precursor compounds referred to as blocked or masked isocyanates.[46] A variety of blocking groups can be used,[47] phenol blocked isocyanates are common. These masked isocyanates can be deblocked in the presence of base or heat, generating a free isocyanate *in-situ* which can then undergo a nucleophilic addition in a controlled manner (Scheme 2.5).

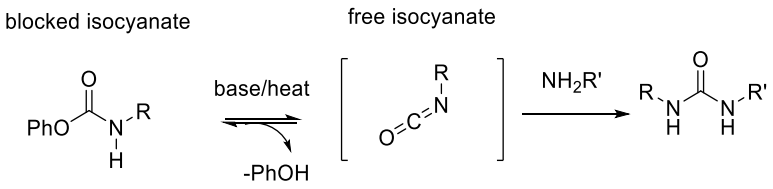

Scheme 2.5: Masked isocyanate reaction strategy

Fragment B was readily formed from commercial aniline building blocks **2a** and **2b** in just one step (Scheme 2.6).[48] This route was used for both the pyrimidine compound **6** and thiazole compound **7**. Gratifyingly, even with the complex sulfonamide structure present on these substrates, reactivity at the aniline position was successful. Exploratory attempts using additional chloroformate reagent, a longer reaction time, or increased reaction temperature did not lead to higher yields.

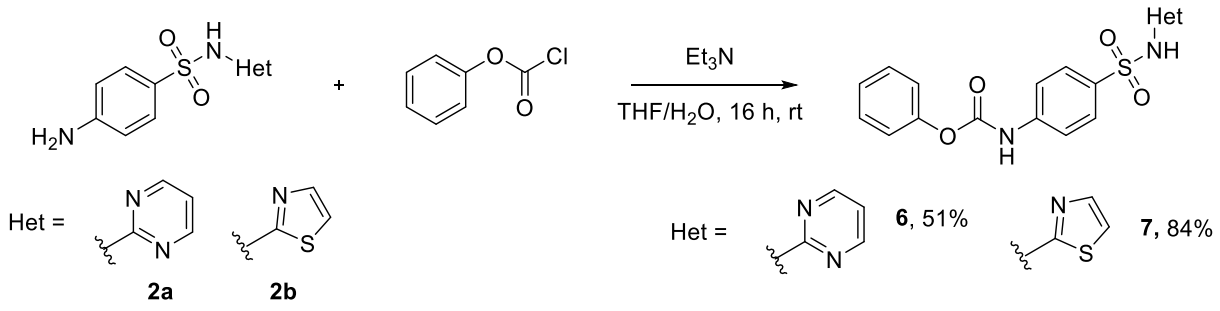

Scheme 2.6: Synthesis of fragment B

With both coupling partners in hand, the next step was to join fragments A and B. This was achieved through a base-mediated isocyanate deblocking and nucleophilic attack at the isocyanate (Scheme 2.7).[48] The amine was included on fragment A and the isocyanate on fragment B based on procedure from Perrey *et al.* [28] The reverse which included the blocked isocyanate on fragment A was attempted but afforded no reaction. The TBS group would undergo cleavage at temperatures greater than 60 °C, so sufficient base was used to ensure complete deblocking of the isocyanate without requiring higher reaction temperature.[46]

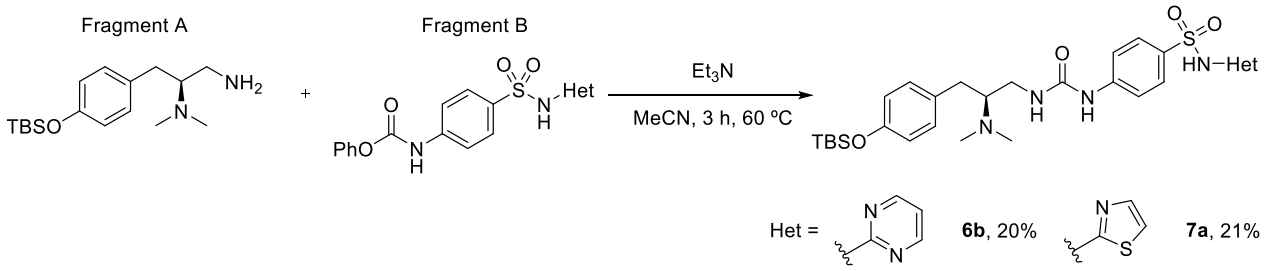

Scheme 2.7: Coupling conditions for generation I compounds

After purification through column chromatography, the protected products **6a** and **7a** were obtained. Yields were very poor for these reactions (Scheme 2.8), but optimization was not conducted at this stage. The goal at this point in the project was to synthesize and purify compounds to deliver for testing. Optimization was not pursued until active compounds and a clear SAR strategy was established, as is a common strategy in medicinal chemistry research.

Deprotection to form **7b** was achieved with excess HF•pyridine at 0 °C (Scheme 2.8).[45] TBAF was first considered as it is the standard for deprotecting TBS and other silyl based protecting groups and a safe and convenient source of F^- ions.[45] TBAF, but the resulting crude material was much easier to purify through column chromatography (Scheme 2.8).

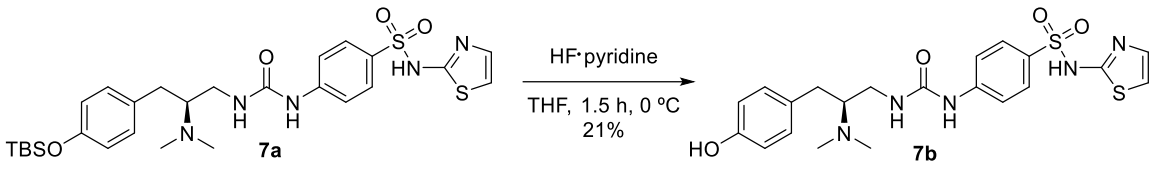

*Scheme 2.8: HF deprotection of **7b***

The use of TBAF was successful in cleaving the TBS group, but the tetrabutylammonium salt remained in the crude material. All attempts failed to separate it from the deprotected product through extractions, column chromatography and preparative TLC. This prompted the use of HF•pyridine which achieved deprotection with similar efficiency to TBAF but allowed easier purification.

One major challenge with this generation of compounds was they contained many heteroatoms, resulting in highly polar products with very poor solubility in common solvents used for flash chromatography purification. This was expected when compounds were designed on paper but proved to be an issue in the laboratory that required creative solutions. Purification techniques using highly polar eluents were often required, and in nearly all cases required MeOH to aid in solubility. Reverse phase chromatography was investigated briefly but was not successful.

In addition to these aryl sulfonamide compounds, a colleague, Mr. Sherif Meshref, also prepared compounds **8a** and **8b** for testing (Figure 2.2). These compounds contained a sulfone in contrast to the sulfonamides and would probe the requirements for $Na_v1.7$ binding. Literature describes an anionic interaction with arginine residues in the VSD4 of $Na_v1.7$,[37] but testing both sulfones and sulfonamides would probe the requirements for this binding.

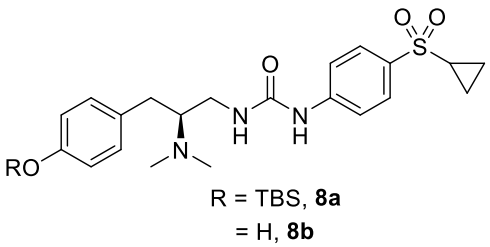

*Figure 2.2: Sulfone compounds **8a** and **8b***

Two additional monofunctional (single point binding) compounds were prepared for this first generation of compounds (Scheme 2.9). These compounds contained the MOR pharmacophore but a truncated right side, excluding the $Na_v1.7$ pharmacophore and only bearing a simple phenyl group in replacement. Compounds **9a** and **9b** would not be tested at $Na_v1.7$ as they lacked the pharmacophore and were not predicted to interact. These compounds were selected for testing to probe only the MOR pharmacophore and validate the use of the PZM21 scaffold and short, rigid urea linker.

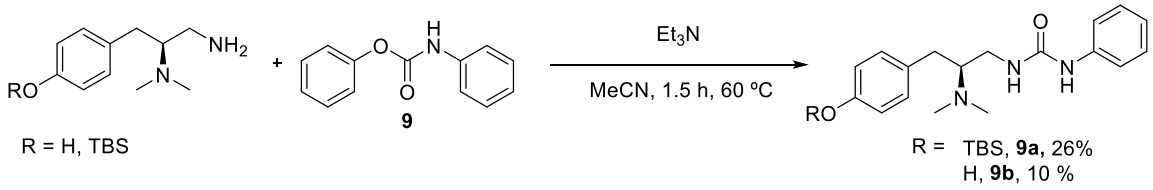

Scheme 2.9: Single point binding (monofunctional) Generation I compounds

Similar to potentially bifunctional (two-point binding) compounds **6a**,**7a** and **8a**, both the TBS protected compound **9a** and free OH compound **9b** were synthesized and prepared for testing. It was not the initial goal to submit TBS protected compounds for testing, as the TBS group was employed for ease of purification purposes only. However, it was decided to test this intermediate as well to understand the importance of the phenol as part of the MOR pharmacophore and learn about the effects of including as sterically large lipophilic group. With these six compounds

completed (Figure 2.3), compounds were delivered to the collaborators and underwent biological testing.

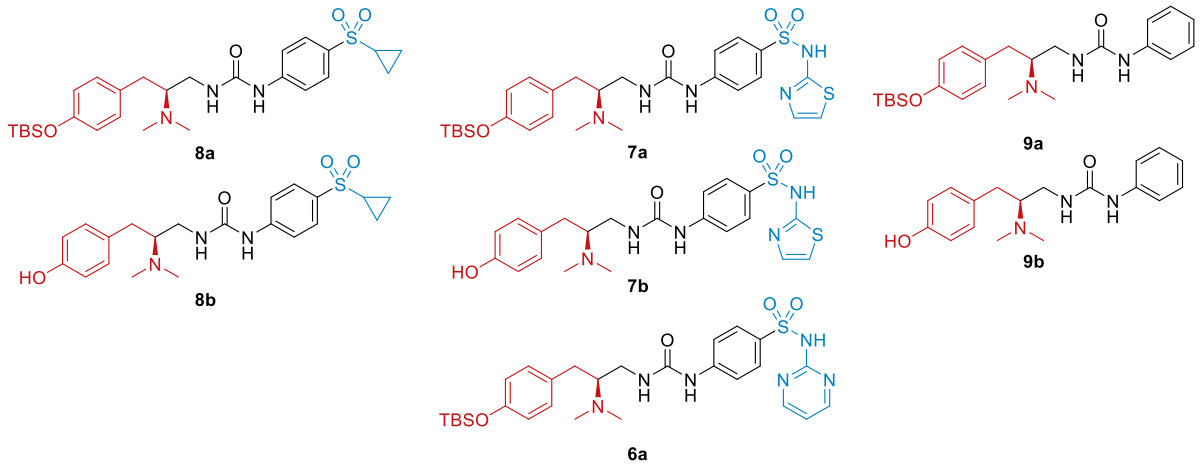

Figure 2.3: Generation I compounds prepared for biological testing

2.3 Results of Urea Linked Aryl Sulfonamide – Generation I

Compounds were tested by the Giguère research group in their laboratory on the medical campus of the University of Ottawa by MSc candidate Shivani Patel. The MOR tests were run on HEK293T cells using the GloSensor assay to measure MOR binding and activation of the G_i/G_o signalling pathway. $Na_v1.7$ tests were also run on HEK293T cells that expressed both human $Na_v1.7$ and K^+ channel Kir7.1, making them excitable and suitable to test neuronal function and signal transmission associated with VSD4 function. The $Na_v1.7$ assay was designed by MSc candidate Shivani Patel in the Giguère lab. All compounds were dissolved in DMSO for testing.

To our delight compounds **6a** and **7a** (Figure 2.3) were both active at $Na_v1.7$. The IC_{50} for the thiazole compound **7a** was 9.24×10^{-8} M comparable to 6.98×10^{-8} M for the control compound PF-771, a known $Na_v1.7$ VSD4 blocker.[49] These results are illustrated in a graph prepared by Dr. Patrick Giguère in Figure 2.4. Compound **6a** shows a change in membrane potential associated with reduced signalling from VSD4 blocking in a similar fashion to PF-771 and achieves a similar

efficacy. The potency of analogue **6b** bearing the free phenol is not sufficient, observed by the shallow curve.

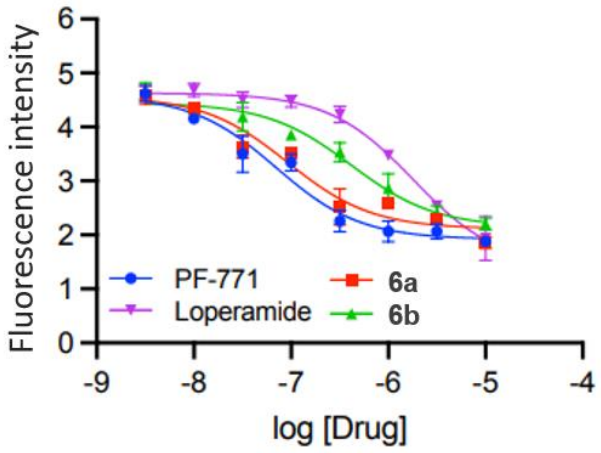

Compound	**Log(IC_{50})**	**IC_{50} (M)**	**SEM**
PF-771	-7.156	6.980×10^{-8}	0.101
Loperamide	-5.743	1.808×10^{-6}	0.074
6a	-7.034	9.248×10^{-8}	0.117
6b	-6.384	4.134×10^{-7}	0.092

Figure 2.4: Results of select compounds from generation I. Fluorescence shown on the Y axis is associated with fluorescent dye travelling across the cell membrane. Reduced fluorescence correlates with $Na_v1.7$ blockage through the VSD4. PF-771is a positive control and Loperamide is a negative control.

These satisfactory binding affinities achieved with aryl sulfonamides did not prompt the need for acyl sulfonamides to be investigated at this time.[42] Lack of activity for compounds **8a** and **8b** (Figure 2.3) confirmed the hypothesis that a sulfonamide was required for ionic contacts with Arg 1602 and Arg 1608,[37] a sulfone was not sufficient. Due to its higher binding affinity, for the design of future compounds targeting $Na_v1.7$ on the project, the thiazole moiety in compounds **7a** and **7b** was selected as the pharmacophore with the understanding that the pyrimidine pharmacophore could be reintroduced at a later stage in the SAR if required.

The monofunctional compounds **9a** and **9b** were not active at MOR, despite containing the same key functionalities as **7a** and PZM21. This result triggered a more thorough investigation into the orientation of compounds when they interact with the MOR binding pocket. This is described in Chapter 2.6, but another a very surprising result was the activity of the TBS bearing compound **7a** and the lack of activity for the OH compound **7b** at $Na_v1.7$. It is curious that the effect of a group relatively far away from the basic amine pharmacophore would have enough of an effect to eliminate binding affinity overall. This resulted in a new synthetic idea for the diamine Fragment A (Scheme 2.3). We sought out to introduce a different functionality on the phenol, something intermediate in size and lipophilicity between the OH and the OTBS. An *O*-methyl was selected for this and was particularly synthetically useful as it represented a securely protected phenol that would be more robust than the OTBS and be able to withstand harsher reaction conditions and temperatures.

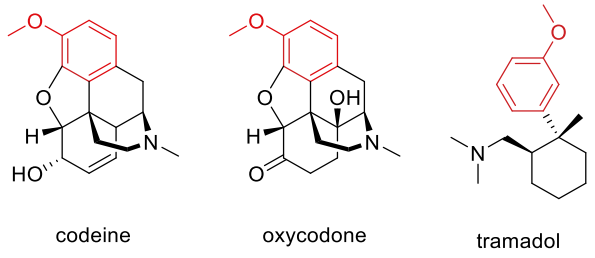

Figure 2.5: Structures of MOR agonists in literature containing an anisole moiety

We were also inspired by opioids such as *codeine*, an active metabolite of *morphine*, which contained the same anisole moiety (Figure 2.5). We also saw no literature evidence for any type of silyl protection employed on the phenol of PZM21, and with this unexpected result from the TBS group, it was decided chose to investigate this position further. We hoped that an *O*-methyl analogue of **7b** could restore activity at $Na_v1.7$ when the OH was inactive, and additionally bind MOR with success.

2.4 Introducing A New Diamine – Alternative Phenol Protection

Forming this new anisole fragment was challenging because it required starting from a different amino acid building block that was not available to purchase at the amide stage, this introduced a new step in the synthesis (Scheme 2.10). One advantage of this route was that the *O*-methyl protected phenol was more stable than the TBS protected phenol, this allowed more aggressive reaction conditions with minimal risk of deprotection. This route was accomplished overall in four steps through a linear synthetic route, it was very successful and time efficient. Purification was achieved at all stages through filtration or extractions, requiring no column chromatography and obtaining the building block quickly and in high yields.

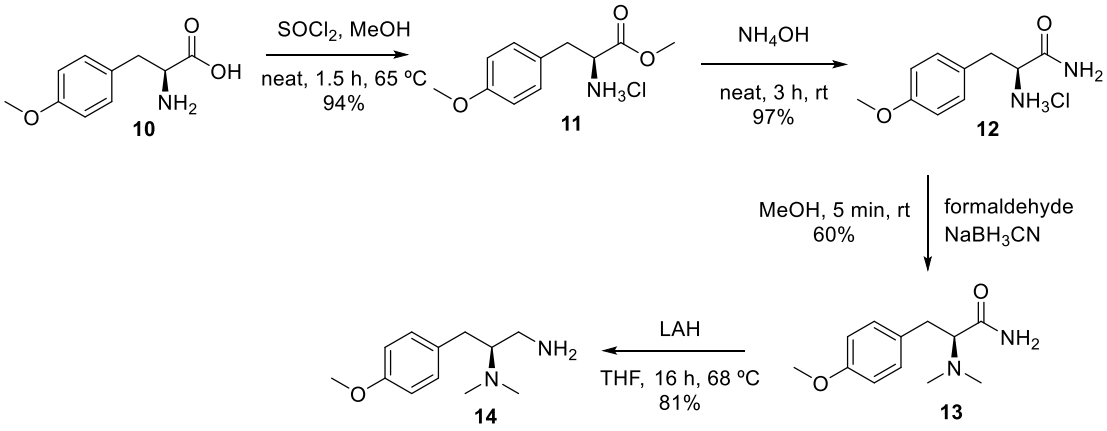

Scheme 2.10: Synthesis of Fragment A'

2.5 Synthesis of *O*-Methyl Diamine

The first step of the synthesis was to methylate 4-methoxy-L-phenylalaine **10** to form **11** (Scheme 2.10)**.** Similar to the strategy for fragment A, the starting material was purchased enantiopure. Esterification was achieved using MeOH and thionyl chloride.[50] This intermediate was taken to the amidation stage as quickly as possible, never storing for longer than 48 hours. Although unlikely, epimerization is a possibility with alpha amino esters and therefore, methyl ester **11** was converted to amide **12** by reacting with aqueous ammonia (Scheme 2.10). NH_3 in

methanol was initially used as the ammonia source but was not as successful as the NH_4OH.[51] The reaction was done neat using the NH_4OH in a large excess and isolating the pure product through a liquid-liquid extraction. This purification utilized the highly polar nature of the compound, isolating in the aqueous phase in the workup.

The next step was dimethylation through a reductive amination with formaldehyde and $NaCNBH_3$ to form **13**.[43] The reaction conditions originally developed utilizing $NaB(OAc)_3H$ were also successful with this substrate, but yields were poor and the one-pot reaction with $NaCNBH_3$ was more feasible and therefore, preferred (Scheme 2.10). The final step to reduce the amide **13** to corresponding amine **14** was accomplished using $LiAlH_4$. Without the risk of cleaving a TBS protecting group, both BH_3 and $LiAlH_4$ mediated reductions were options, and the $LiAlH_4$ conditions proceeded very smoothly, affording the building block **14** for coupling.

Coupling of fragments A' and B proceeded under the same reaction conditions for the OTBS diamine previously optimized (Scheme 2.11). Purification was simpler due to the increased stability of the *O*-Me.

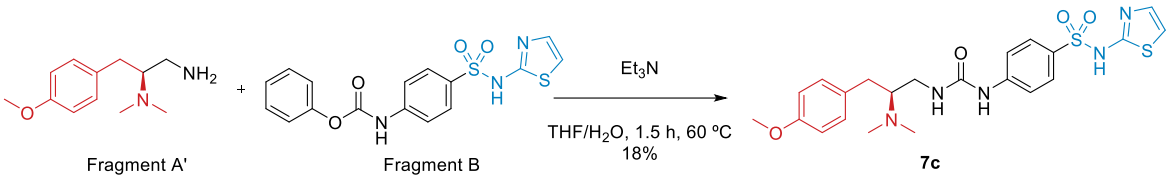

Scheme 2.11: Coupling conditions for compound 15c

Only coupling with the thiazole pharmacophore was completed (Scheme 2.11), as the goal was to probe how changing the phenol protection affected $Na_v1.7$ binding, not the change of heterocycle on the sulfonamide. It was hoped that this intermediately polar *O*-Me compound would be lipophilic enough to maintain $Na_v1.7$ activity, but potentially also hydrophilic enough to restore MOR activity.

2.6 Results of *O*-Methyl Compounds - Generation I

To our surprise, the *O*-methyl compound **7c** (Scheme 2.11) was inactive at both $Na_v1.7$ and MOR. This suggests that the lipophilicity and size of the entire compound is very important for binding at $Na_v1.7$, as this small alteration at the phenol position removed activity. At this point, it was not clear what effect the TBS group was having that caused compounds **6a** and **7a** (Figure 2.3) to be active at $Na_v1.7$. One hypothesis is that the TBS group is required to improve lipophilicity and allow the compound to penetrate or anchor itself in the cell membrane and interact with VDS4 on the surface of the receptor. It could also be due to the physical size of the compound. GX-936, PF-771 and other aryl sulfonamide VSD4 binding analogues (Figure 1.7) have relatively high molecular weights (>500 g/mol). The TBS group adds an additional 100 g/mol to the molecular weight of compounds **6a** and **7a**, making the size of these compounds most comparable of the compounds tested. The implications of this result remain unclear, and more compounds and analogues needed to be tested to better understand the effect of the TBS and other hydrophobic groups on $Na_v1.7$ binding.

A larger concern with new this result is that there was still a lack of activity at MOR. The phenol oxygen interacts with MOR through a water bridge (Figure 1.10), and although this phenolic position is important, it is not as crucial as the basic amine functionality for interaction with the MOR.[19] It was least likely that alterations to this position were disturbing binding and subsequent activity.[19] Additionally, the lack of activity for compound **9b** (Figure 2.3) that did contain the phenol OH supported this hypothesis. Instead of the absence of functionalities preventing binding, it was hypothesized that the lack of MOR activity was caused by a larger effect – orientation of ligand binding.

2.7 Generation I - Orientation and Conformation

Due to the changes made to the right side of the PZM21 scaffold to accommodate the $Na_V1.7$ pharmacophore, it is possible that the overall orientation of generation I compounds became different from that of PZM21. As discussed in Chapter 1.1, it cannot be assumed that pharmacophores will work the same way as a bifunctional ligand as they do independently. The structure and size of the whole molecule effects interactions at the receptor.[6] Generation I compounds (Figure 2.3) which all contain a urea linker, have a clear conformational preference for planarity. Indeed, the section from the distal nitrogen the urea to the sulfonamide group is stabilized by conjugation (Figure 2.6) making the blue highlight of the structure flat. This portion of the molecule could act as a wall, having very little flexibility, and likely prevents generation I compounds from fitting into the MOR binging pocket.

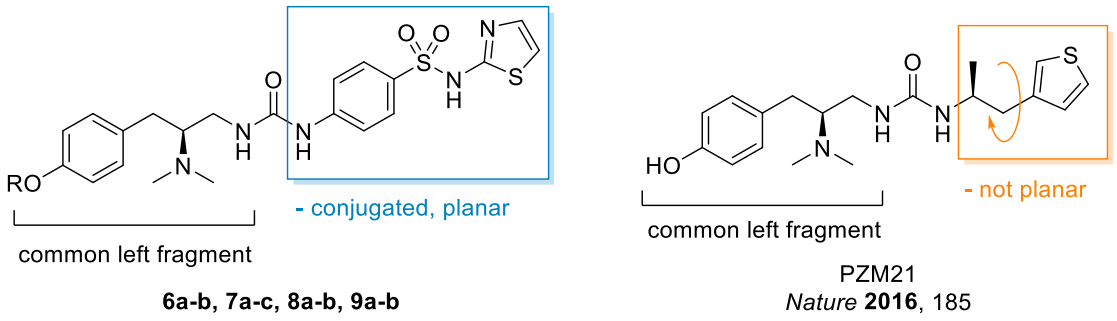

Figure 2.6: Generation I compounds displaying planar right fragment

When compared to PZM21, the right side of the molecule highlighted in orange is composed of sp^3 carbons resulting in a flexible linker which can rotate and adopt a preferred orientation. Molecules often need to flex and bend into appropriate orientations when binding to a receptor.[52] It is hypothesized that the molecule will adopt an orientation that is most suited to the MOR pocket. The hypothesis as to why PZM21 can bind MOR while generation I compounds

cannot when they both contain the same basic amine pharmacophore is based on the ability of PZM21 to adopt this preferred confirmation.

This confirmation is driven by a the A-1,3 strain present in amides and ureas.[53] Indeed, the C-N bond of the urea has partial double bond character through resonance and will rotate in order to orient the smallest atom attached to the α carbon to be in the same plane with the oxygen (Scheme 2.12).

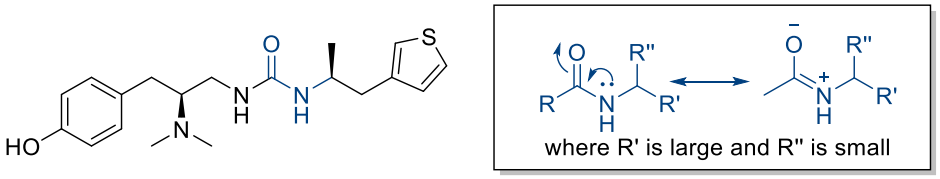

Scheme 2.12: Allylic strain present in amides, such as PZM21

This orientation is favoured to minimize allylic strain, it is highly favourable for PZM21 to adopt a conformation where the H, shown in green, is in plane with the carbonyl oxygen, opposed to the methyl or thiophene group (Scheme 2.13). As a consequence of this stereochemistry, the relative positions of the other groups can also be known when rotation occurs. Steric repulsion caused by eclipsing the methyl group with the carbonyl is a destabilizing interaction of >3.9 kcal/mol. This translates to a ratio of 1000:1 orientation B over A. The predominance of orientation B is potentially what orients PZM21 to fit into the orthosteric pocket of MOR and make the required amino acid contacts for binding, an orientation generation I compounds (Figure 2.3) cannot adopt due to their rigidity.

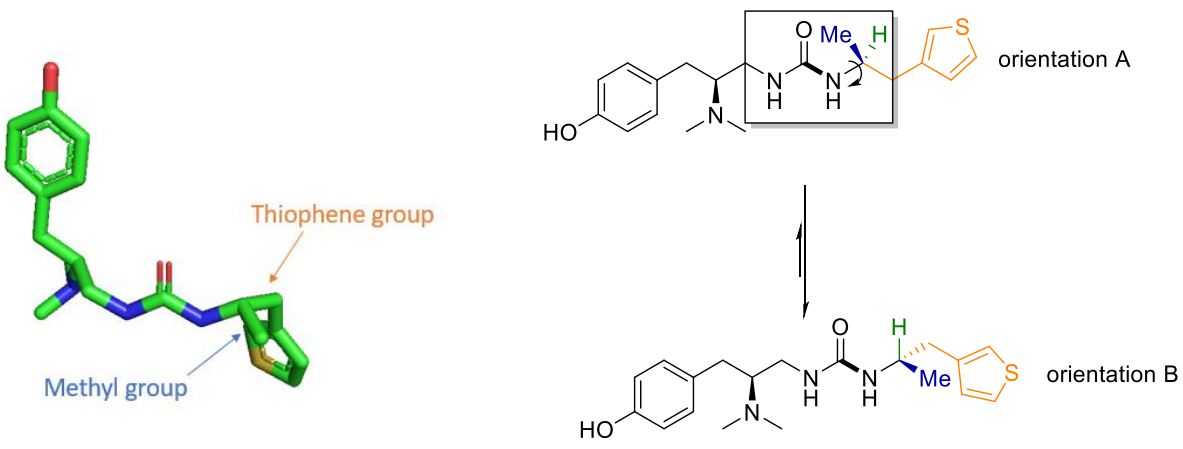

Scheme 2.13: PZM21preffered orientation. Shown from crystal structure in MOR allosteric pocket (PDB: 7SBF) on left.

This hypothesis is further supported with the available data and crystal structure images of the binding pocket of MOR, notably the crystal structure when bound of PZM21 (PBD: 7SBF).[19] The crystal structure of PZM21 was revaluated with this hypothesis in mind (Figure 2.7) and it matches the proposed orientation B hypothesized (Scheme 2.13) and tucks the thiophene residue into a hydrophobic pocket in the orthosteric binding site.[19]

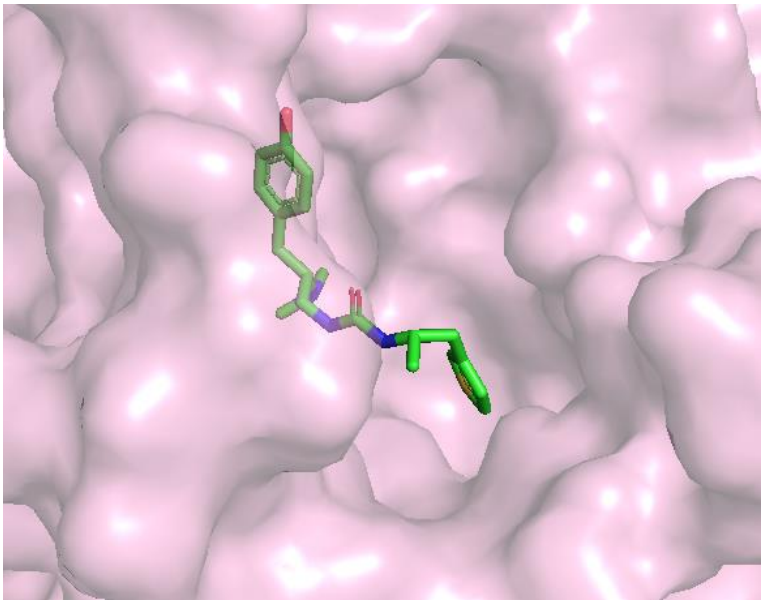

Figure 2.7: PZM21 in MOR binding pocket (PDB: 7SBF). The methyl group is visible coming towards the viewer while the thiophene group is seen pointing away from the viewer, back into the pocket.

With this perspective in mind, we sought to design a second generation of compounds with a more flexible linker that could orient a hydrophobic moiety in the way PZM21 orients the thiophene group into the binding pocket of MOR. This approach is presented in the next chapter.

Chapter 3: SAR Decisions and Insight to MOR binding – Generation II and III

3.1 The Effect of Orientation – Generation II Goals

New compounds required a new scaffold. We sought to maintain $Na_v1.7$ activity by still including the thiazole pharmacophore in generation II compounds. However, the thiazole group would be too polar to act as a hydrophobic group oriented into the MOR pocket. To have both the polar $Na_v1.7$ pharmacophore and a new hydrophobic functionality on the right side of the compounds, generation II compounds were designed with an additional lipophilic substituent (Figure 3.1). Several analogues of $Na_v1.7$ binding drugs also contain lipophilic portions that interact with other parts of the protein while the sulfonamide interacts with the VSD4, so introducing a large hydrophobic portion, shown in orange, was not expected to effect $Na_v1.7$ activity as long as the pharmacophore remained, shown in blue.

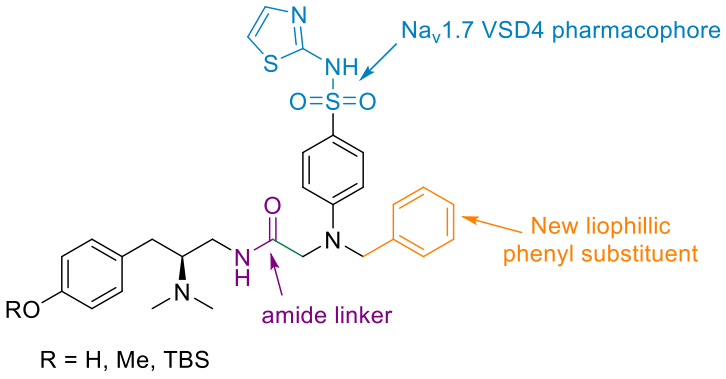

Figure 3.1: General scaffold for second generation of compounds

These compounds were very large and similar in molecular weight to known $Na_v1.7$ inhibitors (Figure 1.7), so although they would likely exhibit poor ADME profiles, the goal was to test how the activity would be affected by introducing a new side chain containing an aromatic ring. Not all compounds in SAR needed to be druggable compounds; the plan was to quickly

assemble compounds that would remain $Na_v1.7$ active to build our SAR, while restoring the MOR binding.

The goal of generation II compounds was to test the hypothesis regarding the preferred activity of PZM21 contributing to binding and activity. Introducing the unsubstituted benzyl ring shown in orange (Figure 3.1) could act like the thiophene sidechain in PZM21 (Figure 2.7) and contribute to anchoring the compound in the MOR pocket. Switching to an amide linker instead of the urea linker was also a new change. Recently published results from Medina *et al.* suggested that amide compounds related to PZM21 would be active at MOR. It was hypothesised that this change could reduce the rigidity of the compound and allow the right side to bend and adopt a similar conformation to PZM21. Although introducing sp^3 carbons would be optimal for flexibility, a nitrogen was selected for connecting the new benzyl ring A and aniline ring B. At this point in the SAR, this was selected for ease of synthesis, and it was not predicted to have a major effect on the rigidity of the compound.

3.2 Synthesis of Amide, Branched Linker, Aryl Sulfonamides - Generation II

The second generation of compounds containing two rings required an entirely new scaffold and design of new building blocks for the right-hand side pharmacophore. A retrosynthetic strategy is shown (Scheme 3.1) beginning with commercially available **2**.

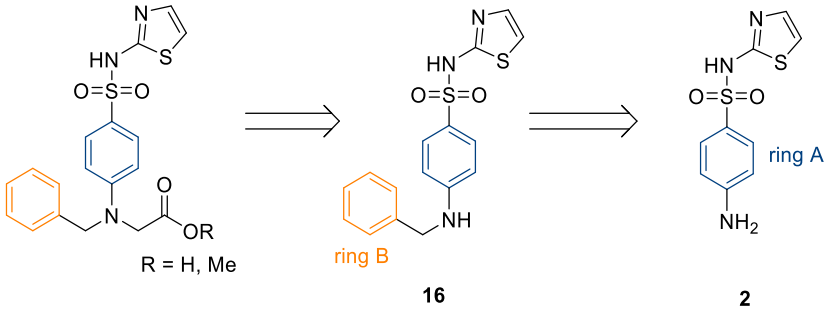

Scheme 3.1: Retrosynthesis of Generation II scaffold, Fragment B'

Addition of ring B was planned through reductive amination with the aniline **2**. This was unsuccessful and ultimately achieved over two steps instead. From amine **16** either a methyl ester or a carboxylic acid would be installed to couple with fragment A' (Scheme 2.10). Both esters and acids could be suitable substrates for nucleophilic addition or peptide coupling respectively with the MOR pharmacophore.

High expectations were set for the reductive amination of **2** with benzaldehyde following literature protocol for the identical substrate.[54] This procedure was attempted several times and adjusted in attempts to achieve success (Table 3.1).

*Table 3.1: Reductive amination attempts to form amide **16***

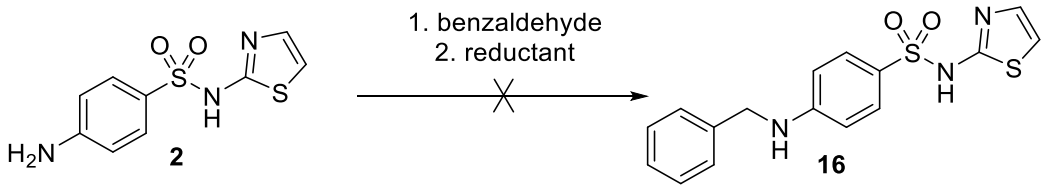

Entry	Time	Reductant	Solvent	Temp
1[a]	20 h	1.2 equiv $NaBH_4$	EtOH	100 °C
2[a]	16 h	1.2 equiv $NaBH_4$	TFE	
3[b]	16 h	2 equiv $NaBH_4$	EtOH	

*a: Conditions: 1. Benzaldehyde (1.7 equiv), amine **2** (1 equiv), 4 M in alcohol, 16-20 h, 100 °C. 2. $NaBH_4$ (1.2 equiv), 30 min, rt.*
*b: Conditions: 1. Benzaldehyde (1 equiv), amine **2** (1 equiv), 4 M in alcohol, 12-16 h, 100 °C. 2. $NaBH_4$ (1.2 equiv), 30 min, rt.*

Imine formation was monitored qualitatively by ^{1}H NMR to attempt to observe complete formation of imine intermediate before addition of the reducing agent. Various reducing agents were used as well, switching from the literature protocol using $NaBH_4$ to $NaBH_3CN$. After many attempts, reductive amination would not proceed as imine formation was never completed sufficiently, and no attempts were successful in obtaining amine product **16**. Attempts were also made to form amine **16** through an S_N2 reaction with benzyl bromide.[55,56]All attempts were unsuccessful (Table 3.2).

*Table 3.2: S_N2 attempts to form amine **16***

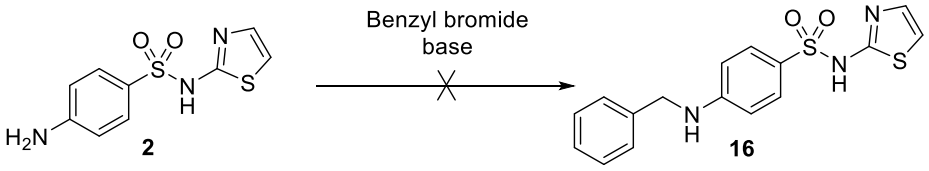

Entry	**Base**	**Solvents**	**Conditions**
1[a]	1.5 equiv K_2CO_3	MeCN	30 min, 120 °C
2[b]		DMF	18 hrs, 80 °C

*a: Conditions: Benzoyl bromide (1 equiv), amine **2** (3 equiv), K_2CO_3 (1.5 equiv), 0.5 M MeCN, 30 min, 120 °C. b: Conditions: Benzoyl bromide (1 equiv), amine **2** (1 equiv), K_2CO_3 (1.5 equiv), 0.3 M DMF, 18 h, 80 °C*

Instead, a two-step approach was used which involved first an acylation of **2** with benzoyl chloride to form amide **15**,[57,58] followed by reduction to amine **16** with $LiAlH_4$ (Scheme 3.2). These two steps proceeded with moderate yields but were still exciting after a time-consuming struggle with reductive amination.

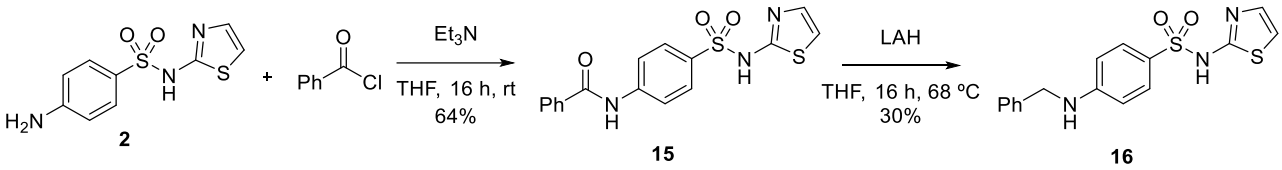

*Scheme 3.2: Reaction pathway to amine **16***

The amine **16** then was reacted with methyl-2-bromo acetate to form methyl ester **17** (Scheme 3.3). This reaction was first performed with K_2CO_3 as the base at 100 °C and proceeded with a poor yield of 21%.[56] It was optimized with to proceed faster through conditions B, with a simpler purification, and in a higher yield when using *N*,*N*-diisopropylethylamine as the base.[59]

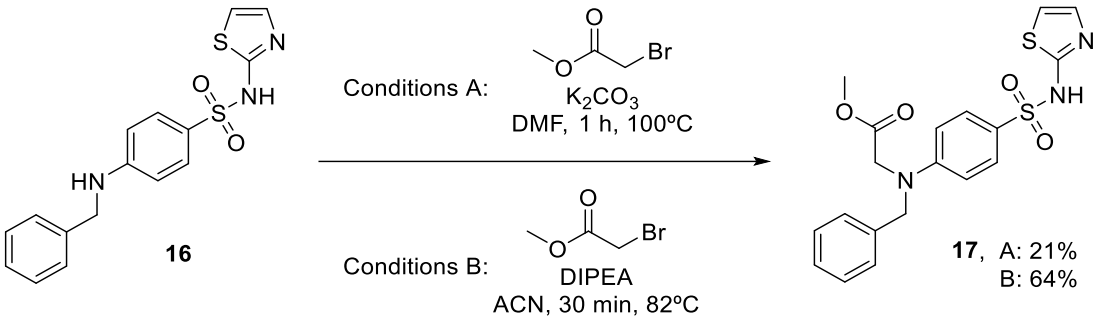

*Scheme 3.3: Synthesis of methyl ester **17***

With methyl ester **17** in hand and completion of fragment B', model reactions were pursued. Reacting **17** with model amines (Figure 3.2) would serve as excellent test reactions to investigate how fragment B' reacted with a basic, dimethyl amines and optimize conditions to employ with the complex diamine fragment A'.

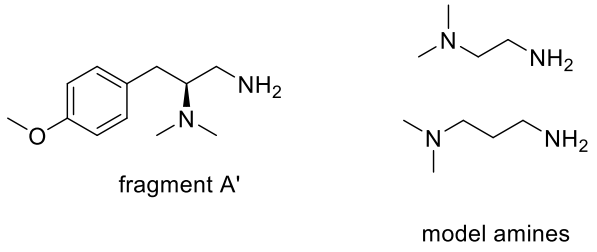

Figure 3.2: Amines selected for coupling with fragment B'

These reactions would help determine if adding an additional hydrolysis step to form carboxylic acids and attempt peptide coupling would necessary, or the methyl ester **17** was a suitable electrophile. *N*,*N*-dimethyl-ethylene diamine and 1-amino-3(dimethylamino)-propane were selected as the amines for model compounds **18a** and **18b** respectively (Scheme 3.4). These amines were readily available in laboratory inventory and although they lack the tyrosine scaffold, they contain a basic dimethyl amine present in the MOR pharmacophore. The dimethyl amine is the most crucial functionality for contact in the MOR binding pocket,[19] so both models would represent this pharmacophore and be testable compounds.

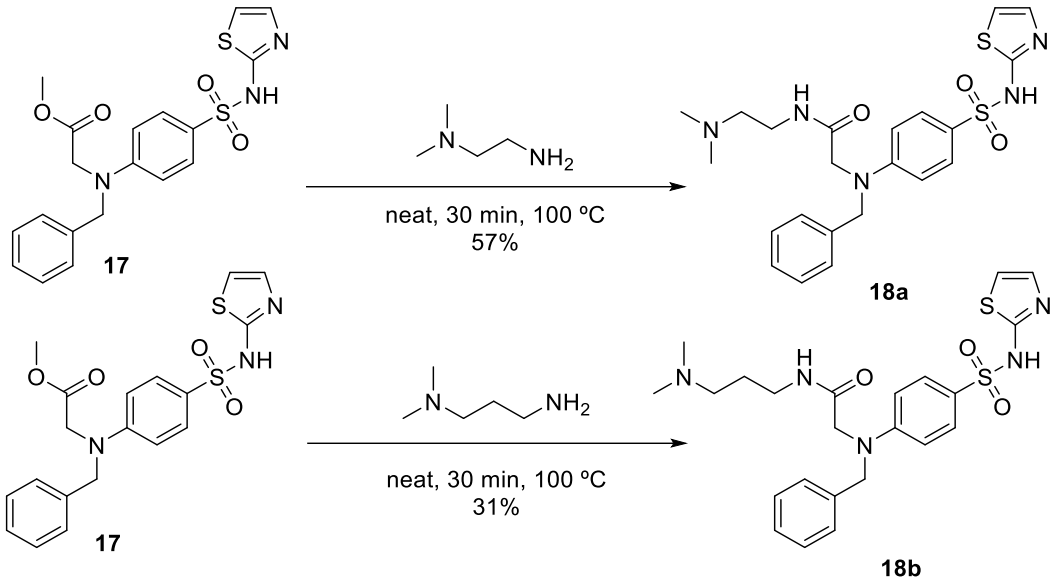

Scheme 3.4: Coupling conditions for generation II model compounds

Reactions were performed according to a literature protocol that contained nearly identical substrates and worked relatively well, in a 57% yield with *N*,*N*-dimethyl-ethylenediamine and 31% yield with 1-amino-3(dimethylamine)-propane (Scheme 3.4).[60] The conditions were solvent free, required amine in a large excess and a high temperature. This was possible as the amines were liquids and both available commercially, so it was not difficult to use them in large excess. Purification was also convenient with these model compounds, as the excess amine was water soluble and removed through liquid liquid extraction.

With these successes, it was clear the methyl ester **17** was a suitable electrophile for coupling with a dimethyl amine containing amine. Unfortunately, as fragment A' was not liquid, and not available in large enough quantities to be used in the same excess as the commercial amines, the protocol would need to be modified. First, other routes were investigated including a promising literature reaction using LiHMDS (Scheme 3.5) This reaction was unsuccessful, no reactivity was observed at all.[61] The LiHMDS failed to react with **17** and model amines as well.

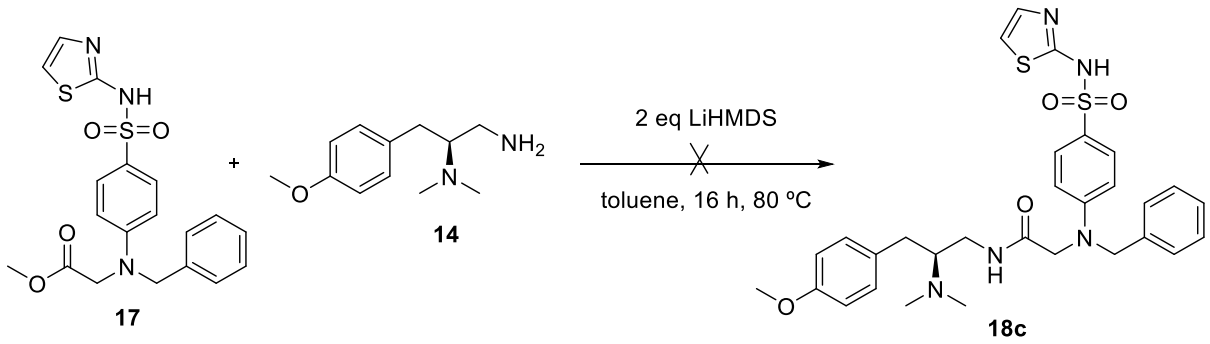

*Scheme 3.5: Failed LiHMDS reaction to form **18c***

Additionally, some trials were made to hydrolyze the methyl ester to the corresponding carboxylic acid, with plans to subject it to peptide coupling. Both LiOH and KOH were attempted (Table 3.3). Hydrolysis was unsuccessful as well, so it was decided to return to the original high temperature, neat conditions and perform the necessary modifications to work with the *O*-methyl amine.

Table 3.3: Failed hydrolysis attempts

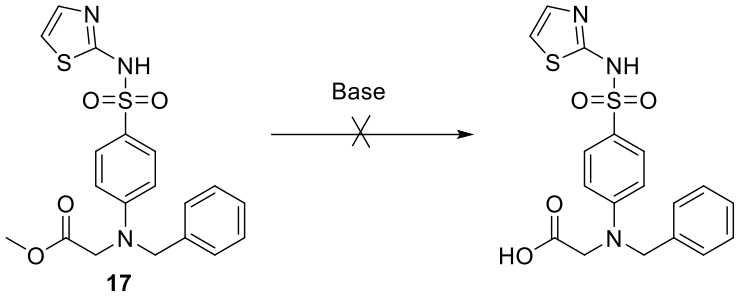

Entry	**Base**	**Solvent**	**Conditions**
1[a]	KOH	H_2O/*i*-PrOH	rt, 48 hrs
2[b]	10 equiv LiOH	H_2O/THF	rt, 16 hrs

a: Conditions: KOH (1 equiv), ester **17** (1 equiv), 0.8 M in 1.8:1 *i*-PrOH:H_2O, 48 h, rt. b: LiOH (10 equiv), ester 17 (1 equiv), 0.1M in THF, 16 h, rt.

When working with fragment A (Scheme 2.3) from generation I compounds, reaction temperature was a limiting factor because above 60 °C the TBS group was liable to cleavage,

making both reactivity and purification challenging. In the case of fragment A' (Scheme 2.10) cleavage of the O-C bond was not expected to be a concern, even at high temperatures. The thermal stability of fragment A' was evaluated to ensure high temperature reaction conditions would be compatible. The compound was heated both neat and in select solvents. DMF was tested for its assistance with solubility and success in other reactions involving the thiazole pharmacophore present in fragment B'. It was found that fragment A' was stable and showed no signs of degradation or *O*-Me cleavage when monitored by both TLC and NMR, up to 200 °C in all cases. With this in mind, the reaction between methyl ester **17** and amine **14** was performed as close to the neat, high temperature model conditions as possible - with only minimal DMF to aid in stirring at 150 °C (Scheme 3.6).

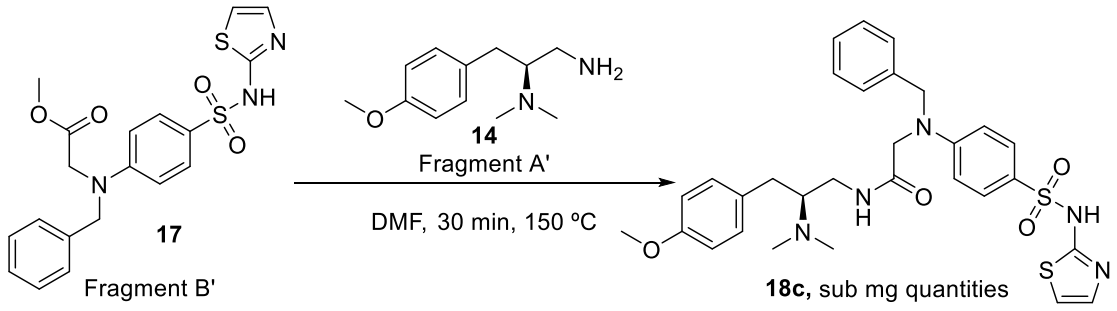

*Scheme 3.6: Coupling conditions for compound **18c***

Gratifyingly, coupling was successful and sub mg quantities were obtained for biological testing. The TLC showed minor impurities. Purification was very challenging and attempted through flash chromatography, extractions, and preparative TLC with no success. The crude ^{1}H NMR is shown (Figure 3.3) and shows a poor signal to noise ratio and some incorrect integrations, excess amine **15** appeared to be present in the ^{1}H NMR and TLC. Nevertheless, the ^{1}H NMR was not lacking any signals expected for **18c**, and a HRMS was also obtained ($[M + Na]^{+}$ Calcd for $C_{30}H_{35}N_5NaO_4S_2$: 616.2025; Found 616.2028). The compound was decided to be tested without

complete characterization with the understanding that if it was successful at activating MOR, it would be pursued again at a later time.

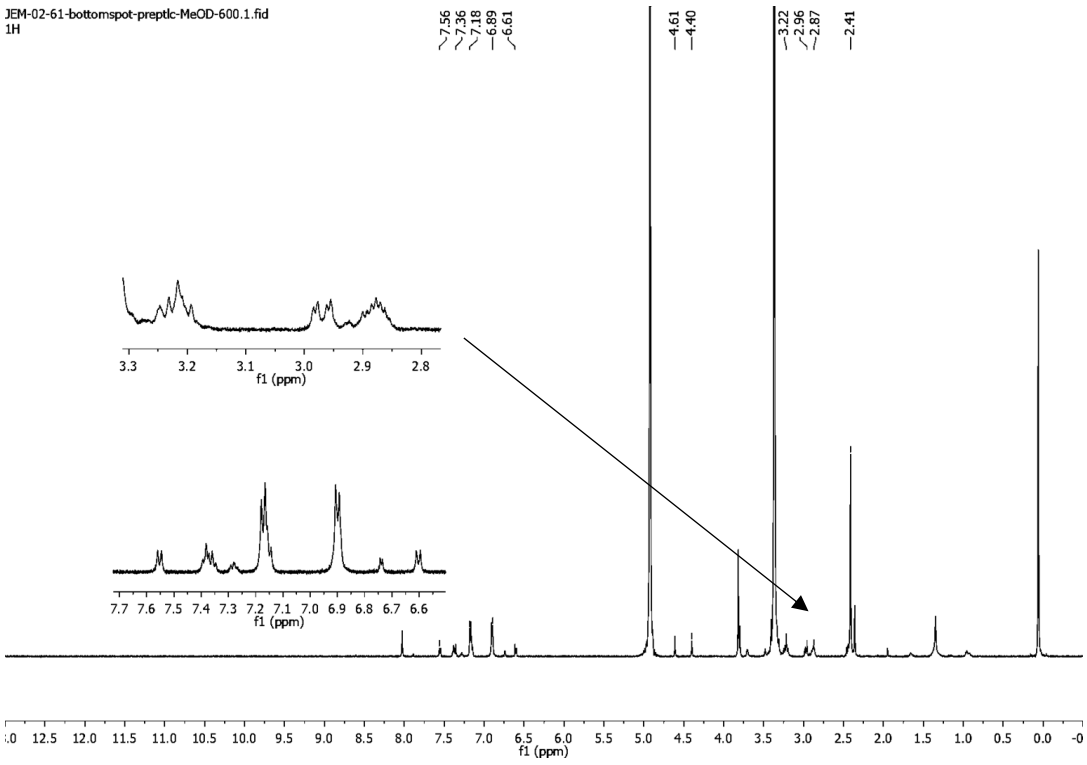

*Figure 3.3: crude ^{1}H NMR of **18c***

Figure 3.4 shows the second generation of compounds sent for testing. It was predicted that activity could be restored at MOR with all of these compounds due to the new scaffold. The lack of phenol OH in compounds **18c** and **19** was not predicted to eliminate MOR binding, potentially it would reduce binding affinity, but the combined presence of cationic amine with the new flexible scaffold could restore binding. Compounds **18a** and **18b** (Figure 3.4) were more difficult to predict, as they contained the basic amine but not the phenyl ring two to three carbons away (Figure 1.4) expected for MOR binding. It was expected that compounds **18a-c** would be active at $Na_v1.7$ containing the thiazole pharmacophore.

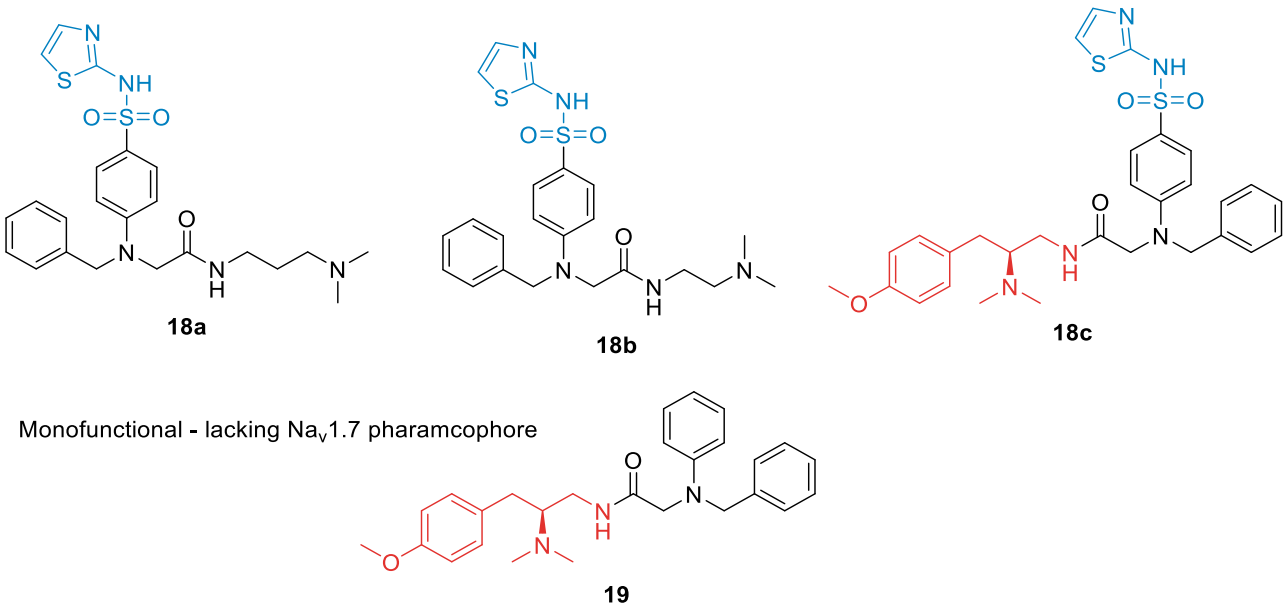

Figure 3.4: Generation II tested compounds

3.3 Results of Amide, Branched Linker, Aryl Sulfonamides – Generation II

Disappointingly, none of the compounds from Generation II (Figure 3.4) were active at either $Na_v1.7$ or MOR. This was frustrating, particularly for compounds **18a** and **18b** which contained the $Na_v1.7$ pharmacophore and had similar size and electronics to known $Na_v1.7$ VSD4 blockers. These results further supported the hypothesis that changes to the entire scaffold can affect orientation and binding, despite still containing identical active pharmacophores.

Lack of MOR activity for compounds **18c** and **19** (Figure 3.4) was also frustrating, as this new scaffold introduced flexibility and lipophilicity predicted to restore MOR activity. Not enough information was available to determine if size, orientation, or electronic effects were why these compounds were not binding to MOR. One hypothesis is that even though the benzyl ring was introduced and *could be* oriented into the hydrophobic pocket of MOR, without the appropriate conformational effects associated with the use of a stereocenter as there is in PZM21, the affinity could be significantly reduced (Figure 3.5). Without known stereochemistry and lack of crystal

structures of our synthesized compounds, limited by NMR alone and physical molecular models it is challenging to really confirm the orientation of the benzyl ring and that it acts in the same fashion as the thiophene in PZM21.

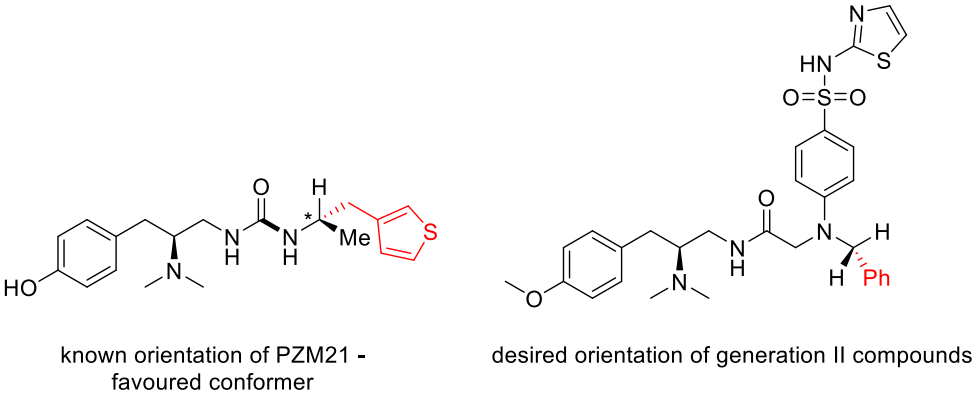

Figure 3.5: Proposed binding orientation of Generation II compounds, compared to known orientation of PZM21

With these conclusions, it was decided to focus on restoring MOR activity as this was the main challenge and a major roadblock in the project. To do this, focus was set on designing *monofunctional compounds* with a scaffold that contained a stereocenter or a simpler, flexible chain with more than one sp^3 carbon linker, closer to PZM21 and other derivatives possessing MOR activity.

3.4 Return to a Linear Scaffold – Generation III

With this in mind, a new series of compounds were designed with a more linear scaffold and an amide linker. New publications on PZM21 analogues **20**, **21** and **22** showed MOR active compounds with a linear scaffold.[62,63] Inspiration was drawn from these compounds (Figure 3.6) for a third generation. With this new and simple linear scaffold, it was hypothesized that MOR activity could be regained.

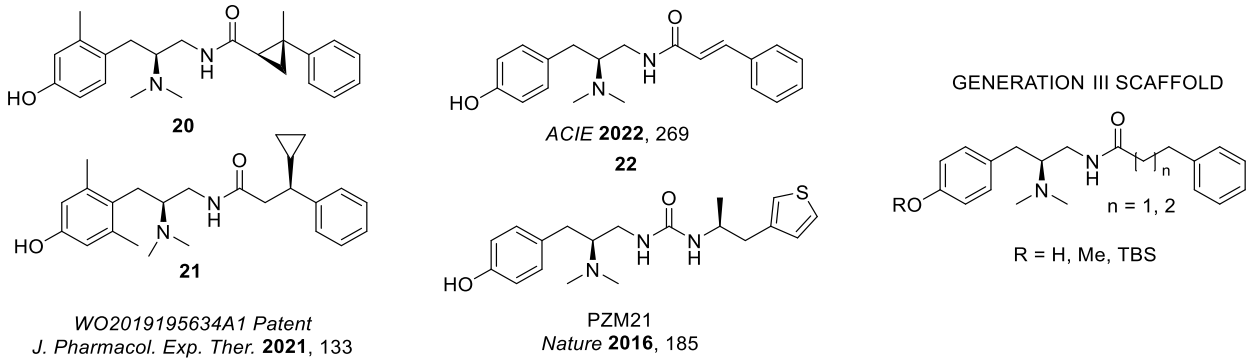

Figure 3.6: Structures of recently published MOR active compounds inspiring the design of Generation III

The OMe, OTBS and OH varieties were planned for synthesis, with hopes that any of the three options would restore MOR activity. Synthesizing and testing all three analogs could confirm that the OH phenol interaction is not essential, and the orientation of the hydrophobic right side is what is crucial in order to gain MOR activity. Two different carbon linkers were selected in order to see how much variability in the length of the chain could be tolerated. This would be valuable information at later stages in the SAR when it was time to re-introduce the $Na_v1.7$ pharmacophore and compounds would require a linear linker.

3.5 Synthesis of Amide Linked Linear Scaffold – Generation III

Generation III synthesis was relatively straightforward, as the major building block for the MOR pharmacophore was already well established (Scheme 2.3, Scheme 2.10). The choice became how to join fragment A or A' to the corresponding right side. Two options arose: addition to an acyl chloride or a peptide coupling through a carboxylic acid. The goal was to assemble the compounds as quickly as possible, as with the recently published cryoEM image of MOR bound to PZM21 and related MOR active compounds from recent publications, it was highly probable these compounds would be active at MOR,[64] so both routes were pursued simultaneously. Compounds with fragment A' **14** were made first, as this left side coupling partner had been the most robust because deprotection was not a risk, easing in purification.

Acyl chloride addition to **14** was efficient with 3-phenyl propionyl chloride (Scheme 3.7). This compound was synthesized and purified through liquid-liquid extraction only, quickly affording **23a** in an 86% yield.

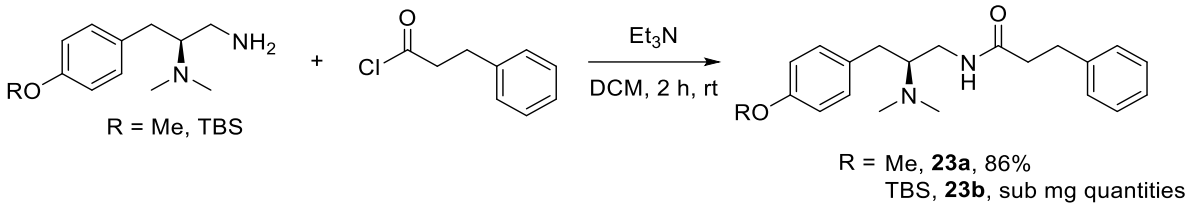

*Scheme 3.7: Synthesis of compound **23a***

As for the reaction with the three-carbon linker, the acid chloride was not available and instead the carboxylic acid was used. A peptide coupling reaction was used that had been previously optimized by Mr. Sherif Meshref with similar substrates. HATU was used as the coupling reagent (Scheme 3.8), and purification of the desired product from the HATU coupling by-product was achieved with little difficulty through column chromatography due to the drastic polarity differences.

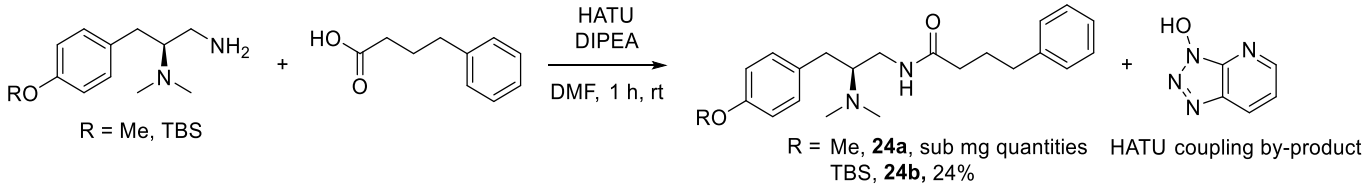

*Scheme 3.8: Peptide coupling conditions for compounds **24a** and **24b***

Compounds containing fragment A were synthesized next using the same reaction conditions. Acid chloride addition with 3-phenyl propionyl chloride (Scheme 3.7) was used for **23b** and peptide coupling with 4-pheynyl butyric acid (Scheme 3.8) for **24b**. Similar to compound **18c** (Figure 3.4), compound **23b** was obtained in sub mg quantities for biological testing. TLC showed minor impurities present, and a HRMS was obtained ($[M + Na]^+$ Calcd for $C_{26}H_{41}N_2O_2Si$:

441.2937; Found 441.2940) of the crude sample. Purification failed repeatedly through flash chromatography, so the compound was tested without complete characterization or further purification, with the understanding it would be revisited if successful. The crude ^{1}H NMR is shown (Figure 3.7) and shows a poor signal to noise ratio, but no peaks are absent for the compound **23b.**

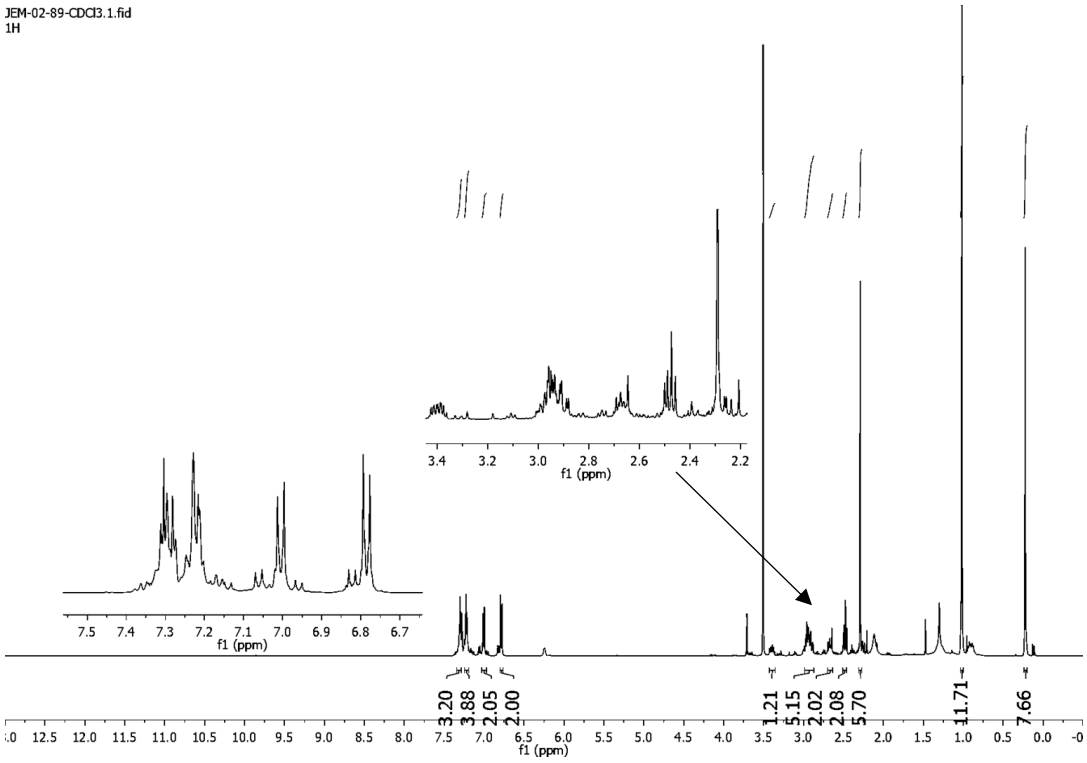

*Figure 3.7: crude ^{1}H NMR of **23b***

HF Deprotection of compounds **23b** and **24b** was attempted, but not completed due to limited amount of compounds and time constraints. Deprotection of *O*-Me compounds **23a** and **24a** were attempted through BBr_3 mediated pathways but were all unsuccessful (Table 3.4).[65,66] Even using a large excess of BBr_3, the *O*-Me bond would not break, and all resulting reaction crude mixtures still contained the *O*-Me intact when observed by ^{1}H NMR.

Table 3.4: Failed BBr_3 mediated deprotection

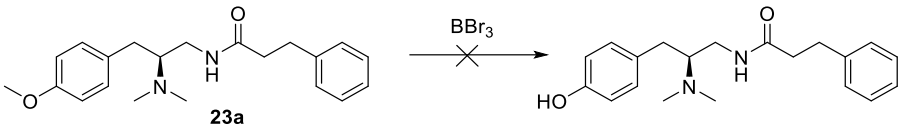

Entry	Equiv of BBr_3	Solvent	Conditions[a]
1	1.1	DCM	0 °C to rt, 3 h
2	10		

a. Conditions: BBr3 (1.1-10equiv), 23a (1equiv), 0.2 M in DCM, inert atmosphere, 3 h, 0 ℃ to rt.

Additionally, an L-Selectride mediated deprotection was attempted. This unusual deprotection strategy was inspired by a literature example on a morphine derivative where one of two *O*-Me groups was transformed to an OH (Scheme 3.9). [45] These conditions also proved unsuccessful on compound **24a**. Even after short reaction times, the conditions destroyed the molecule, and the resulting crude was too difficult to identify or purify the desired product.

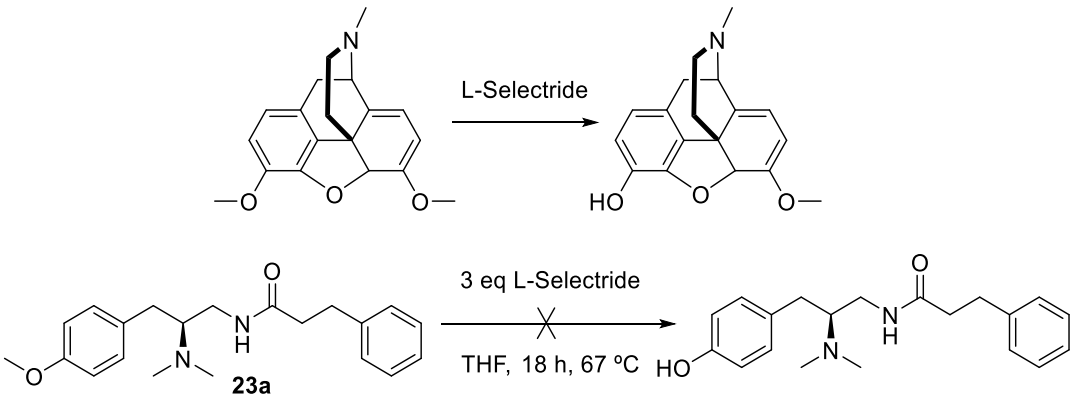

Scheme 3.9: Failed L-Selectride deprotection

A colleague Mr. Sherif Meshref prepared compounds **25a** and **25b**, which contained the same scaffold but an oxygen atom in the linker (Figure 3.8). These compounds would determine the requirements of the linker and probe whether carbons or heteroatoms were better tolerated.

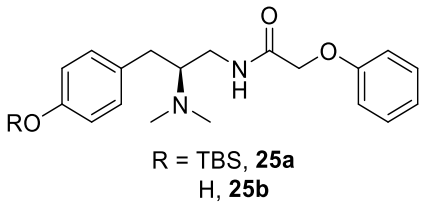

Figure 3.8: Heteroatom linked generation III compounds

Six compounds (Figure 3.9) were sent for testing, with high expectations for activity at MOR. Unlike Generation I and II, these compounds were not tested at $Na_v1.7$ as they lacked the aryl sulfonamide pharmacophore and were not predicted to be active.

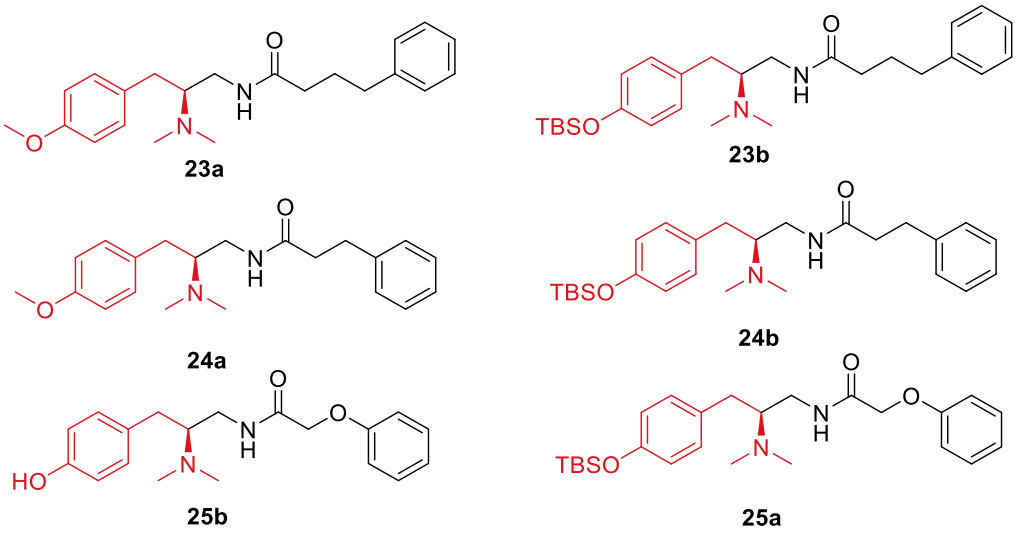

Figure 3.9: Generation III compounds sent for testing

3.6 Results of Amide Linked Linear Scaffold – Generation III

The results of Generation III compounds were very exciting as both the two and three carbon linker compounds **23a** and **24a (**Figure 3.9**)** were active at MOR with an IC_{50} of 2.42 x 10^{-7} M and 6.02 x 10^{-8} M, respectively, similar in affinity to PZM21 with an IC_{50} of 1.05 x 10^{-8} M. These results are illustrated in a graph prepared by Dr. Patrick Giguère in Figure 3.10. cAMP production is associated with activation of the G_i/G_o pathway when ligands bind to and stimulate the MOR. Compounds **23a** and **24a** both show similar efficacy to that of PMZ21, a partial agonist

at MOR. Compound **23a** has a slightly higher potency observed in the left shift of the curve. Compound **25b** containing an oxygen in the linker shows a small amount of potency seen in the inflection of the curve, but cAMP inhibition is still observed correlating with poor efficacy.

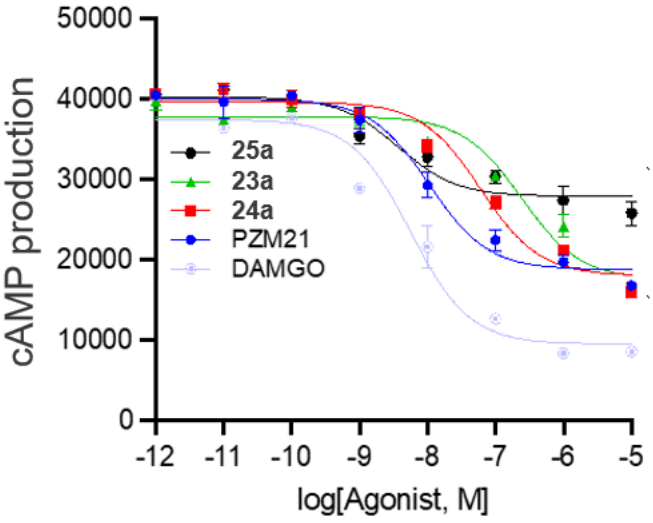

Compound	Log(IC_{50})	IC_{50} (M)	SEM
25a	-3.342	3.691×10^{-9}	0.080
23a	-2.657	2.416×10^{-7}	0.123
24a	-2.694	6.024×10^{-8}	0.096
PZM21	-3.452	1.052×10^{-8}	0.080
DAMGO	-3.158	5.619×10^{-9}	0.103

Figure 3.10: Results of select compounds from generation III illustrating cAMP production associated with G_i/G_o signalling by MOR. PZM21(partial MOR agonist) and DAMGO (full MOR agonist) are both positive controls.

For the first time on the project, compounds were showing binding affinity at the MOR. Compounds bearing the free OH were not synthesized at this time due to time constraints but will be synthesized and tested in the future. Activity is anticipated at potentially an even higher binding affinity than the *O*-methyl compounds as the hydrogen bond donating properties of the phenol would enhance the water bridge formed in the binding pocket.[19] Activity for **23a** and **24a** (Figure 3.9) with the *O*-methyl support the hypothesis that a phenol at this position is only an

intermediately important contact in the MOR pocket. Lack of activity for TBS bearing compounds **23b** and **24b** (Figure 3.9) was interesting, and potentially a consequence of too high of lipophilicity on the left side of the molecules. Further investigations on the left side of compounds are required to understand the impact of this fragment. Some changes made to add to future SAR could include fluorinating the ring or switching from a tyrosine to a naphthyl or tryptophan scaffold (Figure 3.11).

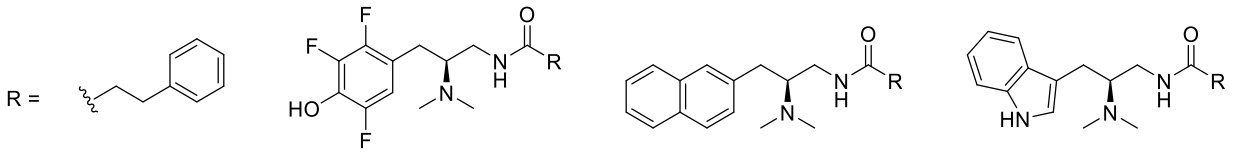

Figure 3.11: Potential fragment A scaffold changes to probe the effects of lipophilicity on the left side of compounds

Compounds **25a** and **25b** (Figure 3.9) showed little to not binding affinity at MOR, (Fig 3.10) indicating that a heteroatom in the linker was not well tolerated, even when reintroducing the phenol OH. Compound **25a** does not display significant cAMP inhibition. It is hypothesized that this oxygen effects the orientation of compounds differently than carbon. As was observed with previous compounds and considering the orientation hypothesis (Scheme 2.13), MOR binding is very sensitive to the orientation of the compound interacting in the receptors orthosteric pocket, both the lipophilicity and orientation need to be considered. These exciting results provide a better understanding of the way compounds bind and what kind of functionalities and linkers can allow compounds to adopt an orientation that is well tolerated in the MOR pocket.

With these results in hand, compounds both binding to the VSD4 of $Na_v1.7$ and the orthosteric pocket of MOR have been achieved. The information from both active and inactive compounds can be used to predict with a much clearer picture what future SAR decisions result in

binding at both receptors. Each tested compound gets one step closer to the ultimate goal of creating a bifunctional compound in the pain network.

Chapter 4: Conclusions and SAR insight

4.1 Hypothesized Requirements for Each Pharmacophore – Hopes for Bifunctional Binding

Even with the encouraging results from Generation I and Generation III compounds, bifunctional binding has not yet been achieved. Despite this, as more compounds are tested and results obtained, a better picture of how compounds bind and what functionalities and orientations are permissible at each receptor emerged. A deeper understanding of binding at each pharmacophore allows SAR decisions to be made with more confidence and results in a higher chance of achieving an active bifunctional compound in the future.

Over the course of the project, 12 compounds have been tested for activity at $Na_v1.7$ and two were capable of $Na_v1.7$ blocking through the VSD4. A summary of relevant compounds and results at $Na_v1.7$ is shown (Figure 4.1). Based on the available results from tested compounds, it is confirmed that aryl sulfonamides **6a** and **7a** interact with the VSD4, as expected when comparing to literature compounds (Figure 1.7). Active compounds contained a urea linker, a linear scaffold, a TBS functionality on the left side of the molecule. The most rigid and linear compounds had highest success binding.

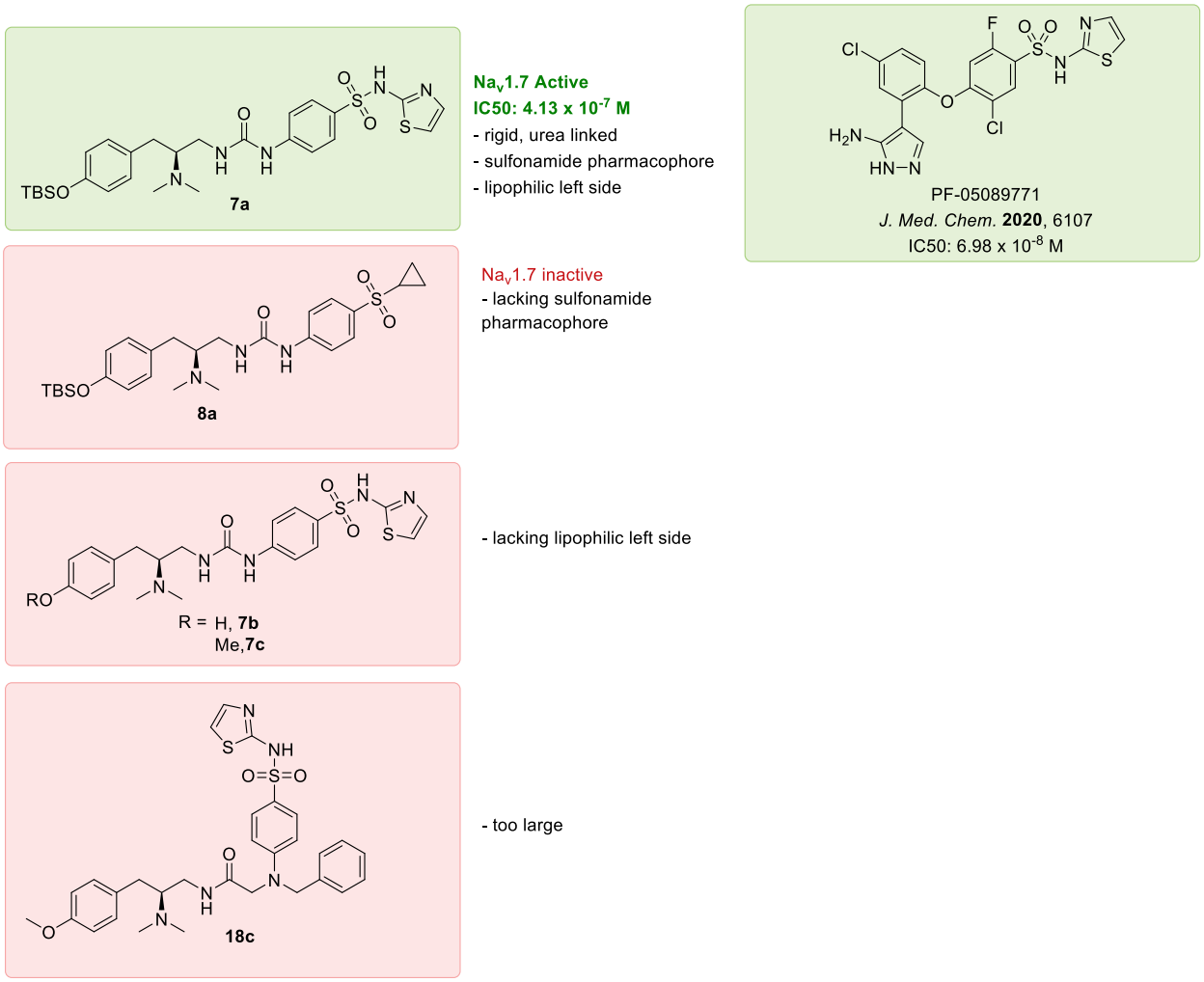

Figure 4.1: Na$_v$ binding summary

As for MOR, 21 compounds were tested for agonist activity and two were active. The relevant compounds are shown (Figure 4.2). Compounds **23a** and **24a** with a flexible linear scaffold and an amide linker were successful for binding. Contrary to Na$_v$1.7, a TBS functionality prevented activity and rigid structures with urea linkers or heteroatoms in the chain were not favourable either.

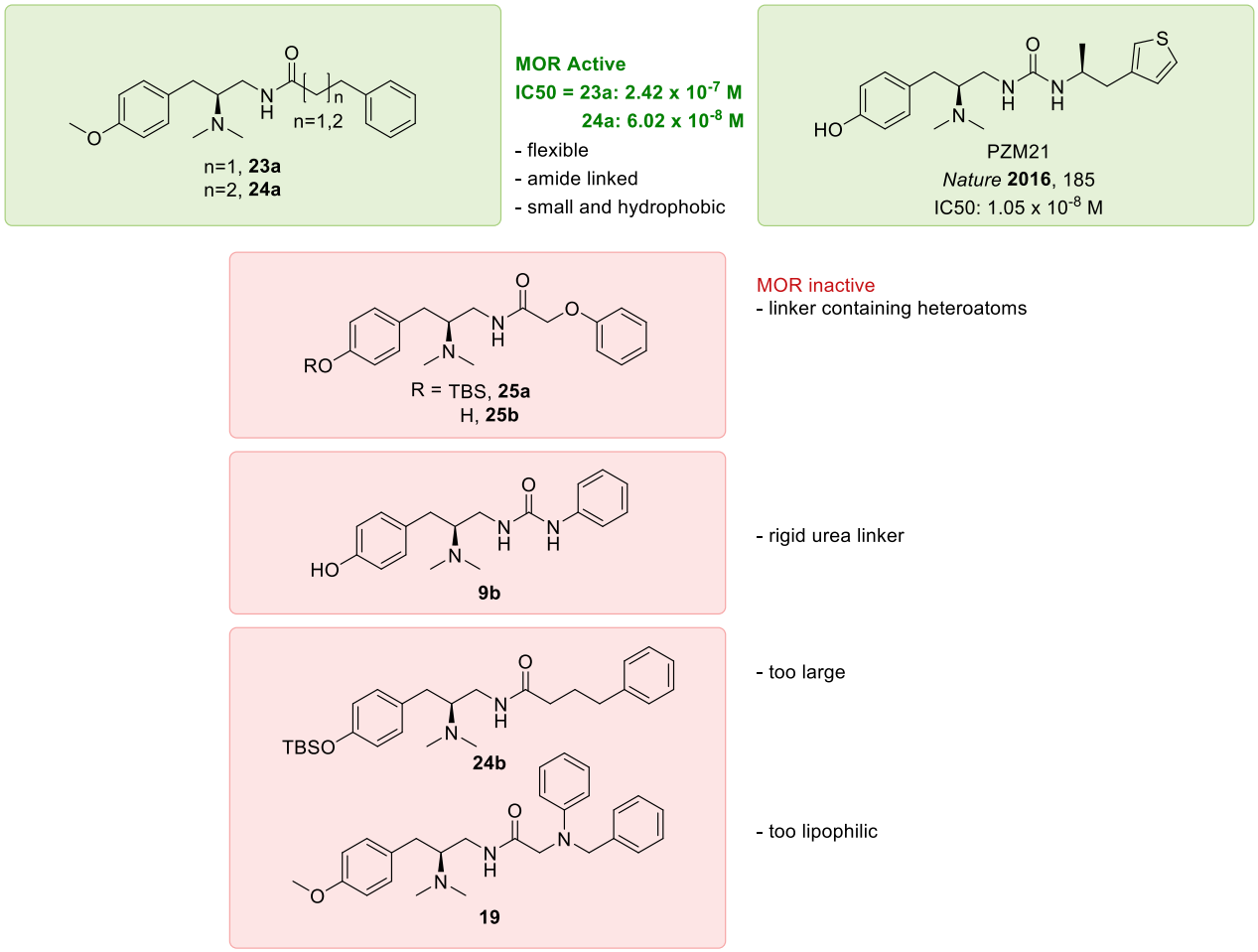

Figure 4.2: MOR binding summary

From these results, it is hypothesized that the orientation of a ligand as it interacts with the MOR pocket is exceptionally important for biological activity. It is suspected that in order to successfully bind, compounds require a flexible linker made of sp^3 carbons so the molecule can bend into an orientation well fitted for the MOR pocket. As for $Na_v1.7$, rigid heteroatom-rich molecules bind and interact with VSD4, that include the heterocyclic sulfonamide pharmacophore. This makes design very challenging, because the binding requirements at each pharmacophore are very different and few functionalities complement each other. A compound must have both properties in order to be successful at achieving a bifunctional binding.

4.2 Future Targets

The compounds shown in Figure 4.3 are the future targets of the project that aim to achieve bifunctional binding. Compounds **26** and **27** are expected to be bifunctional. Fluorination on the ring in compound **26** will contribute to increased lipophilicity. Compound **28** would be a monofunctional test compound and would probe the effect of a stereocenter at the β position. It contains a *R*-Bn at the same position as the *R*-methyl group in PZM21 that contributes to orienting the compound to fit into the MOR binding pocket. The effect of the phenol substituent still remains unclear, and the OH, OTBS and OMe compounds are all still valuable to the SAR at this point. Incorporating larger, lipophilic variations to the left side (Figure 3.11) are also potential targets. OTBS compounds would be expected to be active at Na_v, and *O*-Me and OH analogues at MOR. However, changing the lipophilicity of the molecule overall by fluorinating the ring, or changing the orientation by introducing an oxygen in the linker could affect this prediction.

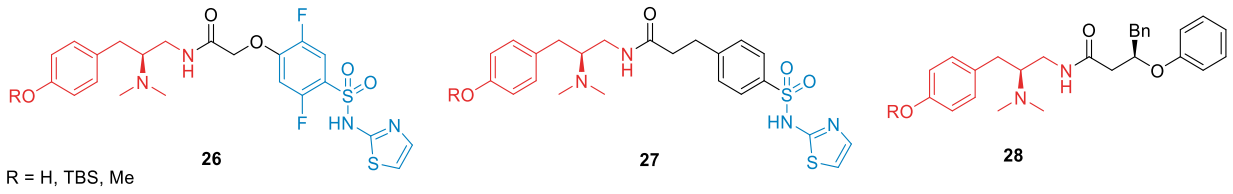

Figure 4.3: Future targets

Only potency has been investigated through IC_{50} values of active compounds. The overall goal at this point in time is to establish a large SAR library of active compounds and continue to work towards bifunctional binding. In the future, other properties such as efficacy and binding affinity through measurements such as K_i values may be investigated.

4.3 Conclusion

The results from this work significantly contributed to the overall goals of the project and have brought new insights into the binding functionalities of $Na_v1.7$ and MOR. In total, 21

compounds were designed, synthesized, characterized and tested over the course of the past three years of the project, 12 of which were synthesized by myself, independently in this thesis.

Through the first generation of compounds (Figure 2.3), it was confirmed that an aryl sulfonamide was required for sufficient binding at $Na_v1.7$. The thiazole moiety in compound **6a** was more potent than the pyrimidine in **7a** and selected as the $Na_v1.7$ VSD4 pharmacophore for future compounds. It was also understood that a rigid structure was not sufficient for MOR binding, even with the crucial cationic dimethyl ammonium salt. Compounds that contained a urea linker were likely too rigid (Scheme 2.13) and required more flexibility to allow compounds to adopt a conformation suitable for the MOR binding pocket. At the phenol position, an anisole is tolerated but an OTBS is not for $Na_v1.7$ binding. Questions about the lipophilicity on the left side of the compounds remain unanswered but plans to change the scaffold (Figure 3.11) will probe this in future SAR rounds.

In Generation II, more flexible compounds containing two rings and an amide linker (Figure 3.4) failed to restore activity at MOR and eliminated activity at $Na_v1.7$. With these results, monofunctional compounds were targeted in Generation III (Figure 3.9) in hopes of restoring MOR binding. This was successfully accomplished through linear compounds with longer amide linkers lacking heteroatoms, much closer in structure to PZM21 and recently published analogues (Figure 3.6). [62,63]

Although no bifunctional compounds have been completed, the knowledge gained to better predict binding at both MOR and $Na_v1.7$ will continue to guide thoughtful SAR, staying true to the original structure-based drug design strategy. Identifying a pharmacophore is challenging, but it is even more difficult to refine SAR and solve the challenges encountered when unexpected results arise from testing new compounds. By achieving binding at both MOR and $Na_v1.7$,

significant progress has been made towards designing a bifunctional ligand through the efforts presented in this thesis. The information gained has laid the groundwork for future students to continue SAR with the ultimate goal of contributing to the design of new, safer analgesics to treat chronic pain.

References

(1) Huggins, D. J.; Sherman, W.; Tidor, B. Rational Approaches to Improving Selectivity in Drug Design. *J. Med. Chem.* **2012**, *55*, 1424.

(2) Corson, T. W.; Aberle, N.; Crews, C. M. Design and Applications of Bifunctional Small Molecules: Why Two Heads Are Better than One. *ACS Chem. Biol.* **2008**, *3*, 677.

(3) Masnoon, N.; Shakib, S.; Kalisch-Ellett, L.; Caughey, G. E. What Is Polypharmacy? A Systematic Review of Definitions. *BMC Geriatr.* **2017**, *17*, 230.

(4) Matos, A.; Bankes, D. L.; Bain, K. T.; Ballinghoff, T.; Turgeon, J. Opioids, Polypharmacy, and Drug Interactions: A Technological Paradigm Shift Is Needed to Ameliorate the Ongoing Opioid Epidemic. *Pharmacy* **2020**, *8*, 154.

(5) Zawilska, J. B.; Wojcieszak, J.; Olejniczak, A. B. Prodrugs: A Challenge for the Drug Development. *Pharmacol. Rep.* **2013**, *65*, 1.

(6) Schiller, P. W. Bi- or Multifunctional Opioid Peptide Drugs. *Life Sci.* **2010**, *86*, 598.

(7) Ding, H.; Kiguchi, N.; Yasuda, D.; Daga, P. R.; Polgar, W. E.; Lu, J. J.; Czoty, P. W.; Kishioka, S.; Zaveri, N. T.; Ko, M.-C. A Bifunctional Nociception and Mu Opioid Receptor Agonist Is Analgesic without Opioid Side Effects in Nonhuman Primates. *Sci. Transl. Med.* **2018**, *10*, 3483.

(8) Cunningham, C. W.; Elballa, W. M.; Vold, S. U. Bifunctional Opioid Receptor Ligands as Novel Analgesics. *Neuropharmacology* **2019**, *151*, 195.

(9) Gao, M.; Zhang, Y.; Wang, B.; Guo, N.; Shao, L.; Zhai, W.; Jiang, L.; Wang, Q.; Qian, H.; Yan, L. Novel Dual-Target M-opioid and TRPV1 Ligands as Potential Pharmacotherapeutics for Pain Management. *Bioorg. Chem.* **2023**, *131*, 106335.

(10) Lane, J. R.; Sexton, P. M.; Christopoulos, A. Bridging the Gap: Bitopic Ligands of G-Protein-Coupled Receptors. *Trends Pharmacol. Sci.* **2013**, *34*, 59.

(11) Fronik, P.; Gaiser, B. I.; Sejer Pedersen, D. Bitopic Ligands and Metastable Binding Sites: Opportunities for G Protein-Coupled Receptor (GPCR) Medicinal Chemistry. *J. Med. Chem.* **2017**, *60*, 4126.

(12) Kamal, M.; Jockers, R. Bitopic Ligands: All-in-One Orthosteric and Allosteric. *Biol. Rep.* **2009**, *10*, 77.

(13) Frimurer, T. M.; Peters, G. H.; Iversen, L. F.; Andersen, H. S.; Møller, N. P. H.; Olsen, O. H. Ligand-Induced Conformational Changes: Improved Predictions of Ligand Binding Conformations and Affinities. *Biophys. J.* **2003**, *84*, 2273.

(14) Bérubé, G. An Overview of Molecular Hybrids in Drug Discovery. *Expert Opin. Drug Discov.* **2016**, *11*, 281.

(15) *Statistics Canada*. https://www.statcan.gc.ca/en/start (accessed 2023-05-31).

(16) Volkow, N. D.; McLellan, A. T. Opioid Abuse in Chronic Pain — Misconceptions and Mitigation Strategies. *N. Engl. J. Med.* **2016**, *374*, 1253.

(17) Neto, J. A.; Costanzini, A.; De Giorgio, R.; Lambert, D. G.; Ruzza, C.; Calò, G. Biased versus Partial Agonism in the Search for Safer Opioid Analgesics. *Molecules* **2020**, *24*, 259.

(18) Przewłocki, R.; Przewłocka, B. Opioids in Chronic Pain. *Eur. J. Pharmacol.* **2001**, *429*, 79.

(19) Manglik, A.; Lin, H.; Aryal, D. K.; McCorvy, J. D.; Dengler, D.; Corder, G.; Levit, A.; Kling, R. C.; Bernat, V.; Hübner, H.; Huang, X. P.; Sassano, M. F.; Giguère, P. M.; Löber, S.; Duan, D.; Scherrer, G.; Kobilka, B. K.; Gmeiner, P.; Roth, B. L.; Shoichet, B. K. Structure-Based Discovery of Opioid Analgesics with Reduced Side Effects. *Nature* **2016**, *537*, 185.

(20) Melchior, C.; Desprez, C.; Wuestenberghs, F.; Leroi, A. M.; Lemaire, A.; Goucerol, G. Impact of Opioid Consumption in Patients With Functional Gastrointestinal Disorders. *Front. Pharmacol.* **2020**, *11*, 596467.

(21) Rosenbaum, D. M.; Rasmussen, S. G. F.; Kobilka, B. K. The Structure and Function of G-Protein-Coupled Receptors. *Nature* **2009**, *459*, 356.

(22) Law, P.-Y.; Wong, Y. H.; Loh, H. H. MOLECULAR MECHANISMS AND REGULATION OF OPIOID RECEPTOR SIGNALING. *Annu. Rev. Pharmacol. Toxicol.* **2000**, *40*, 389.

(23) Valentino, R. J.; Volkow, N. D. Untangling the Complexity of Opioid Receptor Function. *Neuropsychopharmacology* **2018**, *43*, 2514.

(24) Zádor, F.; Király, K.; Essmat, N.; Al-Khrasani, M. Recent Molecular Insights into Agonist-Specific Binding to the Mu-Opioid Receptor. *Front. Mol. Biosci.* **2022**, *9*, 900547.

(25) Pasternak, G. W. Opioids and Their Receptors: Are We There Yet? *Neuropharmacology* **2014**, *76*, 198.

(26) Pathan, H.; Williams, J. Basic Opioid Pharmacology: An Update. *Br. J. Pain.* **2012**, *6*, 11.

(27) Cunningham, C. W.; Elballa, W. M.; Vold, S. U. Bifunctional Opioid Receptor Ligands as Novel Analgesics. *Neuropharmacology* **2019**, 151, 195.

(28) Perrey, D.; Zhang, D.; Nguyen, T.; Carroll, F. I.; Ko, M. C.; Zhang, Y. Synthesis of Enantiopure PZM21: A Biased Agonist of the Mu-Opioid Receptor. *Eur. J. Org. Chem.* **2018**, *2018*, 4006.

(29) Schneider, S.; Provasi, D.; Filizola, M. How Oliceridine (TRV-130) Binds and Stabilizes a μ-Opioid Receptor Conformational State That Selectively Triggers G Protein Signaling Pathways. *Biochemistry* **2016**, *55*, 6456.

(30) Fox, S. I. *Human Physiology*; 2016; Vol. 14.

(31) Sheets, M. F.; Kyle, J. W.; Kallen, R. G.; Hanck, D. A. The Na Channel Voltage Sensor Associated with Inactivation Is Localized to the External Charged Residues of Domain IV, S4. *Biophys. J.* **1999**, *77*, 747.

(32) Ramdas, V.; Talwar, R.; Kanoje, V.; Loriya, R. M.; Banerjee, M.; Patil, P.; Joshi, A. A.; Datrange, L.; Das, A. K.; Walke, D. S.; Kalhapure, V.; Khan, T.; Gote, G.; Dhayagude, U.; Deshpande, S.; Shaikh, J.; Chaure, G.; Pal, R. R.; Parkale, S.; Suravase, S.; Bhoskar, S.; Gupta, R. V.; Kalia, A.; Yeshodharan, R.; Azhar, M.; Daler, J.; Mali, V.; Sharma, G.; Kishore, A.; Vyawahare, R.; Agarwal, G.; Pareek, H.; Budhe, S.; Nayak, A.; Warude, D.; Gupta, P. K.; Joshi, P.; Joshi, S.; Darekar, S.; Pandey, D.; Wagh, A.; Nigade, P. B.;

Mehta, M.; Patil, V.; Modi, D.; Pawar, S.; Verma, M.; Singh, M.; Das, S.; Gundu, J.; Nemmani, K.; Bock, M. G.; Sharma, S.; Bakhle, D.; Kamboj, R. K.; Palle, V. P. Discovery of Potent, Selective, and State-Dependent NaV1.7 Inhibitors with Robust Oral Efficacy in Pain Models: Structure-Activity Relationship and Optimization of Chroman and Indane Aryl Sulfonamides. *J. Med. Chem.* **2020**, *63*, 6107.

(33) Kong, X.; Yinping, L.; Perez-Miller, S.; Luo, G.; Liao, G.; Wu, X.; Liang, S.; Tang, C.; Khanna, R.; Lui, Z. The Small Molecule Compound C65780 Alleviates Pain by Stabilizing Voltage-Gated Sodium Channels in the Inactivated and Slow-Recovering State. *Neuropharmacology* **2022**, *212*, 109057.

(34) Ahuja, S.; Mukund, S.; Deng, L.; Khakh, K.; Chang, E.; Ho, H.; Shriver, S.; Young, C.; Lin, S.; Johnson, J. P.; Wu, P.; Li, J.; Coons, M.; Tam, C.; Brillantes, B.; Sampang, H.; Mortara, K.; Bowman, K. K.; Clark, K. R.; Estevez, A.; Xie, Z.; Verschoof, H.; Grimwood, M.; Dehnhardt, C.; Andrez, J. C.; Focken, T.; Sutherlin, D. P.; Safina, B. S.; Starovasnik, M. A.; Ortwine, D. F.; Franke, Y.; Cohen, C. J.; Hackos, D. H.; Koth, C. M.; Payandeh, J. Structural Basis of Nav1.7 Inhibition by an Isoform-Selective Small-Molecule Antagonist. *Science (1979)* **2015**, *350*, 1491.

(35) Bagal, S. K.; Marron, B. E.; Owen, R. M.; Storer, R. I.; Swain, N. A. Voltage Gated Sodium Channels as Drug Discovery Targets. *Channels (Austin)* **2015**, *9*, 360.

(36) Minett, M. S.; Pereira, V.; Sikandar, S.; Matsuyama, A.; Lolignier, S.; Kanellopoulos, A. H.; Mancini, F.; Iannetti, G. D.; Bogdanov, Y. D.; Santana-Varela, S.; Millet, Q.; Baskozos, G.; MacAllister, R.; Cox, J. J.; Zhao, J.; Wood, J. N. Endogenous Opioids

Contribute to Insensitivity to Pain in Humans and Mice Lacking Sodium Channel Nav1.7. *Nat. Commu.* **2015**, *6*, 8967.

(37) McKerrall, S. J.; Sutherlin, D. P. Nav1.7 Inhibitors for the Treatment of Chronic Pain. *Bioorganic Med. Chem. Lett.* **2018**, *28*, 3141.

(38) Shinozuka, T.; Kobayashi, H.; Suzuki, S.; Tanaka, K.; Karanjule, N.; Hayashi, N.; Tsuda, T.; Tokumaru, E.; Inoue, M.; Ueda, K.; Kimoto, H.; Domon, Y.; Takahashi, S.; Kubota, K.; Yokoyama, T.; Shimizugawa, A.; Koishi, R.; Fujiwara, C.; Asano, D.; Sakakura, T.; Takasuna, K.; Abe, Y.; Watanabe, T.; Kitano, Y. Discovery of DS-1971a, a Potent, Selective NaV1.7 Inhibitor. *J. Med. Chem.* **2020**, *63*, 10204.

(39) Mueller, A.; Starobova, H.; Morgan, M.; Dekan, Z.; Cheneval, O.; Schroeder, C. I.; Alewood, P. F.; Deuis, J. R.; Vetter, I. Antiallodynic Effects of the Selective NaV1.7 Inhibitor Pn3a in a Mouse Model of Acute Postsurgical Pain: Evidence for Analgesic Synergy with Opioids and Baclofen. *Pain* **2019**, *160*, 1766.

(40) Cheng, J.; Giguère, P. M.; Onajole, O. K.; Lv, W.; Gaisin, A.; Gunosewoyo, H.; Schmerberg, C. M.; Pogorelov, V. M.; Rodriguiz, R. M.; Vistoli, G.; Wetsel, W. C.; Roth, B. L.; Kozikowski, A. P. Optimization of 2-Phenylcyclopropylmethylamines as Selective Serotonin 2C Receptor Agonists and Their Evaluation as Potential Antipsychotic Agents. *J. Med. Chem.* **2015**, *58*, 1992.

(41) Liedtke, B. W. H. S. *TRP Ion Channel Function in Sensory Transduction and Cellular Signalling*; CRC Press/Taylor & Francis, 2007.

(42) Safina, B. S.; McKerrall, S. J.; Sun, S.; Chen, C. A.; Chowdhury, S.; Jia, Q.; Li, J.; Zenova, A. Y.; Andrez, J. C.; Bankar, G.; Bergeron, P.; Chang, J. H.; Chang, E.; Chen, J.;

Dean, R.; Decker, S. M.; Dipasquale, A.; Focken, T.; Hemeon, I.; Khakh, K.; Kim, A.; Kwan, R.; Lindgren, A.; Lin, S.; Maher, J.; Mezeyova, J.; Misner, D.; Nelkenbrecher, K.; Pang, J.; Reese, R.; Shields, S. D.; Sojo, L.; Sheng, T.; Verschoof, H.; Waldbrook, M.; Wilson, M. S.; Xie, Z.; Young, C.; Zabka, T. S.; Hackos, D. H.; Ortwine, D. F.; White, A. D.; Johnson, J. P.; Robinette, C. L.; Dehnhardt, C. M.; Cohen, C. J.; Sutherlin, D. P. Discovery of Acyl-Sulfonamide Nav1.7 Inhibitors GDC-0276 and GDC-0310. *J. Med. Chem.* **2021**, *64*, 2953.

(43) Medina, J. C.; Mcgee, L.; Wei, Z.-L.; Sadlowski, C.; Seidl, F.; Bhatt, U.; Xiaodong, W.; Nguyen, T.; Sperandio, D.; Ding, P.; Nerurkar, A.; Yihong, L.; Duquette, J. Opioid Receptor Modulators and Products and Methods Related Thereto. WO2019195634A1, 2019.

(44) Shoichet, K. B.; Gmeiner, P.; Hubner, H.; Roth, L. B.; Dengler, D. G.; Manglik, A.; Kobilka, B. Mu Opioid Receptor Modulators. WO2018129393A1, 2018.

(45) Wuts, G. M. P. *Protective Groups in Organic Synthesis* , 5th ed.; John Wiley & Sons, 2014.

(46) Rolph, M. S.; Markowska, A. L. J.; Warriner, C. N.; O'Reilly, R. K. Blocked Isocyanates: From Analytical and Experimental Considerations to Non-Polyurethane Applications. *Polym. Chem.* **2016**, *7*, 7351.

(47) Rolph, M. S.; Markowska, A. L. J.; Warriner, C. N.; O'Reilly, R. K. Blocked Isocyanates: From Analytical and Experimental Considerations to Non-Polyurethane Applications. *Polym. Chem.* **2016**, *7*, 7351.

(48) Derasp, J. S.; Beauchemin, A. M. Rhodium-Catalyzed Synthesis of Amides from Functionalized Blocked Isocyanates. *ACS Catal.* **2019**, *9*, 8104.

(49) Theile, J. W.; Fuller, M. D.; Chapman, M. L. The Selective Nav1.7 Inhibitor, PF-05089771, Interacts Equivalently with Fast and Slow Inactivated Nav1.7 Channels. *Mol. Pharmacol.* **2016**, *90*, 540.

(50) Gomes, J. C.; Cianni, L.; Ribeiro, J.; dos Reis Rocho, F.; da Costa Martins Silva, S.; Batista, P. H. J.; Moraes, C. B.; Franco, C. H.; Freitas-Junior, L. H. G.; Kenny, P. W.; Leitão, A.; Burtoloso, A. C. B.; de Vita, D.; Montanari, C. A. Synthesis and Structure-Activity Relationship of Nitrile-Based Cruzain Inhibitors Incorporating a Trifluoroethylamine-Based P2 Amide Replacement. *Bioorg. Med. Chem.* **2019**, *27*, 115083.

(51) Girard, A. L.; Enomoto, T.; Yokouchi, S.; Tsukano, C.; Takemoto, Y. Control of 6-Exo and 7-Endo Cyclizations of Alkynylamides Using Platinum and Bismuth Catalysts. *Chem. Asian J.* **2011**, *6*, 1321.

(52) Lovering, F. Escape from Flatland 2: Complexity and Promiscuity. *Med. Chem. Comm.* **2013**, *4*, 515.

(53) Quick, J.; Mondello, C.; Humora, M.; Brennan, T. Synthesis of 2,6-Diacetonylpiperidine. X-Ray Diffraction Analysis of Its N-Benzoyl Derivative. *J. Org. Chem.* **1978**, *43*, 2705.

(54) Luci, D. K.; Jameson, J. B.; Yasgar, A.; Diaz, G.; Joshi, N.; Kantz, A.; Markham, K.; Perry, S.; Kuhn, N.; Yeung, J.; Kerns, E. H.; Schultz, L.; Holinstat, M.; Nadler, J. L.; Taylor-Fishwick, D. A.; Jadhav, A.; Simeonov, A.; Holman, T. R.; Maloney, D. J. Synthesis and Structure-Activity Relationship Studies of 4-((2-Hydroxy-3-

Methoxybenzyl)Amino)Benzenesulfonamide Derivatives as Potent and Selective Inhibitors of 12-Lipoxygenase. *J. Med. Chem.* **2014**, *57*, 495.

(55) Ling, X.; Xiong, Y.; Huang, R.; Zhang, X.; Zhang, S.; Chen, C. Synthesis of Benzidine Derivatives via FeCl3·6H 2O-Promoted Oxidative Coupling of Anilines. *J. Org. Chem.* **2013**, *78*, 5218.

(56) Ilić, M.; Kikelj, D.; Ilaš, J. Fluorinated Dual Antithrombotic Compounds Based on 1,4-Benzoxazine Scaffold. *Eur. J. Med. Chem.* **2012**, *50*, 255.

(57) Navidpour, L.; Karimi, L.; Amini, M.; Vosooghi, M.; Shafiee, A. Syntheses of 5-Alkylthio-1,3-Diaryl-1,2,4-Triazoles. *J. Heterocycl. Chem.* **2004**, *41*, 201.

(58) Xu, Z. M.; Li, H. X.; Young, D. J.; Zhu, D. L.; Li, H. Y.; Lang, J. P. Exogenous Photosensitizer-, Metal-, and Base-Free Visible-Light-Promoted C-H Thiolation via Reverse Hydrogen Atom Transfer. *Org. Lett.* **2019**, *21*, 237.

(59) Everett, R. K.; Wolfe, J. P. Aza-Wittig Rearrangements of N-Benzyl and N-Allyl Glycine Methyl Esters. Discovery of a Surprising Cascade Aza-Wittig Rearrangement/Hydroboration Reaction. *J. Org. Chem.* **2015**, *80*, 9041.

(60) Lou, J.; Wang, Q.; He, Y.; Yu, Z. A Simple Aliphatic Diamine Auxiliary for Palladium-Catalyzed Arylation of Unactivated β-C(Sp3)-H Bonds. *Adv. Synth. Catal.* **2018**, *360*, 4571.

(61) Li, G.; Ji, C. L.; Hong, X.; Szostak, M. Highly Chemoselective, Transition-Metal-Free Transamidation of Unactivated Amides and Direct Amidation of Alkyl Esters by N-C/O-C Cleavage. *J. Am. Chem. Soc.* **2019**, *141*, 11161.

(62) Wang, H.; Hetzer, F.; Huang, W.; Qu, Q.; Meyerowitz, J.; Kaindl, J.; Hübner, H.; Skiniotis, G.; Kobilka, B. K.; Gmeiner, P. Structure-Based Evolution of G Protein-Biased μ-Opioid Receptor Agonists. *Angew. Chem.* **2022**, *61*, 269.

(63) Youngblood, B.; Li, K.; Gehlert, D. R.; Medina, J. C.; Schwartz, N. A Novel Maintenance Therapeutic for Opioid Use Disorder. *J. Pharmacol. Exp. Ther.* **2021**, *378*, 133.

(64) Pasquini, C.; Coniglio, A.; Bassetti, M. Controlled Dealkylation by BBr3: Efficient Synthesis of Para-Alkoxy-Phenols. *Tetrahedron Lett.* **2012**, *53*, 6191.

(65) Majetich, G.; zhang, Y.; Wheless, K. Hydride-Promoted Demethylation of Methyl Phenyl Ethers. *Tetrahdron Lett.* **1994**, *35*, 872743730.

(66) Jacquemard, U.; Bénéteau, V.; Lefoix, M.; Routier, S.; Mérour, J. Y.; Coudert, G. Mild and Selective Deprotection of Carbamates with Bu 4NF. *Tetrahedron* **2004**, *60*, 10039.

Claims to Original Research

1. Synthetic routes towards complex PZM21 analogues were developed;

2. New structure-activity relationship data was obtained that suggests that some flexibility in the scaffold is essential to MOR activity, and that

3. These new $Na_v1.7$ inhibitor scaffolds highlight the importance of hydrophobic groups for biological activity of the PZM21 analogues.

Supporting Information

General information

Analytical Thin layer chromatography (TLC) was performed on aluminum backed silica plates cut to side. Visualization was achieved with UV light and staining with potassium permanganate, cerium molybdate (universal), ninhydrin (for amines) and anisaldehyde (phenols) solutions and heated to intensify color. Purification of compounds was performed where indicated with standard flash column chromatography using 40-63 μL silica.

^{1}H NMR spectra were recorded on Bruker AVANCE 300 MHz, 400 MHz, 500 MHz and 600 MHz spectrometers at room temperature. NMR data was reported in ppm, using deuterated solvents as internal standards (CDCl3 at 7.26 ppm, DMSO-d_6 at 2.50 ppm, acetone-d_6 at 2.05 ppm and MeOH-d_4 at 3.31 ppm). NMR data is reported as: multiplicity (br = broad, s = singlet, d = doublet, t = triplet, q = quartet, quint = quintet, m = multiplet), coupling constant(s) in Hz, integration. Additional unresolved fine splitting observed where indicated. ^{13}C spectra were recorded at 101, 126 and 151 MHz on Bruker AVANCE 400, 500 and 600 MHz spectrometers respectively at room temperature. NMR data was reported in ppm, using deuterated solvents as internal standards ($CDOCl_3$ at 77.16 ppm, DMSO-d_6 at 39.52 ppm and acetone-d_6 at 29.84 ppm). High-Resolution Mass Spectrometry (HRMS) was performed on Kratos Concept IIH mass spectrometer with an electron beam of 70 eV. Fourier Transmission Infrared Spectrometry (FTIR) was performed on Agilent Technologies Cary 630 FTIR.

Materials

Unless otherwise indicated, all commercially available materials were used without further purification. Reaction solvents were used as HPLC solvents, and/or degassed prior to use where

indicated. Compound **9** was prepared according to literature procedure and used without further purification.[67]

Experimental procedures and Characterization data

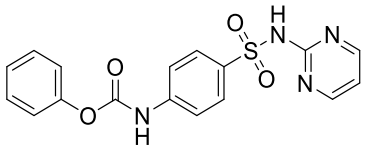

phenyl (4-(N-(pyrimidin-2-yl)sulfamoyl)phenyl)carbamate (6): Sulfadiazine (0.249 g, 0.998 mmol, 1.00 equiv) was suspended in a solution of 0.05 mL of THF and 1.10 mL of water in a microwave vial charged with a stir bar. The solution was cooled in an ice bath for 10 minutes. Sodium bicarbonate (0.160 g, 1.89 mmol, 1.90 equiv) was added and the reaction was stirred for 30 minutes. Phenyl chloroformate (0.20 mL, 1.2 mmol, 1.2 equiv) was added dropwise. The reaction was allowed to warm to room temperature and was stirred for 16 hours. After complete consumption of sulfadiazine judged by TLC (20% toluene/EtOAc) and 10 mL of water was added. The aqueous layer was extracted with 3 x 10 mL EtOAc. The organic layers were collected and washed 3 x 10 mL with NaCl brine. The resulting organic solution was dried over Na_2SO_4 and filtered through cotton. The organic extracts were concentrated *in vacuo*. Purification was achieved by dissolving the crude in minimal hot ethanol. Ice water was added, and the crude was cooled at -20 °C for 16 hours to precipitate the solid. The resulting solution was concentrated *in vacuo* to remove ethanol. The resulting aqueous solution was extracted 3 x 10 mL with EtOAc. The organic extracts were dried over Na_2SO_4, filtered through cotton, concentrated *in vacuo* and dried under high vacuum for 16 hours resulting in 0.104 g (28%) of a flaky, white solid.

TLC R*f*: 0.77 [85% EtOAc/Hex]

^{1}H NMR (500 MHz, DMSO-*d*$_6$): δ 11.69 (br , 1H), 10.66 (s, 1H), 8.49 (d, *J* = 4.9 Hz, 2H), 7.94 (d, *J* = 8.8 Hz, 2H), 7.66 (d, *J* = 8.8 Hz, 2H), 7.43 (t, *J* = 7.9 H, 2H), 7.27 (t, *J* = 7.4 Hz, 1H), 7.25 – 7.21 (d, *J* = 7.9 Hz, 2H), 7.02 (t, *J* = 4.9 Hz, 1H)

^{13}C NMR (126 MHz, DMSO-*d*$_6$): δ 151.6, 150.3, 129.8, 129.5, 129.4, 129.1, 125.7, 121.9, 118.8, 117.7, 115.2, 112.1.

IR (FTIR): 3352, 2932, 1732, 1339 cm^{-1}

HRMS (ESI): $[M + Na]^+$ Calcd for $C_{17}H_{15}N_4NaO_4S$: 393.0633; Found 393.0607

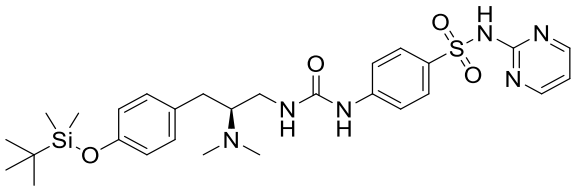

(*S*)-4-(3-(3-(4-((tert-butyldimethylsilyl)oxy)phenyl)-2-(dimethylamino)propyl)ureido)-*N*-(pyrimidin-2-yl)benzenesulfonamide (6a): Blocked isocyanate **6** (0.0780 g, 0.212 mmol, 1.00 equiv) was suspended in 0.3 mL of MeCN in a microwave vial charged with a stir bar. Triethylamine (0.035 mL, 0.25 mmol, 1.2 equiv) was added dropwise. Diamine **5** (0.0657 g, 0.212 mmol, 1 equiv) was added slowly, using an additional 0.5 mL of MeCN to transfer it to the reaction vessel. The reaction vessel was sonicated for 1 minute. The reaction vessel was sealed with a microwave septum and purged with Ar balloon. The reaction was heated at 60 ºC for 1.5 hours After full disappearance of blocked isocyanate, as judged by TLC (5% MeOH/DCM), the reaction was removed from heat, allowed to cool to room temperature and 15 mL of EtOAc was added. The mixture was washed 3 x 10 mL with a Na_2CO_3/$NaHCO_3$ buffer (pH=10) and 1 x 10 mL with NaCl brine. The organic extracts were dried over Na_2SO_4,

filtered through cotton, and concentrated *in vacuo*. Purification was achieved via column chromatography with a gradient eluent system of [5% MeOH/DCM] increasing to [15% MeOH/DCM]. Concentration *in vacuo* and drying under high vacuum for 24 hours resulted in 0.0268 g (21%) of a yellow oil.

TLC R*f*: 0.31 [10%MeOH/DCM]

^{1}H NMR (500 MHz, DMSO-d_6): δ 9.21 (s, 1H), 8.48 (d, *J* = 4.8 Hz, 2H), 7.80 (d, *J* = 8.0 Hz, additional unresolved fine coupling observed, 2H), 7.48 (d, *J* = 8.0 Hz, additional unresolved fine coupling observed, 2H), 7.09 (d, *J* = 8.3 Hz, 2H), 7.02 (t, *J* = 4.9 Hz, 1H), 6.76 (d, *J* = 8.3 Hz, 2H), 6.25 (s, 1H), 3.18 – 3.13 (m, 1H), 2.94 (t, *J* = 10.3 Hz, 1H), 2.83 (dd, *J* = 13.7, 3.4 Hz, 1H), 2.77 br, 1H), 2.33 (, 6H), 2.38 - 2.29 (m, 1H) 0.94 (s, 9H), 0.16 (s, 6H).

^{13}C NMR (126 MHz, DMSO-d_6): δ 158.3 157.1, 154.5, 153.2, 144.7, 131.4, 130.1, 128.9, 119.6, 116.3, 115.7, 64.9, 30.1, 25.6, 17.9, -4.5. Data from DEPT experiments indicate 2 signals overlapping with DMSO-d_6 peak (40.4, 39.4).

HRMS (ESI): $[M + H]^+$ Calcd for $C_{28}H_{41}N_6O_4SSi$: 585.2679; Found 585.2667

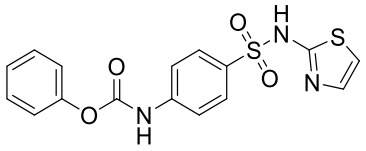

phenyl (4-(N-(thiazol-2-yl)sulfamoyl)phenyl)carbamate (7): Sulfathiazole (0.250 g, 0.980 mmol, 1.00 equiv) was suspended in a solution of 3.0 mL of THF and 1.1 mL of water in a microwave vial charged with a stir bar. The solution was cooled in an ice bath for 10 minutes. Sodium bicarbonate (0.0994 g, 1.17 mmol, 1.20 equiv) was added and the reaction was stirred for 30 minutes. Phenyl chloroformate (0.1 mL, 1.08 mmol, 1.10 equiv) was added dropwise. The

reaction was allowed to warm to room temperature and was stirred for 24 hours. After complete consumption of sulfathiazole, as judged by TLC (5% MeOH/DCM), 10 mL of water was added. The aqueous layer was extracted 3 x 10 mL with EtOAc. The organic layers were collected and washed 3 x 10 mL with NaCl brine. The organic extracts were dried over Na_2SO_4 and filtered through cotton. The organic extracts were concentrated *in vacuo* and dried under high vacuum for 16 hours resulting in 0.308 g (84%) of pale-yellow solid.

TLC R*f*: 0.46 [5% MeOH/DCM]

^{1}H NMR (500 MHz, DMSO-*d*$_6$): δ 10.61 (s, 1H), 7.77 (d, *J* = 8.8 Hz, additional unresolved fine coupling observed, 2H), 7.64 (d, *J* = 8.8 Hz, additional unresolved fine coupling observed, 2H), 7.43 (t, *J* = 7.6 Hz, 2H), 7.29 – 7.21 (m, 4H), 6.80 (d, *J* = 4.6 Hz, 1H).

^{13}C NMR (126 MHz, DMSO-*d*$_6$): δ 168.7, 151.6, 150.3, 142.0, 136.3, 129.5, 127.1, 125.7, 124.7, 121.9, 118.0, 108.1.

IR (FTIR): 3212, 3201, 1742, 1317 cm^{-1}

HRMS (ESI): $[M + Na]^+$ Calcd for $C_{16}H_{13}N_3NaO_4S_2$: 398.0245; Found 398.0220.

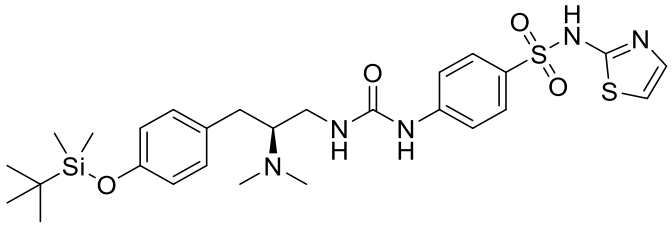

(*S*)-4-(3-(3-(4-((tert-butyldimethylsilyl)oxy)phenyl)-2-(dimethylamino)propyl)ureido)-N-(thiazol-2-yl)benzenesulfonamide (7a): Blocked isocyanate **7** (0.080 g, 0.22 mmol, 1.0 equiv) was suspended in 0.3 mL of MeCN in a microwave

vial charged with a stir bar. Triethylamine (0.035 mL, 0.25 mmol, 1.2 equiv) was added dropwise while stirring. Diamine **5** (0.065 g, 0.22 mmol, 1.0 equiv) was added slowly, using an additional 0.5 mL of MeCN to transfer. The reaction vessel was sonicated for 1 minute. The reaction vessel was sealed with a microwave septum and purged with an Ar balloon. The reaction was heated at 60 ºC for 3 hours. After full disappearance of blocked isocyanate, as judged by TLC (10% MeOH/DCM), the reaction was removed from heat and allowed to cool to room temperature and 15 mL of EtOAc was added. The mixture was washed 3 x 10 mL with a Na_2CO_3/$NaHCO_3$ buffer (pH=10) and 1 x 10 mL with NaCl brine. The organic extracts were dried over Na_2SO_4, filtered through cotton and concentrated *in vacuo*. Purification was achieved via column chromatography, [10% MeOH/DCM]. Concentration *in vacuo* and drying under high vacuum for 24 hours resulted in 0.0262 g (20%) of a yellow oil.

TLC R*f*: 0.33 [10% MeOH/DCM]

^{1}H NMR (400 MHz, Acetone-d_6): δ 7.62 (d, *J* = 8.5 Hz, 2H), 7.25 – 7.17 (m, 5H), 6.86 – 6.81 (m, 2H), 6.73 (d, *J* = 4.3 Hz, 1H), 3.52 (d, *J* = 3.7 Hz, 1H), 3.35 – 3.22 (m, 2H), 3.18 (dd, *J* = 13.4, 3.6 Hz, 1H), 2.77 (d, *J* = 2.6 Hz, 6H), 2.70 (dd, *J* = 13.5, 10.1 Hz, 1H), 0.98 (d, *J* = 0.8 Hz, 9H), 0.20 (d, *J* = 0.8 Hz, 6H).

^{13}C NMR (101 MHz, Acetone-d_6): δ 171.0, 155.8, 154.9, 144.2, 136.8, 132.6, 131.1, 128.0, 120.8, 117.4, 109.0, 66.7, 40.7, 39.5, 31.8, 26.0, 18.7, 9.6, -4.3.

HRMS (ESI): $[M + H]^+$ Calcd for $C_{27}H_{40}N_5O_4S_2Si$: 590.2291; Found 590.2300.

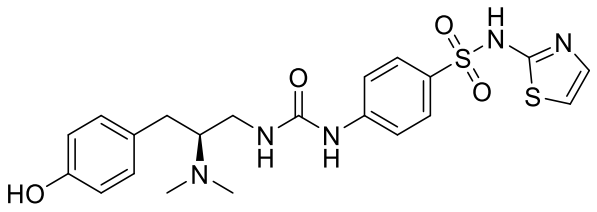

(*S*)-4-(3-(2-(dimethylamino)-3-(4-hydroxyphenyl)propyl)ureido)-*N*-(thiazol-2-yl)benzenesulfonamide (7b): TBS protected compound **7a** (0.0158 g, 0.0260 mmol, 1.00 equiv) was dissolved in 0.1 mL of dry THF in an Eppendorf tube charged with a stir bar. The reaction was cooled in an ice bath to 0 ºC for 10 minutes. The reaction vessel was purged with argon through an upside-down funnel set over top of the tube. HF•pyridine (0.025 mL, 0.93 mmol, 37 equiv) was added using a micropipette. The tube was closed and purged with an Ar balloon. The reaction was stirred in an ice bath at 0 ºC for 1 hour. After 1 hour, the ice bath was removed and the reaction was allowed to come to room temperature, stirring for an additional 75 minutes. After full disappearance of starting material judged by TLC (20% MeOH/DCM) 10 mL of saturated $NaHCO_3$ solution was added and the mixture was extracted with 3 x 10 mL of EtOAc. The organic extracts were collected and dried over Na_2SO_4, filtered over cotton and concentrated *in vacuo*. Purification was achieved via column chromatography, [20% MeOH/DCM]. Concentration *in vacuo* and drying under high vacuum for 24 hours resulted in 0.0027 g (22%) of a clear oil.

TLC R*f*: 0.26 [20%MeOH/DCM]

^{1}H NMR (500 MHz, Acetone-d_6): δ 8.39 (s, 1H) 7.65 (dd, *J* = 9.0, 2.2 Hz, 2H), 7.35 (dd, *J* = 9.0, 2.2 Hz, 2H), 7.19 (d, *J* = 4.5 Hz, 1H), 7.11 (d, *J* = 8.4 Hz, 2H), 6.78 (d, *J* = 8.4 Hz, additional unresolved fine coupling observed, 2H), 6.72 (d, *J* = 4.5 Hz, 1H), 3.44 (m, 1H), 3.13 (t, *J* = 9.0, additional unresolved fine coupling observed, 1H), 3.08 – 3.01 (m, 2H), 2.59 (s, 6H), 2.54 – 2.47 (m, 1H)

^{13}C NMR (151 MHz, Acetone-*d*$_6$): δ 170.6, 162.2, 156.8, 155.5, 144.5, 136.3, 131.0, 128.0, 117.3, 116.2, 114.8, 108.9, 66.8, 40.6, 39.6, 31.3.

HRMS (ESI): $[M + H]^+$ Calcd for $C_{21}H_{26}N_5O_4S_2$: 476.1426; Found 476.1443.

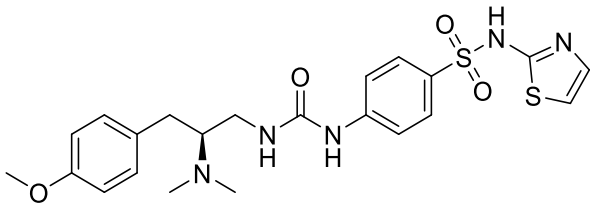

(*S*)-4-(3-(2-(dimethylamino)-3-(4-methoxyphenyl)propyl)ureido)-*N*-(thiazol-2-yl)benzenesulfonamide (7c): Blocked isocyanate **6** (0.0452 g, 0.220 mmol, 1.00 equiv) was suspended in 0.6 mL of MeCN in a microwave vial charged with a stir bar. Triethylamine (0.006 mL, 0.04 mmol, 0.2 equiv) was added dropwise while stirring. Diamine **14** (0.0871 g, 0.230 mmol, 1.10 equiv) was added slowly. The reaction vessel was sonicated for 1 minute. The reaction vessel was sealed with a microwave septum and purged with an Ar balloon. The reaction was heated at 60 ºC for 1.5 hours After full disappearance of blocked isocyanate judge by TLC (10% MeOH/DCM) the reaction was removed from heat and allowed to cool to room temperature and 15 mL of EtOAc was added. The mixture was washed 3 x 10 mL with a Na_2CO_3/$NaHCO_3$ buffer (pH=10) and 1 x 10 mL with NaCl brine. The organix extracts were dried over Na_2SO_4, filtered through cotton and concentrated *in vacuo*. Purification was achieved via column chromatography, [5% MeOH/DCM]. Concentration *in vacuo* and drying under high vacuum for 24 hours resulted in 0.0199 g (18%) of a yellowish oil.

TLC R*f*: 0.28 [10%MeOH/DCM]

^{1}H NMR (600 MHz, Acetone-*d*$_6$): δ 7.62 (d, *J* = 8.9 Hz, additional unresolved fine coupling observed, 2H), 7.24 – 7.21 (m, 4H), 7.19 (d, *J* = 4.3 Hz, 1H), 6.87 (d, *J* = 8.9 Hz, additional

unresolved fine coupling observed, 2H), 6.72 (d, *J* = 4.3 Hz, 1H), 3.76 (s, 3H), 3.46 (d, *J* = 9.94, 1H), 3.19 (dd, *J* = 9.0, 3.3 Hz, 2H), 3.13 (d, *J* = 13.4 Hz, 1H), 2.69 (s, 6H), 2.62 (t, *J* = 9.7, 1H).

^{13}C NMR (151 MHz, Acetone-d_6): 160.1, 157.7 144.7, 136.2, 131.2, 130.6, 128.5, 118.8, 115.3, 107.1, 68.0, 55.7, 47.84, 40.7, 40.2, 32.1, 9.2.

HRMS (ESI): $[M + H]^+$ Calcd for $C_{22}H_{28}N_5O_4S_2$: 490.1583; Found 490.1569.

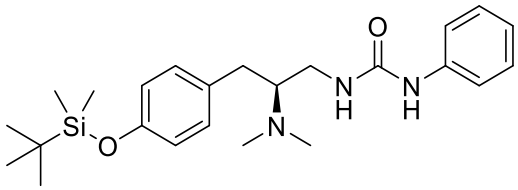

(*S*)-1-(3-(4-((*tert*-butyldimethylsilyl)oxy)phenyl)-2-(dimethylamino)propyl)-3-phenylurea (9a): Blocked isocyanate **9** (0.0497 g, 0.234 mmol, 1.00 equiv) was suspended in 0.5 mL of MeCN in a microwave vial charged with a stir bar. Triethylamine (0.039 mL, 0.28 mmol, 1.2 equiv) was added dropwise while stirring. Diamine **5** (0.0741 g, 0.0234 mmol, 1.00 equiv) was added slowly. The reaction vessel was sonicated for 1 minute. The reaction vessel was sealed with a microwave septum and purged with an Ar balloon. The reaction was heated at 60 ºC for 1.5 hours. After full disappearance of blocked isocyanate judge by TLC (10% MeOH/DCM) the reaction was removed from heat and allowed to cool to room temperature and 15 mL of EtOAc was added. The mixture was washed 3 x 10 mL with a Na_2CO_3/$NaHCO_3$ buffer (pH=10) and 1 x 10 mL with NaCl brine. The organic extracts were dried over Na_2SO_4, filtered through cotton and concentrated *in vacuo*. Purification was achieved via column chromatography, [5% MeOH/DCM]. Concentration *in vacuo* and drying under high vacuum for 24 hours resulted in 0.0257 g (26%) of a yellowish oil.

TLC R*f*: 0.19 [5%MeOH/DCM]

^{1}H NMR (500 MHz, Acetone-d_6): δ 8.30 (s, 1H), 7.46 (d, *J* = 7.7 Hz, 2H), 7.18 (t, *J* = 7.9 Hz, 2H), 7.13 (d, *J* = 8.4 Hz, 2H), 6.87 (t, *J* = 7.4 Hz, 1H), 6.80 (d, *J* = 8.4 Hz, 2H), 5.95 (s, 1H), 3.36 (m, 1H), 3.02 (t, *J* = 12.2 Hz, additional unresolved fine coupling observed, 1H), 2.94 (dd, *J* = 13.4, 4.0, 1H), 2.85 (sext, *J* = 5.3, 1H), 2.40-2.37 (m, 1H), 2.39 (s, 6H), 0.99 (s, 9H), 0.20 (s, 6H).

^{13}C NMR (151 MHz, Acetone-d_6): δ 156.1, 154.8, 141.9, 133.5, 130.5, 131.0, 129.4, 121.9, 120.8, 118.7, 66.7, 40.4, 31.3, 26.1, 18.7, -4.29.

HRMS (ESI): $[M + H]^+$ Calcd for $C_{24}H_{38}N_3O_2Si$: 428.2733; Found 428.2710.

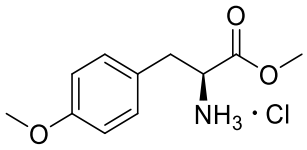

methyl (*S*)-2-amino-3-(4-methoxyphenyl)propanoate HCl (11): Optima grade methanol (5.0 mL) was added trough a septum to a microwave vial that had been purged with argon and charged with a stir bar. The reaction was cooled 0 ºC with an ice bath for 10 minutes. Thionyl chloride (0.49 mL, 4.9 mmol, 3.8 equiv) was added dropwise over 5 minutes through a septum. The ice bath was removed, and the mixture was stirred for an additional 10 minutes. The septum was removed and 4-methyoxy-L-phenylalaine (1.28 mmol, 0.250 g, 1.00 equiv) was added quickly as a solid. The reaction was re-sealed with a microwave septum and heated at 65 ºC for 90 minutes. After full disappearance of 4-methyoxy-L-phenylalaine by TLC (40% MeOH/DCM) reaction was removed from heat, allowed to cool to room temperature and concentrated *in vacuo* to dryness. The crude solid was triturated, suspended in diethyl ether, and filtered through a frit and washed with additional diethyl ether resulting in 0.294 g (94%) of a fluffy, pale-yellow solid. Although not confirmed with HRMS, based on the presence of an additional br peak (1H) in the ^{1}H NMR

and the reaction conditions, it is highly plausible that the product is an HCl salt, or a mixture of the salt and free base.

TLC R*f*: 0.21 [90%EtOAc/Hex]

^{1}H NMR (600 MHz, DMSO-*d*$_6$): δ 8.59 – 8.45 (br, 3H), 7.14 (d, *J* = 8.1 Hz, 2H), 6.90 (d, *J* = 8.1 Hz, 2H), 4.23 (m, 1H), 3.73 (s, 3H), 3.68 (s, 3H), 3.06 (q, *J* = 13.4 Hz, additional unresolved fine coupling observed, 2H).

^{13}C NMR (126 MHz, DMSO-*d*$_6$): δ 169.4, 158.5, 130.5, 126.4, 114.0, 55.1, 53.4, 52.5, 35.0.

HRMS (ESI): $[M + Na]^+$ Calcd for $C_{11}H_{15}NO_3Na$: 232.0950; Found 232.0957

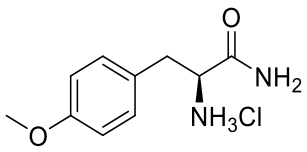

(*S*)-2-amino-3-(4-methoxyphenyl)propenamide (12): Methyl ester **11** (2.85 mmol, 0.703 g, 1.00 equiv) was added to a round bottom flask charged with a stir bar. NH_4OH (99.8 mmol, 14.2 mL, 35.0 equiv) was added slowly. The reaction was stirred at room temperature for 3 hours. After full disappearance of methyl ester by TLC (2.5% MeOH/DCM) the reaction was concentrated *in vacuo*. The crude was dissolved in 10 mL of deionized water and washed 3 x 10mL with DCM. The aqueous extracts were concentrated *in vacuo* followed by high vacuum resulting in 0.639 g (97%) of pale-orange solid. Although not confirmed with HRMS, based on the presence of an additional br peak (1H) in the ^{1}H NMR and the reaction conditions, it is highly plausible that the product is an HCl salt or a mixture of the salt and free base.

TLC R*f*: 0.23 [2.5% MeOH/DCM]

^{1}H NMR (600 MHz, DMSO-*d*$_6$): δ 7.92 (br , 1H), 7.48 (br, 1H), 7.19 (d, *J* = 8.6 Hz, 2H), 6.88 (d, *J* = 8.6 Hz, 2H), 3.87 (t, *J* = 6.9 Hz, 1H), 3.87 (t, *J* = 6.6 Hz, 1H), 3.73 (s, 3H), 3.03 (dd, *J* = 14.0, 6.1 Hz, 1H), 2.93 (dd, J = 14.0, 7.3 Hz, 1H).

^{13}C NMR (126 MHz, DMSO-*d*$_6$): δ 170.3, 158.8, 131.1, 127.4, 114.3, 55.5, 54.0, 36.3.

IR (FTIR): 3216, 2873, 1660, 1613, 1243 cm^{-1}.

HRMS (ESI): $[M + Na]^+$ Calcd for $C_{10}H_{14}N_2O_2Na$: 217.0953; Found 217.0964.

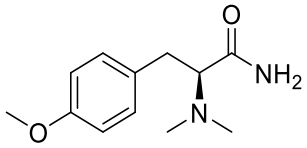

(*S*)-2-(dimethylamino)-3-(4-methoxyphenyl)propenamide (13): Optima grade methanol (16.2 mL) was added to a round bottom flask charged with a stir bar. Formaldehyde as a 37% w/w solution (52.0 mmol, 5.18 mL, 13.0 equiv) was added, followed by a few drops of glacial acetic acid. Amide **12** was added (4.00 mmol, 0.778 g, 1 equiv). The reaction was cooled to 0 ºC with an ice bath for 10 minutes. Sodium cyanoborohydride (6.00 mmol, 0.385 g, 1.50 equiv) was added slowly at 0 ºC and the reaction was sealed with a plastic cap. The ice bath was removed, and the reaction stirred for 5 minutes. After full disappearance of amide by TLC (10% MeOH/DCM) the reaction was concentrated *in vacuo*. 15 mL of saturated $NaHCO_3$ was added. The mixture was extracted 5 x 10 mL of DCM. The organic extracts were dried over Na_2SO_4, filtered through cotton and concentrated *in vacuo* followed by high vacuum for 16 hours resulting in 0.535 g (60%) of a sticky, white solid.

TLC R*f*: 0.42 [10% MeOH/DCM]

^{1}H NMR (500 MHz, DMSO-*d*$_6$): δ 7.10 (d, *J* = 8.6 Hz, additional unresolved fine coupling observed, 2H), 6.80 (d, *J* = 8.6 Hz, additional unresolved fine coupling observed, 2H), 3.70 (s, 3H), 3.11 (dd, *J* = 9.0, 5.5 Hz, 1H), 2.85 (dd, *J* = 13.4, 9.0 Hz, 1 H), 2.66 (dd, *J* = 13.4, 5.5 Hz, 1H), 2.24 (s, 3H).

^{13}C NMR (126 MHz, DMSO-*d*$_6$): 171.9, 157.5, 131.2, 130.0, 113.5, 69.0, 54.9, 41.7, 33.4.

IR (FTIR): 3271, 2844, 1660, 1613, 1243 cm^{-1}.

HRMS (ESI): $[M + H]^+$ Calcd for $C_{12}H_{19}N_2O_2$: 223.1447; Found 223.1445

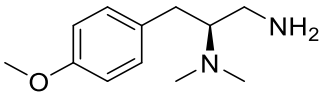

(*S*)-3-(4-methoxyphenyl)-*N*,*N*-dimethylpropane-1,2-diamine (14): Amide **13** (1.10 mmol, 0.253 g, 1.00 equiv) was added to a RBF charged with a stir bar. The amide was suspended in 17 mL of dry THF and the reaction was cooled to 0 ºC for 10 minutes. LAH (0.214 g, 5.62 mmol, 5.0 equiv) was added portion wise while stirring. The reaction was warmed to room temperature and then heated to 68 ºC for 20 hours. After full disappearance of amide judged by TLC (20%MeOH/DCM) the reaction was removed and cooled to 0 ºC for 30 minutes. The reaction was quenched with excess saturated Rochelle salt solution and stirred vigorously for 5 hours. The solution was extracted 3 x 15 mL with DCM. The organic extracts were dried over Na_2SO_4, filtered through cotton, and concentrated *in vacuo* followed by high vacuum for 16 hours resulting in 0.185 g (81%) of a yellow oil.

TLC R*f*: 0.23 [20% MeOH/DCM]

^{1}H NMR (300 MHz, Acetone-d_6): δ 7.19 – 7.08 (m, 2H), 6.87 – 6.73 (m, 2H), 3.74 (s, 6H), 3.34 (dd, *J* = 14.0, 5.8 Hz, 1H), 3.11 (dd, *J* = 14.0, 6.2 Hz, 1H), 2.95 – 2.83 (m, 1H), 2.69 (d, *J* = 7.0 Hz, 2H), 2.29 (s, 6H).

^{13}C NMR (126 MHz, Acetone-d_6): 158.7, 134.2, 130.9, 114.2, 67.7, 55.4, 51.2, 41.5, 34.7.

IR (FTIR): 3409, 2931, 1421, 1237, 1174 cm^{-1}

HRMS (ESI): $[M + H]^+$ Calcd for $C_{12}H_{21}N_2O$: 209.1654; Found 223.1656

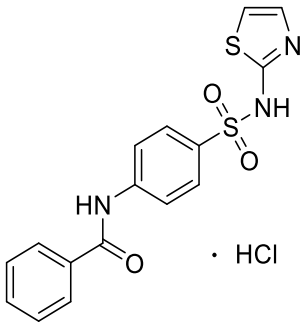

***N*-(4-(*N*-(thiazol-2-yl)sulfamoyl)phenyl)benzamide HCl (15):** Sulfathiazole (0.763 g, 3.00 mmol, 1.00 equiv) was suspended in 8 mL of dry THF in a microwave vial charged with a stir bar. The vial was sealed with a septum and purged with Ar. Benzoyl chloride (0.5 mL, 4.5 mmol, 1.5 equiv) was dissolved in 4 mL of dry THF. The solution of benzoyl chloride in THF was added to the reaction vessel dropwise through the septum, in an ice bath at 0 °C. Triethylamine (0.4 mL, 3.1 mmol, 1.02 equiv) was added dropwise through the septum. The reaction was allowed to warm to room temperature and was stirred for 16 hours. After complete consumption of sulfathiazole by TLC (10% MeOH/DCM), the formed solids were filtered through a fritted funnel, washed with additional THF and dried under high vacuum for 24 hours yielding 0.691 g (64%) of a white solid. Although not confirmed with HRMS, based on the presence of an additional br peak (1H) in the

^{1}H NMR and the reaction conditions, it is highly plausible that the product is an HCl salt or a mixture of the salt and free base.

TLC R*f*: 0.55 [10%MeOH/DCM]

^{1}H NMR (300 MHz, DMSO-*d*$_6$): δ 12.71 (br, 1H), 10.56 (s, 1H), 8.00 – 7.88 (m, 4H), 7.79 (d, *J* = 8.7 Hz, 2H), 7.67 – 7.49 (m, 3H), 7.25 (d, *J* = 4.6 Hz, 1H), 6.82 (d, *J* = 4.6 Hz, 1H).

^{13}C NMR (126 MHz, DMSO-*d*$_6$): δ 168.8, 166.0, 142.4, 136.8, 134.5, 131.9, 128.4, 127.8, 126.8, 124.3, 119.8, 108.1.

IR (FTIR): 1656, 1392 cm^{-1}.

HRMS (ESI): $[M + Na]^+$ Calcd for $C_{16}H_{13}N_3O_3NaS_2$: 382.0296; Found 382.0274

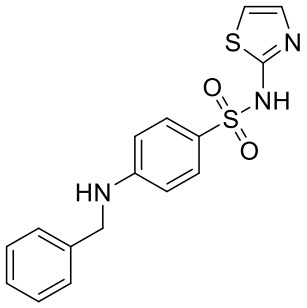

4-(benzylamino)-*N*-(thiazol-2-yl)benzenesulfonamide (16): Amide **15** (0.286 g, 0.790 mmol, 1.00 equiv) was suspended in 1.3 mL of dry THF in an RBF charged with a stir bar. The reaction was cooled to 0 ºC for 10 minutes. LAH (0.099 g, 2.4 mmol, 3.0 equiv) was added portion wise while stirring. The reaction was warmed to room temperature and then heated to 68 ºC for 16 hours. After full disappearance of amide judged by TLC (3% MeOH/DCM), the reaction was removed from heat and cooled to 0 ºC in an ice bath for 30 minutes. A modified Fieser quench was performed, 1.0 mL of H_2O was added slowly, followed by 1.0 mL of 10% NaOH, then 3.0 mL of H_2O. The ice bath was removed, and the reaction was stirred at room temperature for 15

minutes. Excess Mg_2SO_4 was added and stirred at room temperature for 15 minutes. Resulting solids were filtered through a frit and washed with MeOH. The resulting filtrate was concentrated *in vacuo* followed by high vacuum for 16 hours resulting in 0.237 g (30%) of white solid.

The TFA salt of compound **16** is reported in the literature and characterization data is agreeable.[54]

^{1}H NMR (500 MHz, DMSO-d_6): δ 7.45 (d, *J* = 8.8 Hz, additional unresolved fine coupling observed, 2H), 7.34 – 7.28 (m, 4H), 7.32-7.30 (m, 1H), 7.16 (d, *J* = 4.6 Hz, 1H), 6.99 (t, *J* = 5.9 Hz, 1H), 6.71 (d, *J* = 4.5 Hz, 1H), 6.59 (d, *J* = 8.8, additional unresolved fine coupling observed, 2H), 4.30 (d, *J* = 6.0 Hz, 2H).

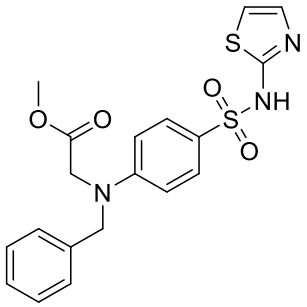

methyl *N*-benzyl-*N*-(4-(N-(thiazol-2-yl)sulfamoyl)phenyl)glycinate (17): Amine **16** (1.24 g, 3.60 mmol, 1.00 equiv) was suspended in 15 mL of optima grade acetonitrile in a microwave vial charged with a stir bar. *N*,*N*-diisopropylethylamine (1.8 mL, 11 mmol, 3.0 equiv) was added. Methyl-2-bromoacetate (0.8 mL, 9.0 mmol, 2.5 equiv) was added. The reaction was sealed with a microwave septum and heated at 82 ºC for 30 minutes. After full disappearance of amine starting material judged by TLC (15% MeOH/DCM) the reaction was removed from heat and cooled to 0 ºC in an ice bath for 10 minutes. Resulting solids were filtered through a frit and washed with additional cold acetonitrile. Solids were collected resulting in 0.971 g (64%) of white crystals.

TLC R*f*: 0.64 [15%MeOH/DCM]

^{1}H NMR (500 MHz, DMSO-*d*$_6$): δ 7.42 (d, *J* = 8.8 Hz, additional unresolved fine coupling observed, 2H), 7.32-7.31 (m, 5H), 7.23 (m, 1H), 7.04 (t, J= 6.0 Hz, 1H), 6.82 (d, *J* = 4.7 Hz, 1H), 6.59 (d, *J* = 8.8 Hz, additional unresolved fine coupling observed, 2H), 4.74 (s, 2H), 4.31 (d, *J* = 6.0 Hz, 2H), 3.55 (s, 1H).

^{13}C NMR (126 MHz, DMSO-*d*$_6$): 167.5, 166.1, 151.6, 139.3, 128.4, 128.3, 127.7, 127.6, 127.2, 111.0, 106.2, 52.3, 48.2, 45.9.

IR (FTIR): 1736, 1289, 1135 cm^{-1}.

HRMS (ESI): $[M + Na]^+$ Calcd for $C_{19}H_{19}N_3O_4NaS_2$ 440.0715; Found 440.0698.

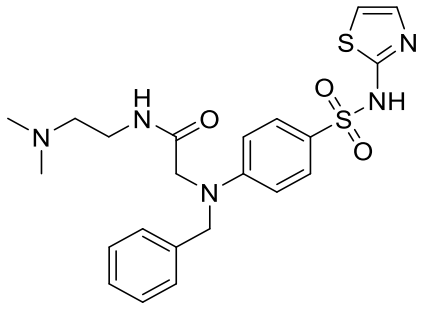

2-(benzyl(4-(*N*-(thiazol-2-yl)sulfamoyl)phenyl)amino)-*N*-(2-(dimethylamino)ethyl)acetamide (18a): Methyl ester **17** (0.0460 g, 0.110 mmol, 1.00 equiv) was added to a microwave vial charged with a stir bar. *N*,*N*-dimethylethylenediamine (0.4 mL, 5.8 mmol, 53 equiv) was added. The reaction was sealed with a microwave septum and heated at 100 ºC for 30 minutes. After full disappearance of methyl ester judged by TLC (10% MeOH/DCM), the reaction was removed from heat and cooled to room temperature. The reaction was diluted with 5 mL of EtOAc and extracted 3 x 10 mL of H_2O. The organic extracts were dried over Na_2SO_4,

filtered through cotton and concentrated *in vacuo* followed by high vacuum for 16 hours resulting 0.0297 g (57%) of a white solid.

TLC R*f*: 0.23 [15% MeOH/DCM]

^{1}H NMR (500 MHz, Chloroform-*d*): δ 7.70 (d, *J* = 8.8 Hz, additional unresolved fine coupling observed, 2H), 7.39 – 7.27 (m, 5H), 6.94 (d, *J* = 4.8 Hz, 1H), 6.71 (br, 1H), 6.57 (d, *J* = 8.8 Hz, additional unresolved fine coupling observed, 2H), 6.44 (d, *J* = 4.8 Hz, 1H), 4.52 (s, 2H), 4.35 (d, *J* = 5.4 Hz, 2H), 3.22 (q, *J* = 5.7 Hz, 2H), 2.32 (t, *J* = 6.1 Hz, 2H), 2.19 (s, 6H).

^{13}C NMR (126 MHz, Chloroform-*d*): δ 165.6, 151.2, 138.3, 128.9, 128.6, 127.7, 127.5, 127.2, 111.8, 106.2, 57.5, 51.0, 50.9, 47.8, 45.1, 37.2, 29.8.

IR (FTIR): 3240, 2925, 1684, 1654, 1480, 1283, 1095 cm^{-1}

HRMS (ESI): $[M + H]^+$ Calcd for $C_{22}H_{28}N_5O_3S_2$ 474.1634; Found 474.1632

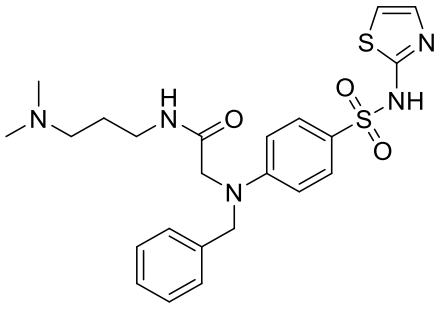

2-(benzyl(4-(*N*-(thiazol-2-yl)sulfamoyl)phenyl)amino)-*N*-(3-(dimethylamino)propyl)acetamide (18b): Methyl ester **17** (0.0583 g, 0.130 mmol 1.00 equiv) was added to a microwave vial charged with a stir bar followed by 1-amino-3(dimethylamino)-propane (0.5 mL, 2.5 mmol, 19 equiv). The reaction was sealed with a microwave septum and heated at 100 ºC for 30 minutes. After full disappearance of methyl ester judged by TLC (10% MeOH/DCM), the reaction was removed from heat and cooled to room temperature. The reaction

was diluted with 5 mL of EtOAc and extracted 3 x 10 mL of H_2O. The organic extracts were dried over Na_2SO_4, filtered through cotton and concentrated *in vacuo* followed by high vacuum for 16 hours resulting 0.0195 g (31%) of a white solid.

TLC R*f*: 0.28 [100% EtOAc]

^{1}H NMR (500 MHz, Chloroform-*d*): δ 8.00 (s, 1H), 7.70 (d, *J* = 8.8 Hz, additional unresolved fine coupling observed, 2H), 7.39 – 7.27 (m, 5H), 6.88 (d, *J* = 4.8 Hz, 1H), 6.58 (d, *J* = 8.8 Hz, additional unresolved fine coupling observed, 2H), 6.46 (d, *J* = 4.8 Hz, 1H), 4.51 (s, 2H), 4.36 (d, *J* = 3.7 Hz, 2H), 3.26 (dd, *J* = 12.1, 6.2 Hz, 2H), 2.41 (t, *J* = 6.2 Hz, 2H), 2.21 (s, 6H), 1.61 (p, *J* = 6.2 Hz, 2H).

^{13}C NMR (126 MHz, Chloroform-*d*): δ 165.7, 151.2, 138.6, 129.6, 129.0, 128.6, 127.7, 127.5, 126.9, 111.8, 106.4, 58.6, 51.0, 47.8, 45.2, 39.9, 29.9, 24.9.

IR (FTIR): 1695, 1495, 1289, 1134 cm^{-1}.

HRMS (ESI): $[M + H]^+$ Calcd for $C_{23}H_{30}N_5O_3S_2$ 488.1790; Found 488.1802

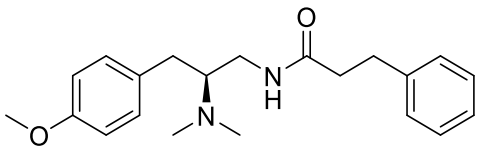

(*S*)-*N*-(2-(dimethylamino)-3-(4-methoxyphenyl)propyl)-3-phenylpropanamide (23a): Diamine **14** (0.105 g, 0.500 mmol, 1.05 equiv) was dissolved in 7 mL of dry DCM in a microwave vial charged with a stir bar. The vial was sealed with a septum and purged with Ar gas. Triethylamine (0.1 mL, 0.72 mmol, 1.5 equiv) was added slowly through the septum. 3-phenyl propionyl chloride (0.074 mL, 0.48 mmol, 1.0 equiv) was added dropwise through the septum. The reaction was stirred for 2 hours. After full disappearance of acid chloride judged by TLC (25%

Hexane/75% EtOAc), the reaction was concentrated *in vacuo*. The resulting crude was dissolved in 5 mL of EtOAc and extracted 2 x 5 mL with saturated $NaHCO_3$ and 1 x 5 mL with NaCl brine. Organic extracts were dried over Na_2SO_4, filtered through cotton and concentrated *in vacuo* followed by high vacuum for 16 hours resulting 0.146 g (86%) of a yellow oil.

TLC R*f*: 0.39 [5% MeOH/DCM]

^{1}H NMR (300 MHz, Chloroform-*d*): δ 7.34 – 7.25 (m, 2H), 7.24 – 7.16 (m, 3H), 7.05 (d, *J* = 8.5 Hz, additional unresolved fine coupling observed, 2H), 6.84 (d, J = 8.5 Hz, additional unresolved fine coupling observed, 2H), 6.19 (s, 1H), 3.79 (s, 3H), 3.43 – 3.33 (m, 1H), 3.02 – 2.82 (m, 4H), 2.68 – 2.58 (m, 1H), 2.46 (t, *J* = 7.6 Hz, 2H), 2.28 (s, 6H), 2.26 – 2.19 (m, 1H).

^{13}C NMR (126 MHz, Chloroform-*d*): δ 171.9, 158.1, 141.0, 131.1, 129.9, 128.5, 128.4, 126.1, 114.1, 64.8, 55.3, 40.1, 39.5, 38.4, 31.8, 30.1.

IR (FTIR): 3305, 2928, 1666, 1453, 1242 cm^{-1}.

HRMS (ESI): $[M + H]^+$ Calcd for $C_{21}H_{29}N_2O_2$: 341.2229; Found 341.2234

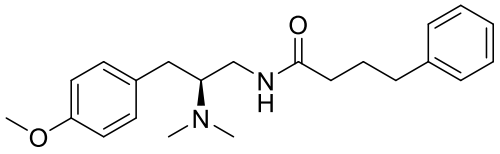

(*S*)-*N*-(2-(dimethylamino)-3-(4-methoxyphenyl)propyl)-4-phenylbutanamide (24a): In a small vial, 4-phenyl butyric acid (0.0303 g, 0.160 mmol, 1.00 equiv) was dissolved in 0.4 mL of DMF. HATU (0.0962 g, 0.240 mmol, 1.50 equiv) was added, followed by DIPEA (0.1 mL, 0.7 mmol, 3 equiv). This solution was stirred at room temperature for 1 hour. In a separate reaction flask charged with a stir bar, diamine **14** (0.0564 g, 0.240 mmol, 1.50 equiv) was dissolved in 0.3 mL of DMF. The solution of 4-phenyl butyric acid, HATU and DIPEA was added to the reaction

flask containing **14**. The reaction stirred at room temperature for 16 hours. After full disappearance of 4-phenyl butyric acid judged by TLC (5% MeOH/DCM) the reaction was concentrated *in vacuo*. The crude was purified via column chromatography, [1% Et_3N, 5% MeOH/DCM]. Concentration *in vacuo* and drying under high vacuum for 24 hours resulting in sub-mg quantities sent for biological testing.

TLC R*f*: 0.30 [5%MeOH/DCM]

^{1}H NMR (500 MHz, Chloroform-*d*): δ 7.33 – 7.28 (m, 2H), 7.24 – 7.19 (m, 3H), 7.09 (d, *J* = 8.6 Hz, additional unresolved fine coupling observed, 2H), 6.86 (d, *J* = 8.6 Hz, additional unresolved fine coupling observed, 2H), 3.82 (s, 3H), 3.45 (m, 1H), 2.97 (dt, *J* = 9.5, 2.4 Hz, additional unresolved fine coupling observed, 2H), 2.79 - 2.75 (m, 1H) 2.67 (t, *J* = 7.6 Hz, 2H), 2.38 (s, 6H), 2.35 – 2.29 (m, 1H), 2.18 (t, *J* = 7.3 Hz, 2H), 2.00-1.94 (m, 2H).

^{13}C NMR (126 MHz, Chloroform-*d*): δ 172.7, 158.2, 141.8, 131.0, 130.0, 128.6, 128.4, 126.0, 114.2, 65.0, 55.4, 40.2, 39.5, 35.3, 30.7, 27.2, 8.2.

HRMS (ESI): $[M + Na]^+$ Calcd for $C_{22}H_{30}N_2O_2Na$: 377.2205; Found 377.2203

Compound **24b**

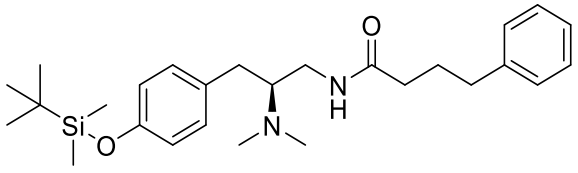

(*S*)-*N*-(3-(4-((tert-butyldimethylsilyl)oxy)phenyl)-2-(dimethylamino)propyl)-4-phenylbutanamide (24b): In a small vial, 4-phenyl butyric acid (0.0185 g, 0.120 mmol, 1.00 equiv) was dissolved in 0.2 mL of DMF. HATU (0.0514 g, 0.160 mmol, 1.50 equiv) was added, followed by DIPEA (0.056 mL, 0.32 mmol, 3.0 equiv). This solution was stirred at room

temperature for 1 hour. In a separate reaction flask charged with a stir bar, diamine **5** (0.0463 g, 0.160 mmol, 1.50 equiv) was dissolved in 0.3 mL of DMF. The solution of 4-phenyl butyric acid, HATU and DIPEA was added to the reaction flask containing **15**. The reaction stirred at room temperature for 16 hours. After full disappearance of 4-phenyl butyric acid judged by TLC (5% MeOH/DCM) the reaction was concentrated *in vacuo*. The crude was purified via column chromatography, [5% MeOH/DCM]. Concentration *in vacuo* and drying under high vacuum for 24 hours resulted in 0.0116 g (24%) of a yellowish oil.

TLC R*f*: 0.40 [5% MeOH/DCM]

HRMS (ESI): $[M + Na]^+$ Calcd for $C_{27}H_{42}N_2O_2NaSi$: 477.2913; Found 477.2911.

^{1}H NMR (500 MHz, Chloroform-*d*): δ 7.27-7.24 (m, 2H), 7.18-7.15 (m, 3H), 7.05 (d, *J* = 8.5 Hz, additional unresolved fine splitting observed, 2H), 6.79 (d, *J* = 8.5 Hz, additional unresolved fine splitting observed, 2H), 6.41 (s, 1H), 3.31 (s, 2H). 2.95 (d, *J* = 14 Hz, additional unresolved fine splitting observed, 2H), 2.62 (s, 6H), 2.66-2.60 (m, 2H), 2.58-2.53 (m, 1H), 2.23 (dt, *J* = 7.4, 3.5, 2H) 1.91 (quint, J = 7.7, 2H), 0.97 (s, 9H), 0.18 (s, 6H).

^{13}C NMR (126 MHz, Chloroform-*d*): δ 155.0, 141.6, 130.1, 128.7, 128.5, 126.1, 120.8, 40.0, 35.5, 35.3, 31.2, 27.0, 25.8, 18.3, -4.3.

Spectra

6

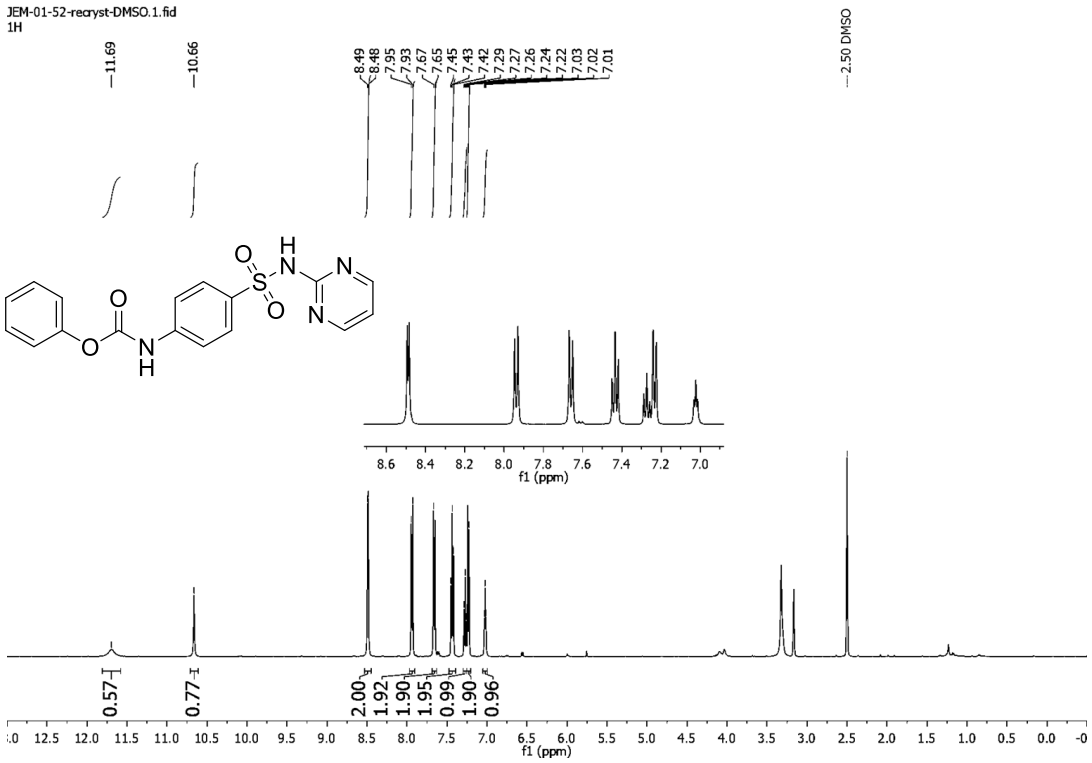
JEM-01-52-recryst-DMSO.1.fid
1H
11.69
10.66
8.49
8.48
7.95
7.93
7.67
7.65
7.45
7.43
7.42
7.29
7.27
7.26
7.24
7.22
7.03
7.02
7.01
2.50 DMSO
f1 (ppm)
0.57
0.77
2.00
1.92
1.90
1.95
0.99
1.90
0.96

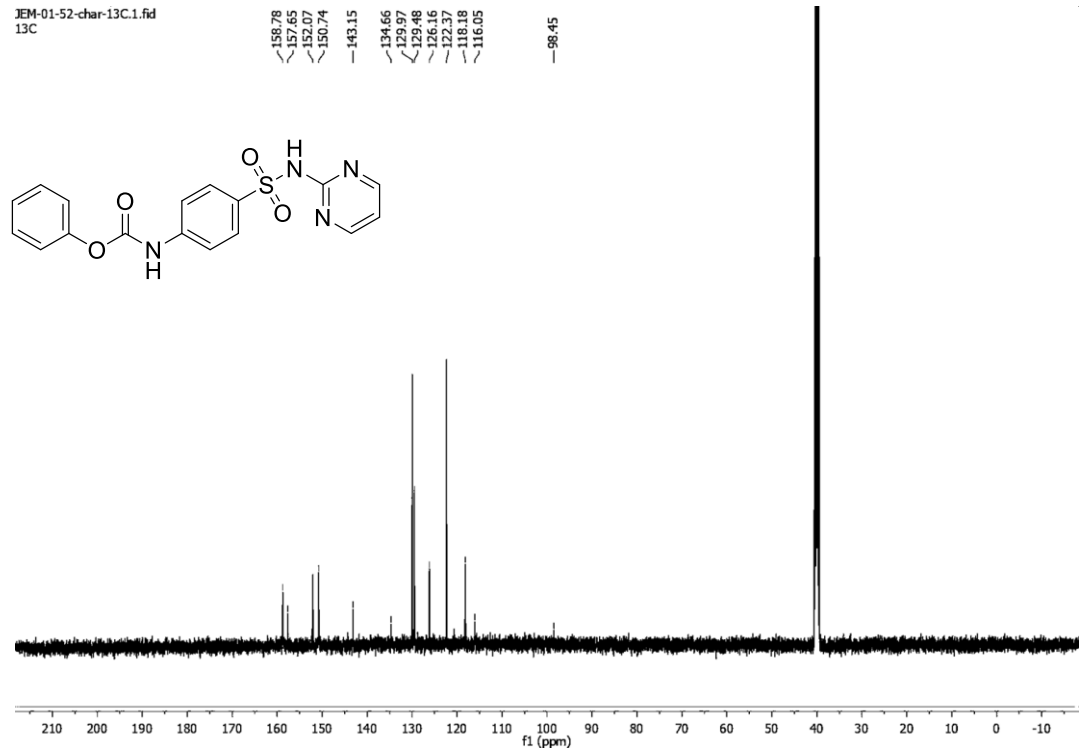
JEM-01-52-char-13C.1.fid
13C
158.78
157.65
152.07
150.74
143.15
134.66
129.97
129.48
126.16
122.37
118.18
116.05
98.45
f1 (ppm)

6a

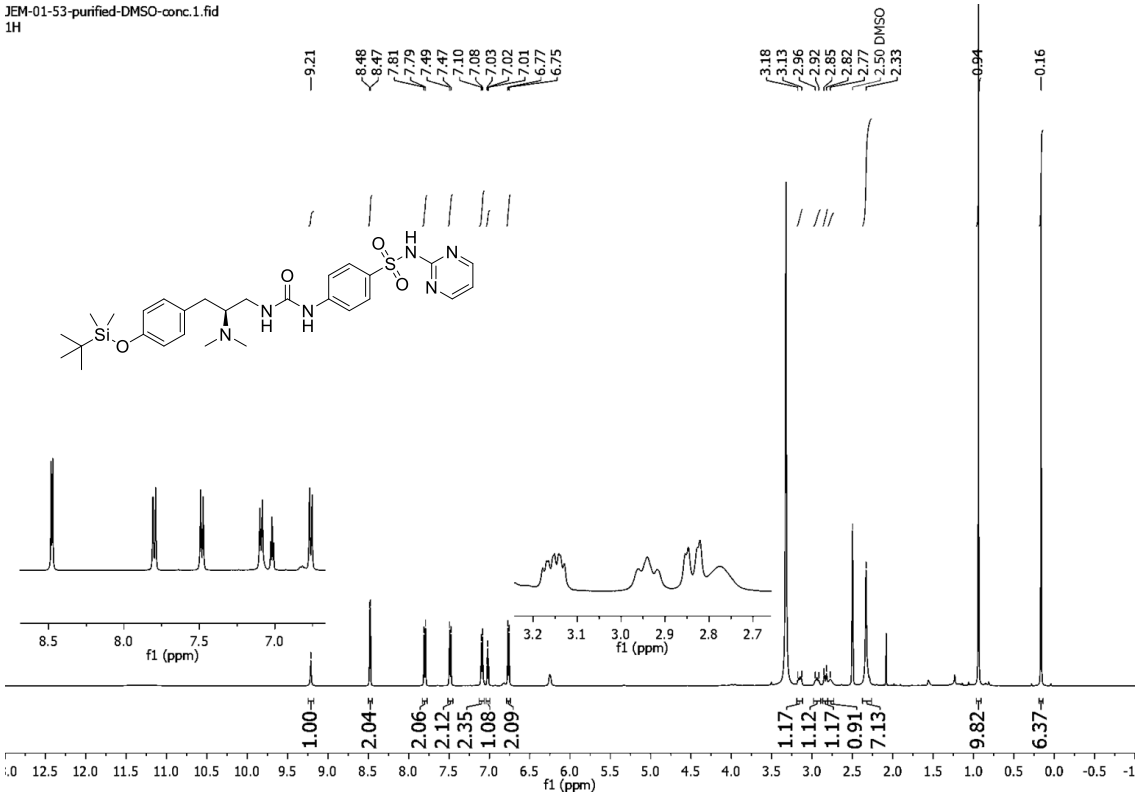
JEM-01-53-purified-DMSO-conc.1.fid
1H
9.21
8.48
8.47
7.81
7.79
7.49
7.47
7.10
7.08
7.03
7.02
7.01
6.77
6.75
3.18
3.13
2.96
2.92
2.85
2.82
2.77
2.50 DMSO
2.33
0.94
0.16
1.00
2.04
2.06
2.12
2.35
1.08
2.09
1.17
1.12
1.17
0.91
7.13
9.82
6.37
f1 (ppm)

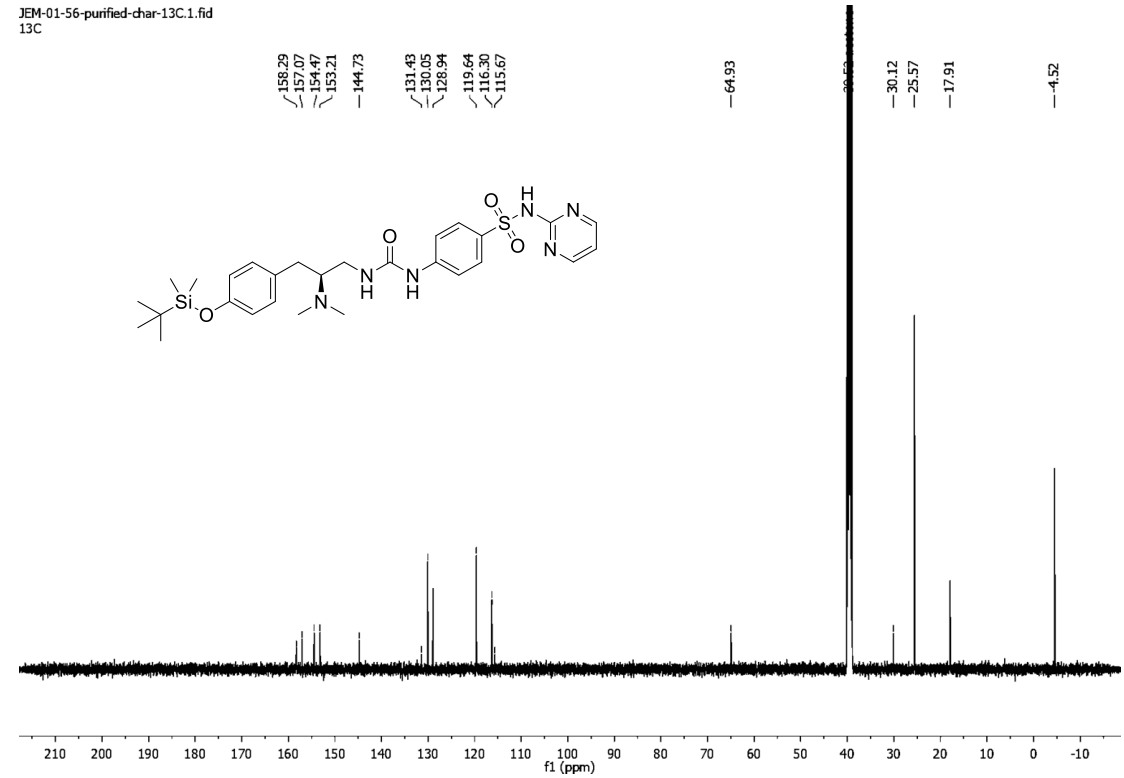
JEM-01-56-purified-char-13C.1.fid
13C
158.29
157.07
154.47
153.21
144.73
131.43
130.05
128.94
119.64
116.30
115.67
64.93
30.12
25.57
17.91
-4.52
f1 (ppm)

7

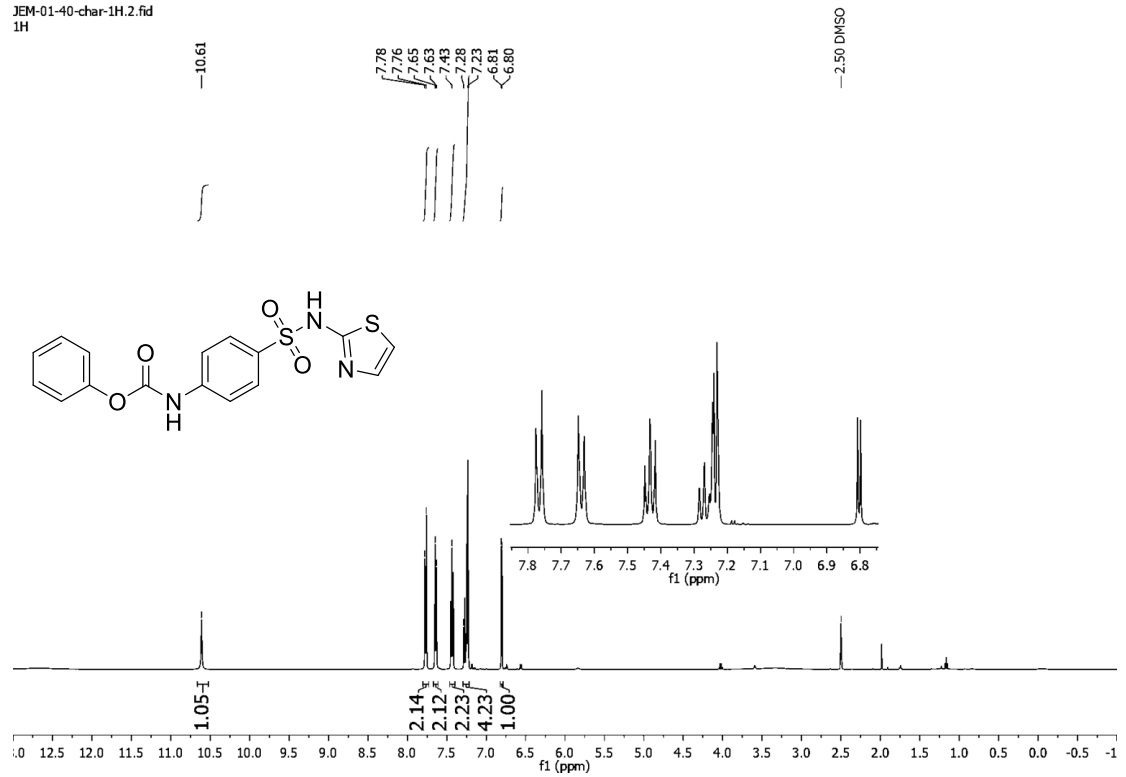
JEM-01-40-char-1H.2.fid
1H
10.61
7.78
7.76
7.65
7.63
7.43
7.28
7.23
6.81
6.80
2.50 DMSO
1.05
2.14
2.12
2.23
4.23
1.00
f1 (ppm)

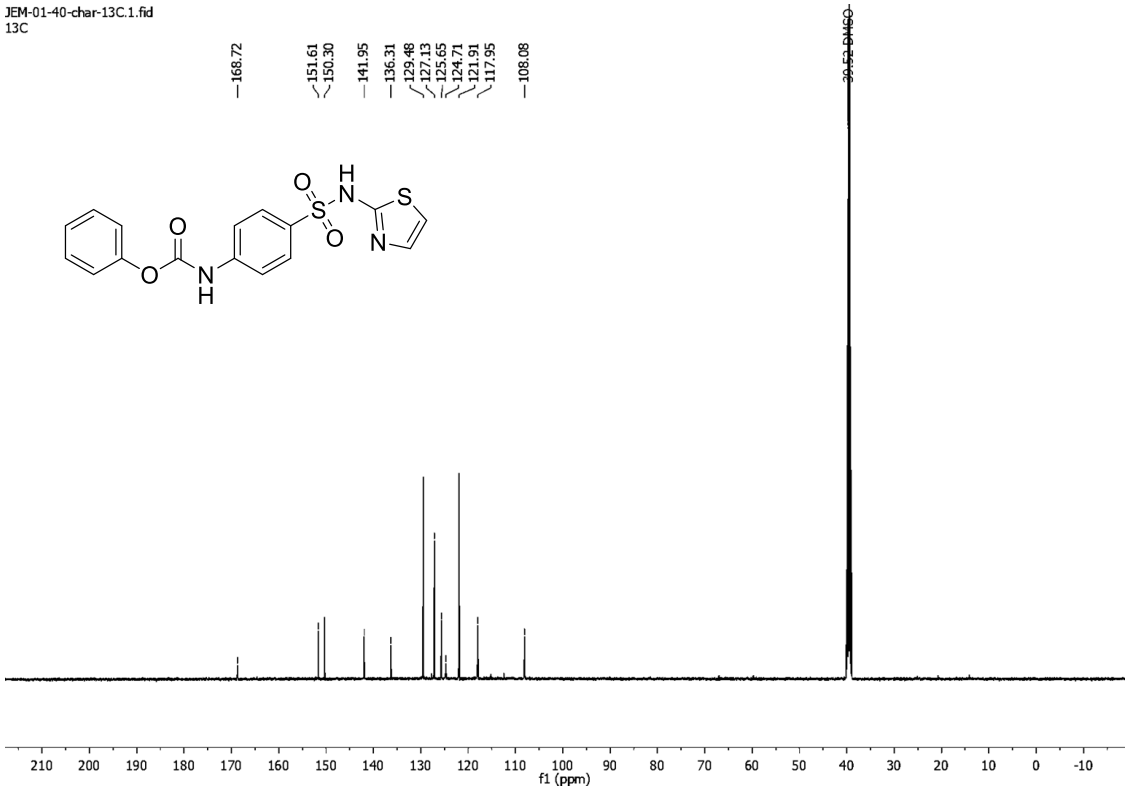
JEM-01-40-char-13C.1.fid
13C
168.72
151.61
150.30
141.95
136.31
129.48
127.13
125.65
124.71
121.91
117.95
108.08
39.52 DMSO
f1 (ppm)

7a

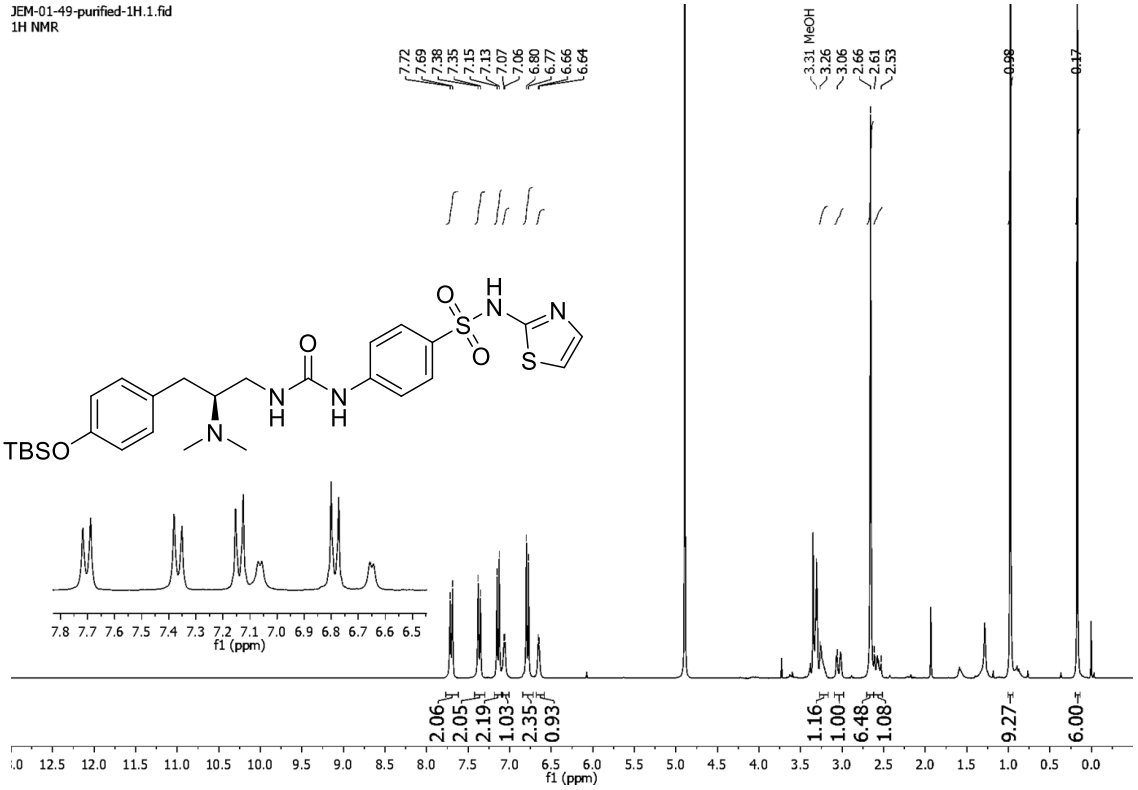
JEM-01-49-purified-1H.1.fid
1H NMR
7.72
7.69
7.38
7.35
7.15
7.13
7.07
7.06
6.80
6.77
6.66
6.64
3.31 MeOH
3.26
3.06
2.66
2.61
2.53
0.98
0.17
TBSO
2.06
2.05
2.19
1.03
2.35
0.93
1.16
1.00
6.48
1.08
9.27
6.00
f1 (ppm)

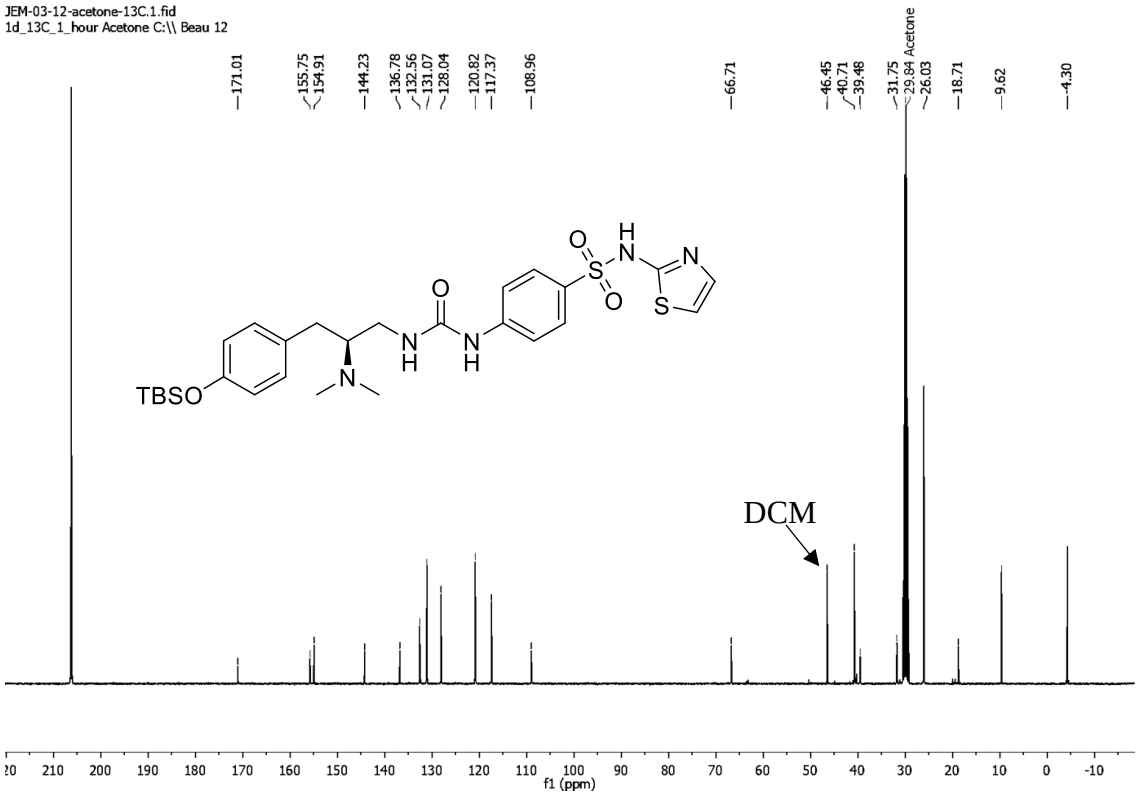
JEM-03-12-acetone-13C.1.fid
1d_13C_1_hour Acetone C:\\ Beau 12
171.01
155.75
154.91
144.23
136.78
132.56
131.07
128.04
120.82
117.37
108.96
66.71
46.45
40.71
39.48
31.75
29.84 Acetone
26.03
18.71
9.62
-4.30
TBSO
DCM
f1 (ppm)

7b

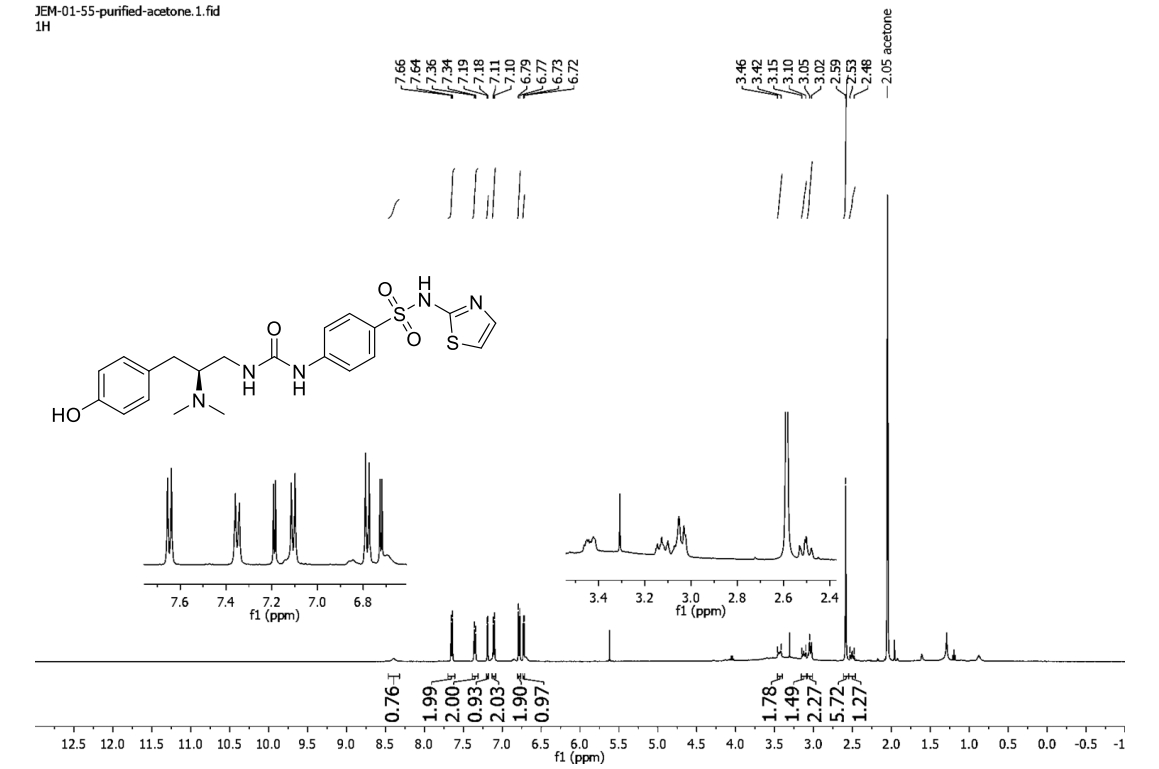
JEM-01-55-purified-acetone.1.fid
1H
7.66
7.64
7.36
7.34
7.19
7.18
7.11
7.10
6.79
6.77
6.73
6.72
3.46
3.42
3.15
3.10
3.05
3.02
2.59
2.53
2.48
2.05 acetone
HO
f1 (ppm)
0.76
1.99
2.00
0.93
2.03
1.90
0.97
1.78
1.49
2.27
5.72
1.27

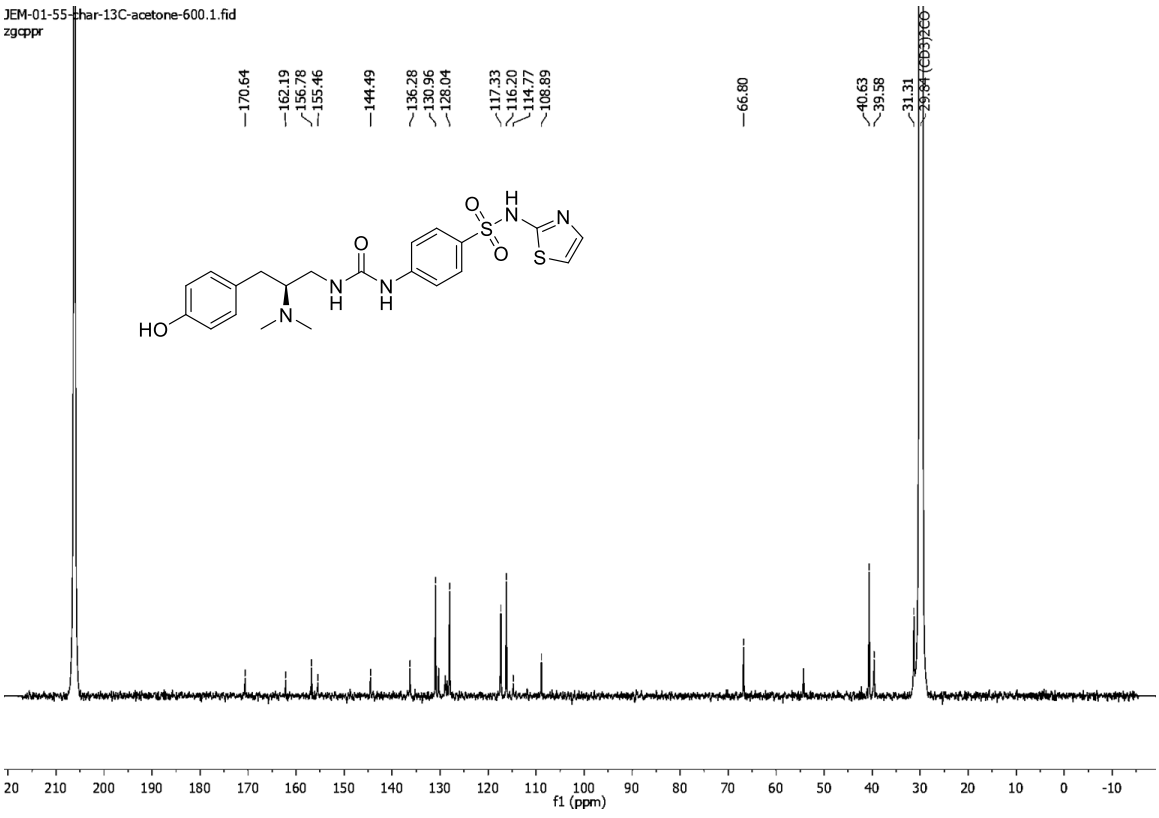
JEM-01-55-char-13C-acetone-600.1.fid
zgcppr
170.64
162.19
156.78
155.46
144.49
136.28
130.96
128.04
117.33
116.20
114.77
108.89
66.80
40.63
39.58
31.31
29.84 (CD3)2CO
HO
f1 (ppm)

7c

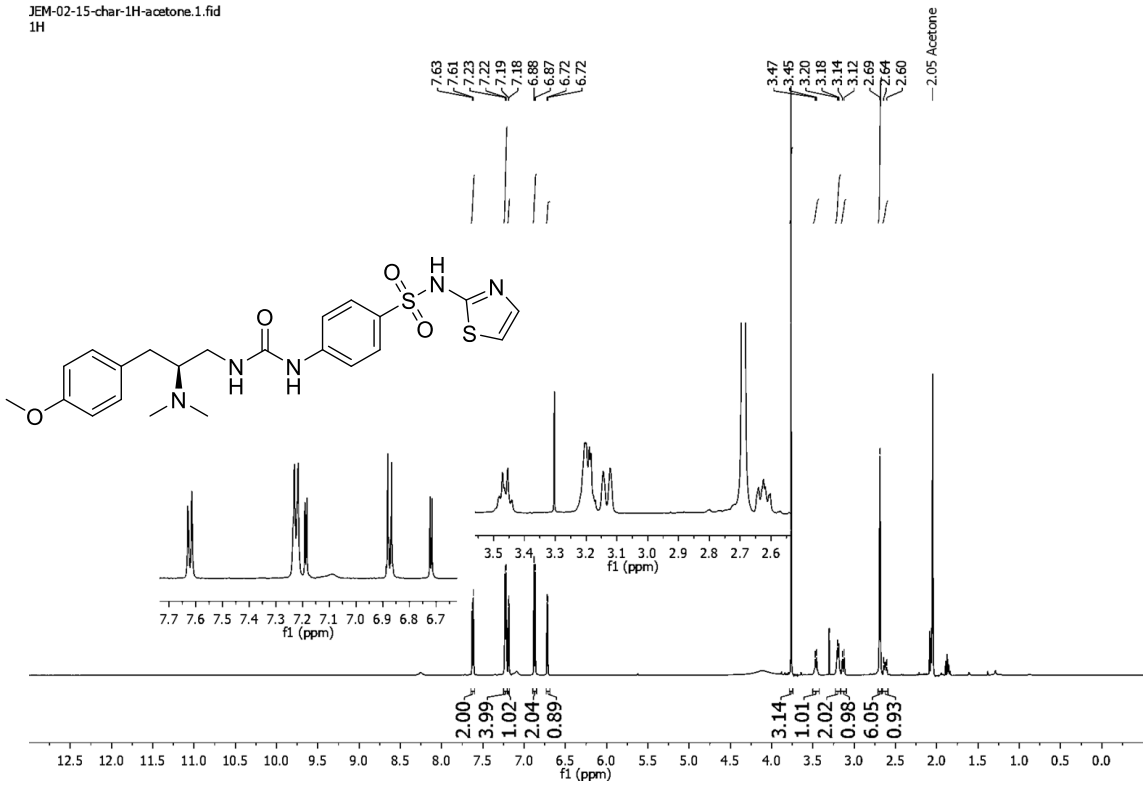
JEM-02-15-char-1H-acetone.1.fid
1H
7.63
7.61
7.23
7.22
7.19
7.18
6.88
6.87
6.72
6.72
3.47
3.45
3.20
3.18
3.14
3.12
2.69
2.64
2.60
2.05 Acetone
2.00
3.99
1.02
2.04
0.89
3.14
1.01
2.02
0.98
6.05
0.93
f1 (ppm)

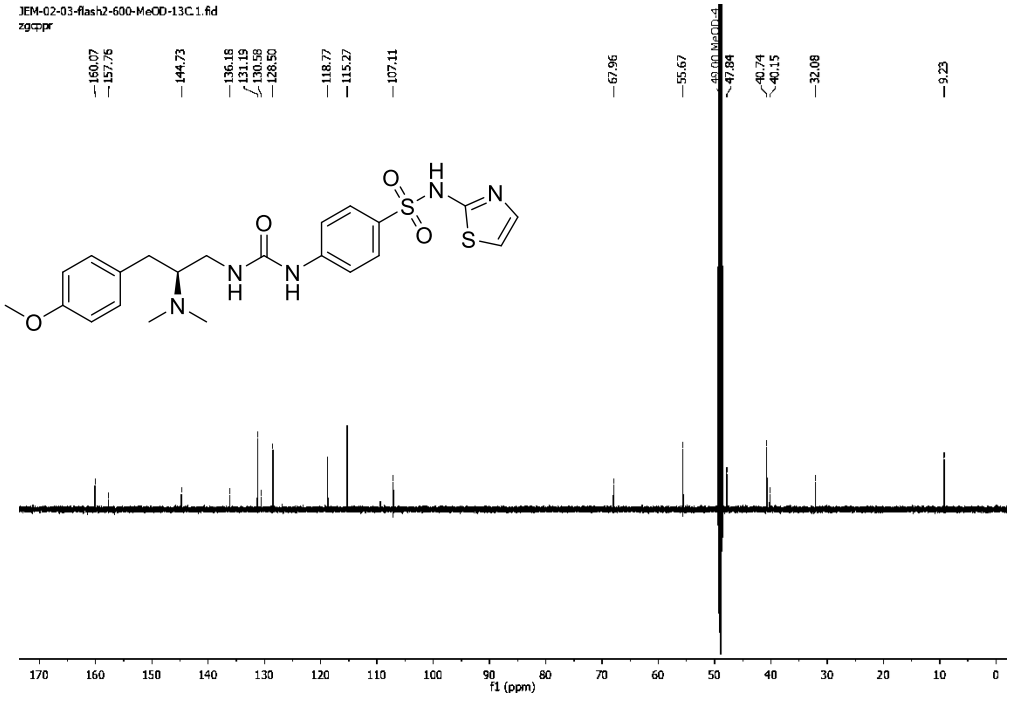
JEM-02-03-flash2-600-MeOD-13C.1.fid
zgcppr
160.07
157.76
144.73
136.18
131.19
130.98
128.50
118.77
115.27
107.11
67.96
55.67
49.00 MeOD-d4
47.84
40.74
40.15
32.08
9.23
f1 (ppm)

9a

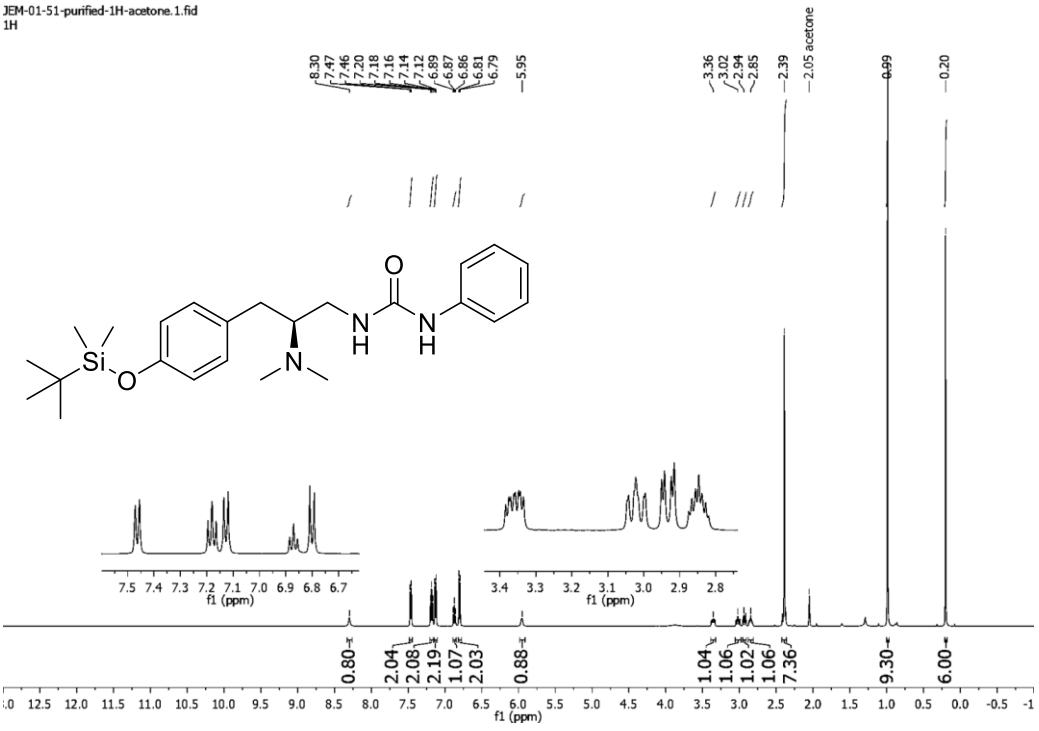
JEM-01-51-purified-1H-acetone.1.fid
1H
8.30
7.47
7.46
7.20
7.18
7.16
7.14
7.12
6.89
6.87
6.86
6.81
6.79
5.95
3.36
3.02
2.94
2.85
2.39
2.05 acetone
0.99
0.20
0.80
2.04
2.08
2.19
1.07
2.03
0.88
1.04
1.06
1.02
1.06
7.36
9.30
6.00
f1 (ppm)

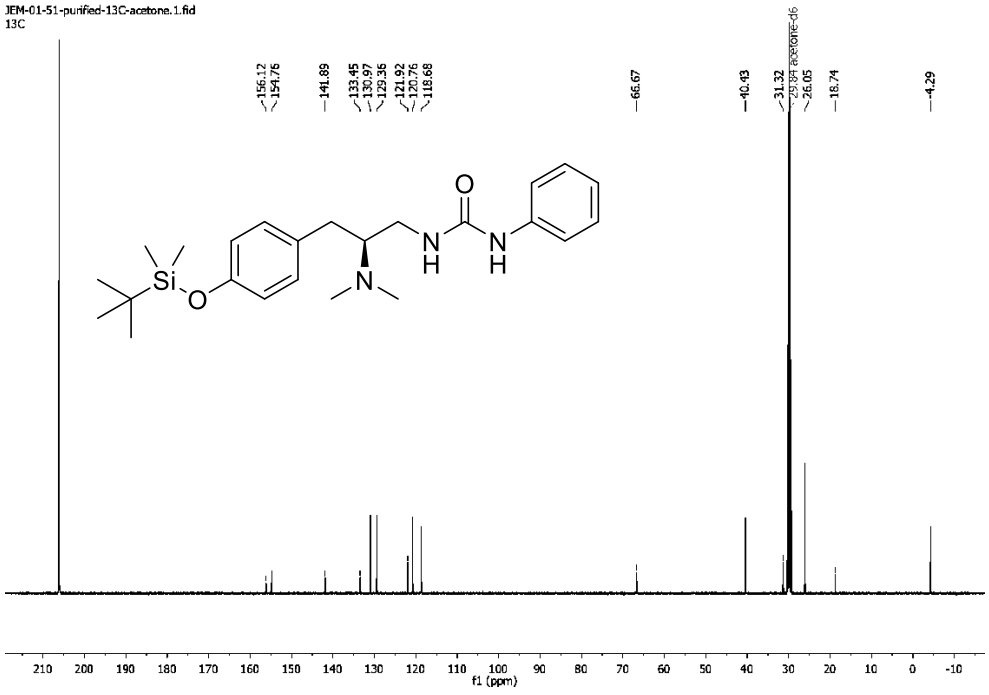
JEM-01-51-purified-13C-acetone.1.fid
13C
156.12
154.76
141.89
133.45
130.97
129.36
121.92
120.76
118.68
66.67
40.43
31.32
29.84 acetone-d6
26.05
18.74
-4.29
f1 (ppm)

11

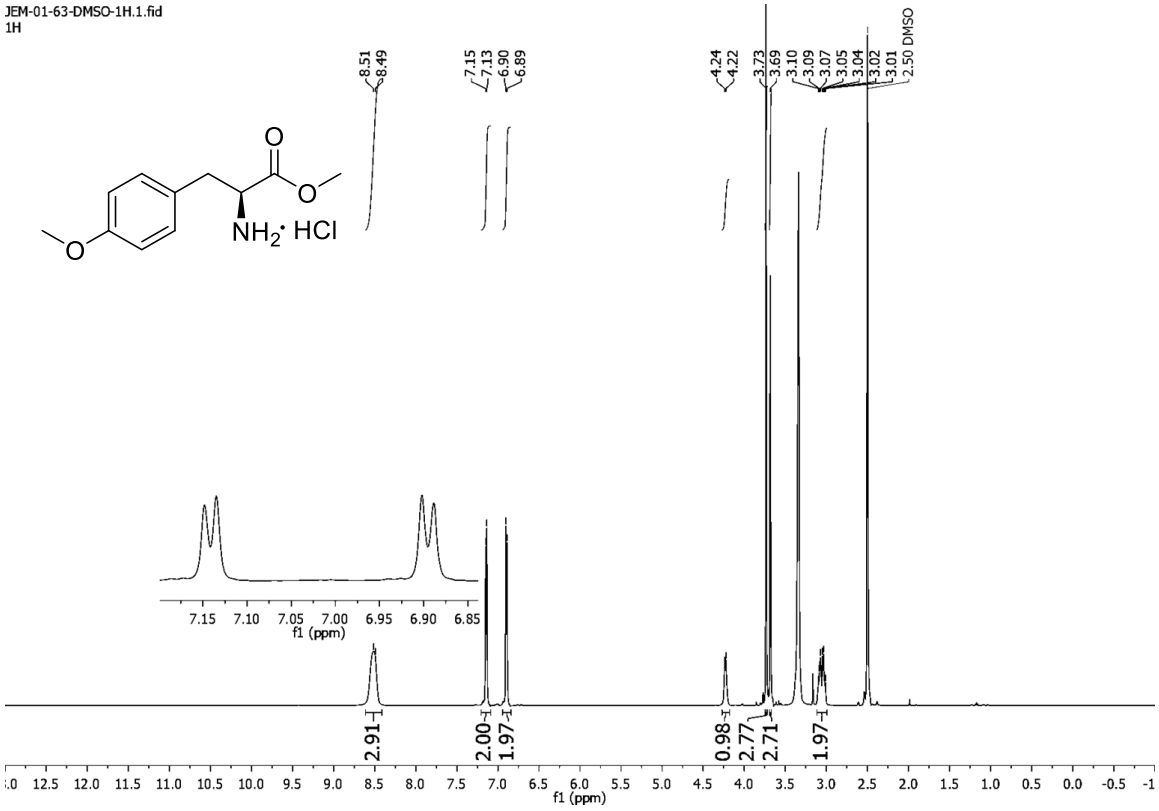
JEM-01-63-DMSO-1H.1.fid
1H
8.51
8.49
7.15
7.13
6.90
6.89
4.24
4.22
3.73
3.69
3.10
3.09
3.07
3.05
3.04
3.02
3.01
2.50 DMSO
O
O
NH2· HCl
O
7.15 7.10 7.05 7.00 6.95 6.90 6.85
f1 (ppm)
2.91
2.00
1.97
0.98
2.77
2.71
1.97
f1 (ppm)

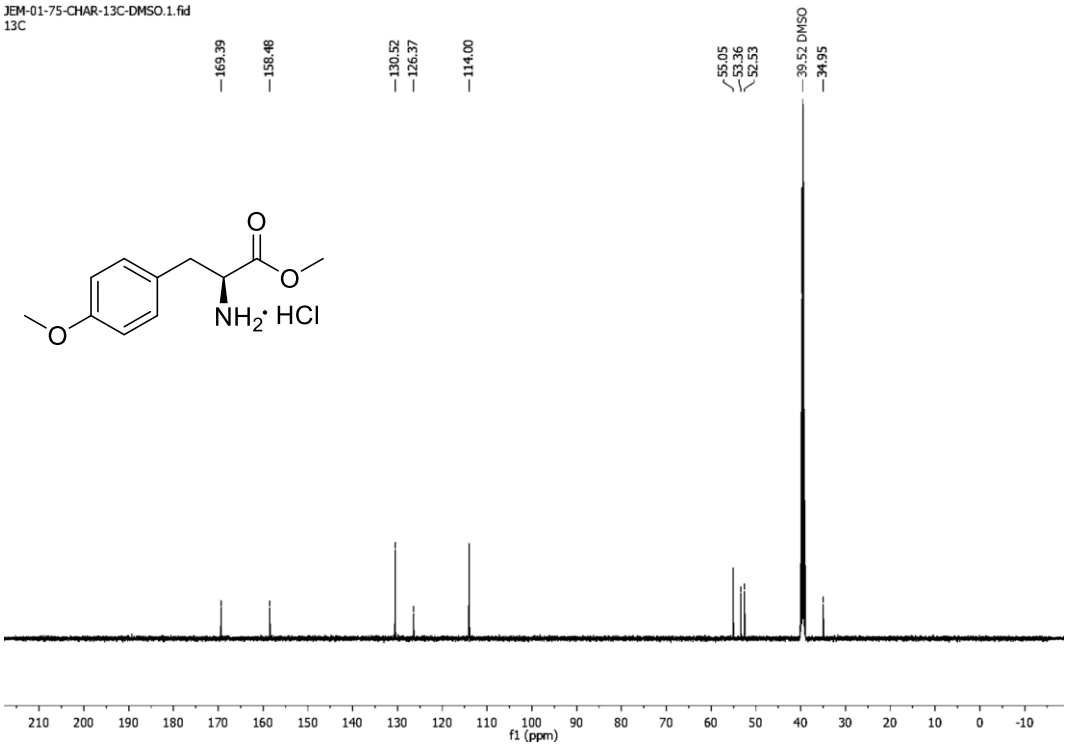
JEM-01-75-CHAR-13C-DMSO.1.fid
13C
169.39
158.48
130.52
126.37
114.00
55.05
53.36
52.53
39.52 DMSO
34.95
O
O
NH2· HCl
O
f1 (ppm)

12

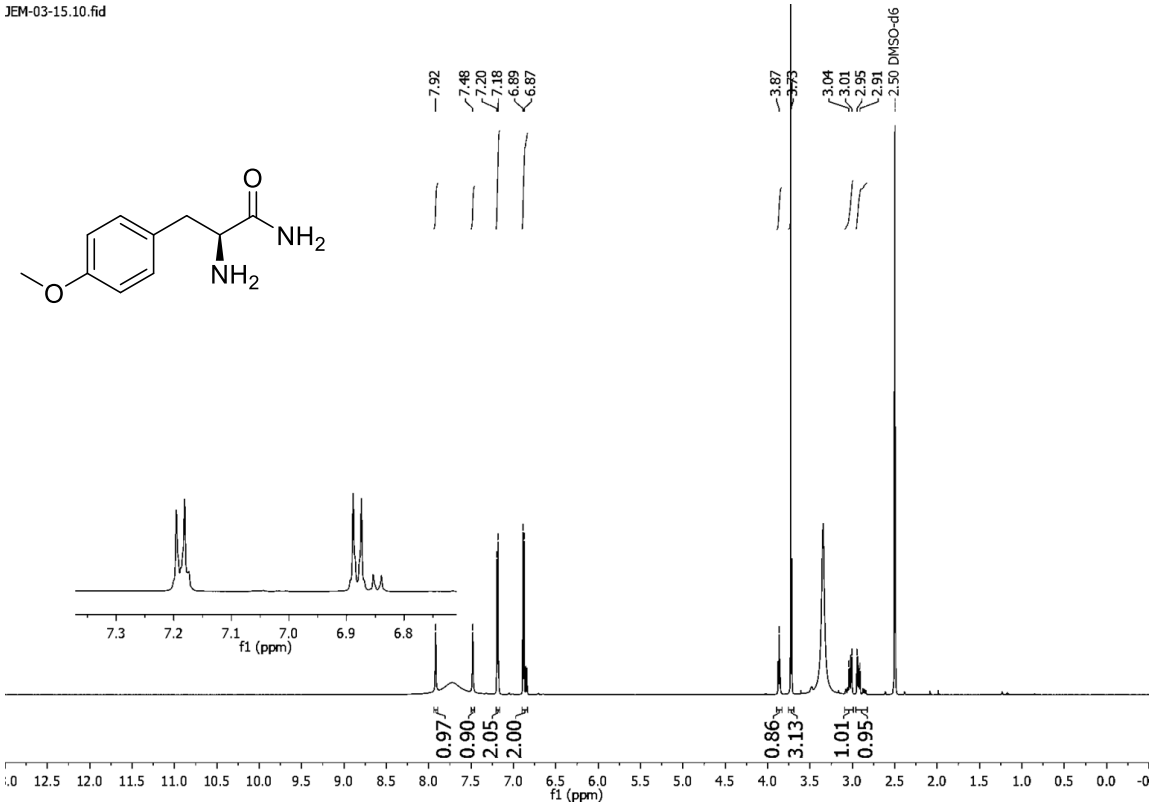
JEM-03-15.10.fid
7.92
7.48
7.20
7.18
6.89
6.87
3.87
3.73
3.04
3.01
2.95
2.91
2.50 DMSO-d6
O
NH2
NH2
O
7.3
7.2
7.1
7.0
6.9
6.8
f1 (ppm)
0.97
0.90
2.05
2.00
0.86
3.13
1.01
0.95
f1 (ppm)

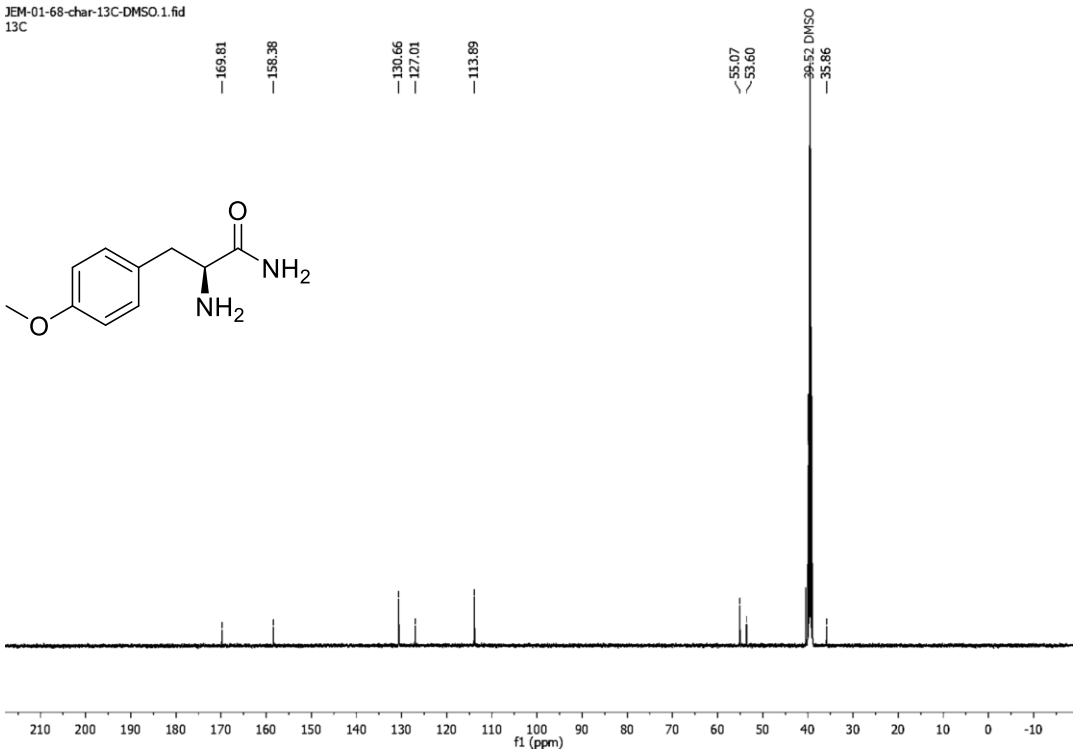
JEM-01-68-char-13C-DMSO.1.fid
13C
169.81
158.38
130.66
127.01
113.89
55.07
53.60
39.52 DMSO
35.86
O
NH2
NH2
O
f1 (ppm)

13

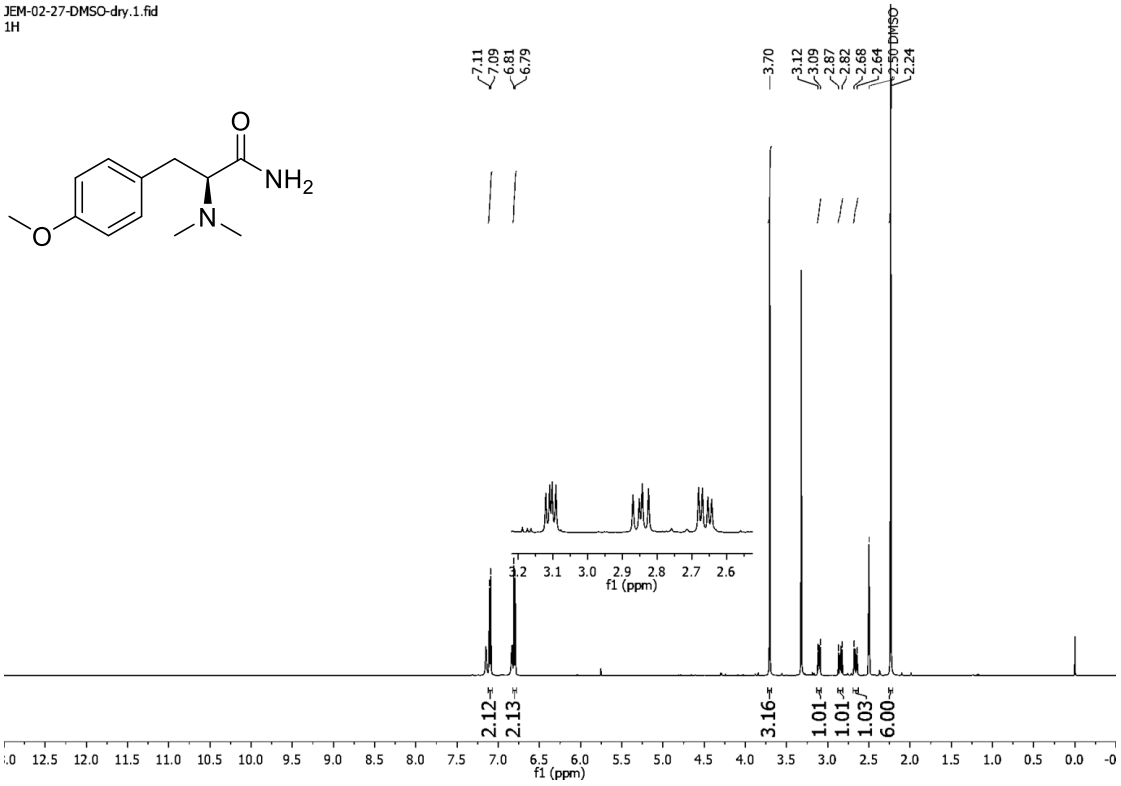
JEM-02-27-DMSO-dry.1.fid
1H
7.11
7.09
6.81
6.79
3.70
3.12
3.09
2.87
2.82
2.68
2.64
2.50 DMSO
2.24
O
NH2
N
O
3.2 3.1 3.0 2.9 2.8 2.7 2.6
f1 (ppm)
2.12
2.13
3.16
1.01
1.01
1.03
6.00
f1 (ppm)

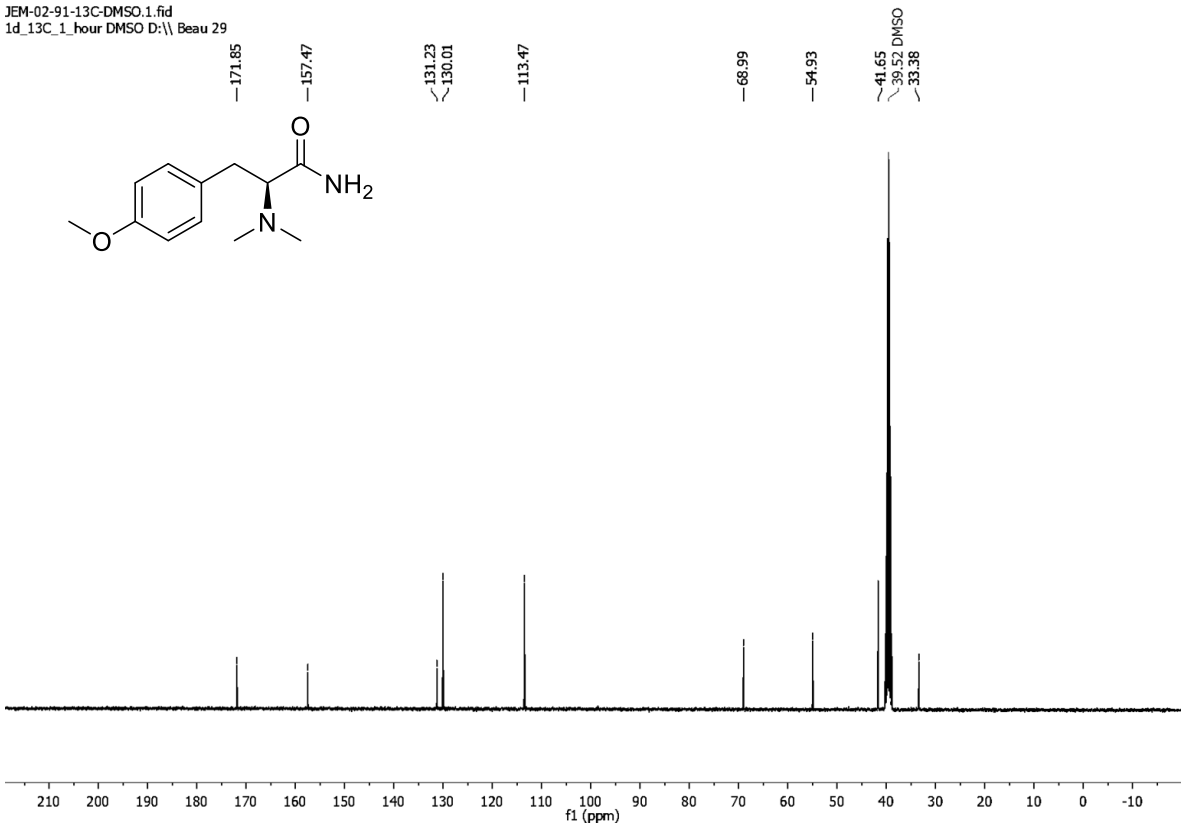
JEM-02-91-13C-DMSO.1.fid
1d_13C_1_hour DMSO D:\\ Beau 29
171.85
157.47
131.23
130.01
113.47
68.99
54.93
41.65
39.52 DMSO
33.38
O
NH2
N
O
f1 (ppm)

14

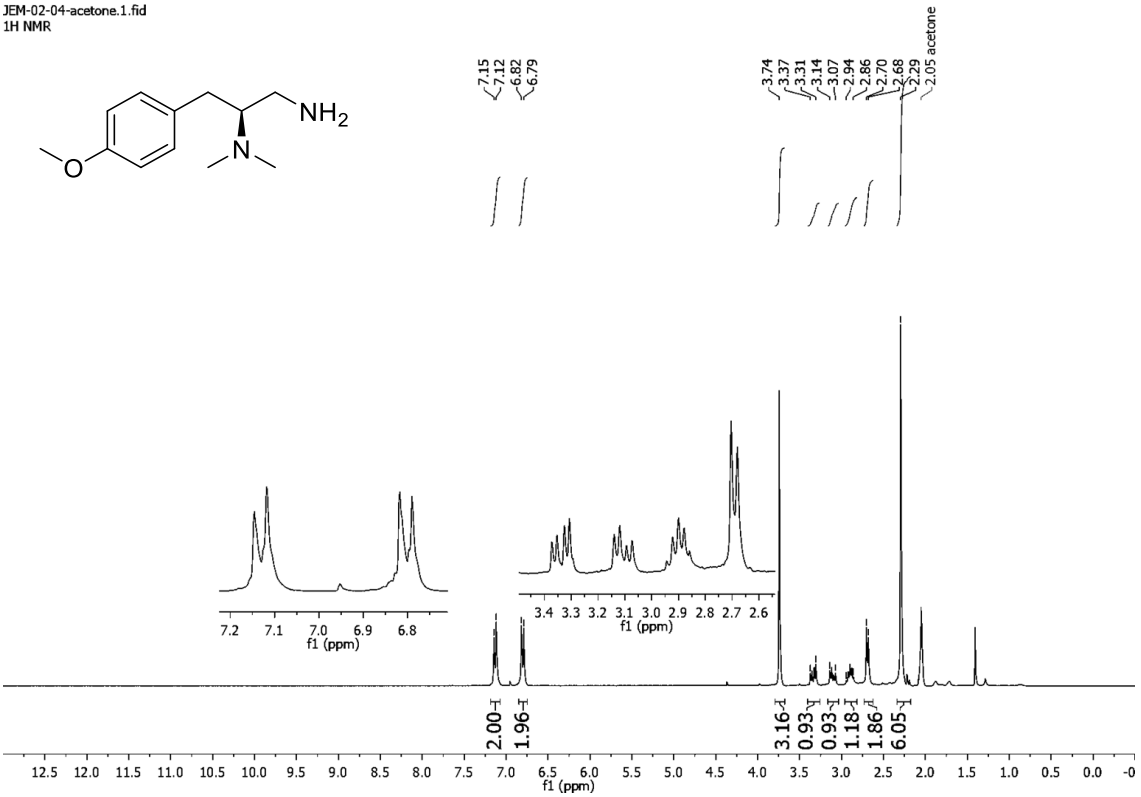
JEM-02-04-acetone.1.fid
1H NMR
NH2
O
N
7.15
7.12
6.82
6.79
3.74
3.37
3.31
3.14
3.07
2.94
2.86
2.70
2.68
2.29
2.05 acetone
2.00
1.96
3.16
0.93
0.93
1.18
1.86
6.05
f1 (ppm)

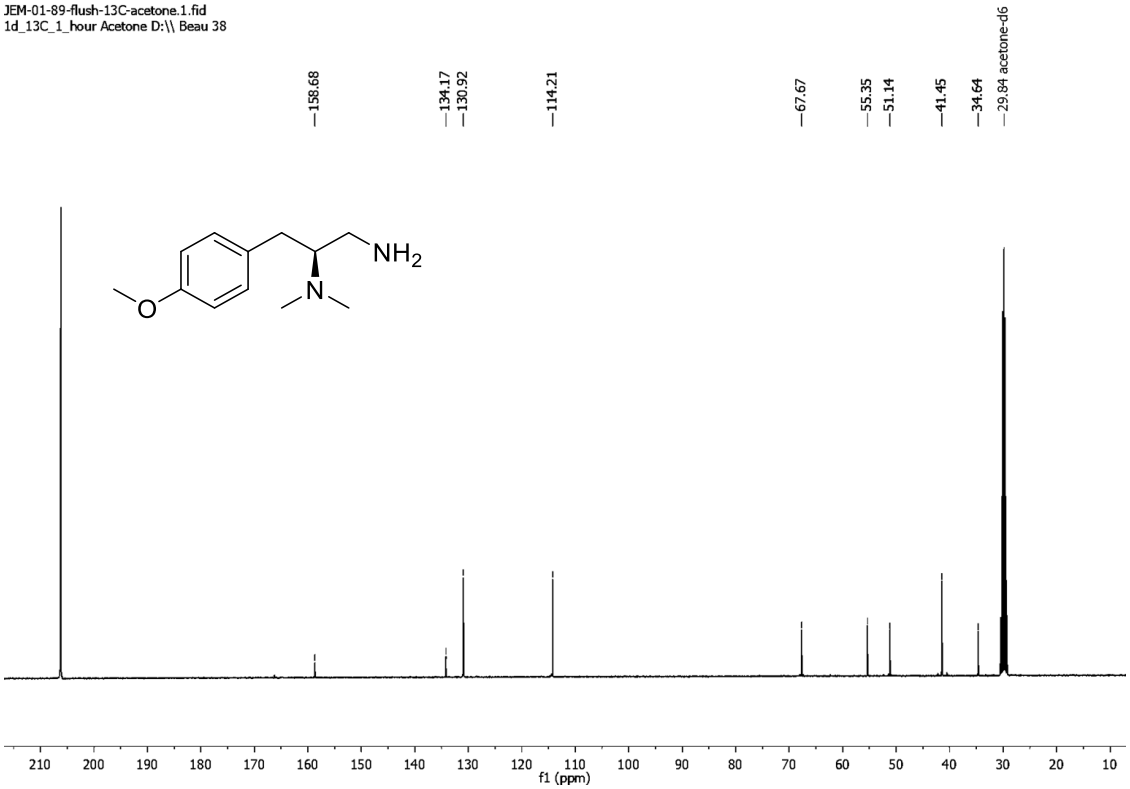
JEM-01-89-flush-13C-acetone.1.fid
1d_13C_1_hour Acetone D:\\ Beau 38
158.68
134.17
130.92
114.21
67.67
55.35
51.14
41.45
34.64
29.84 acetone-d6
NH2
O
N
f1 (ppm)

15

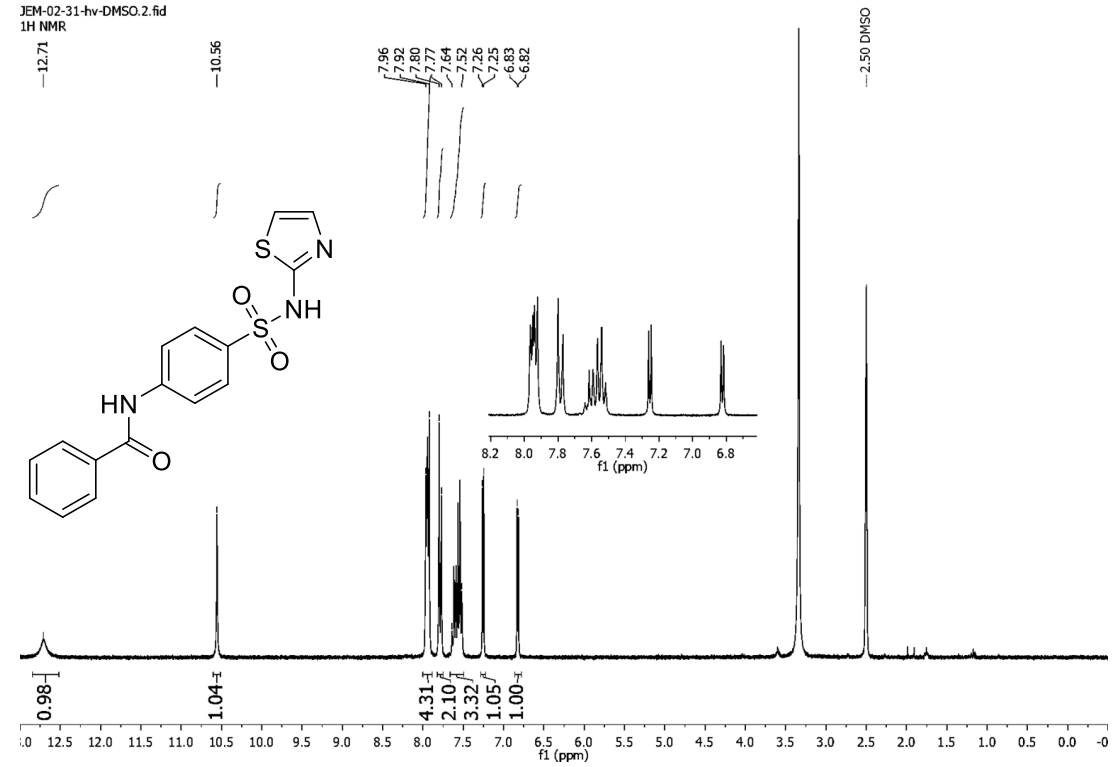
JEM-02-31-hv-DMSO.2.fid
1H NMR
12.71
10.56
7.96
7.92
7.80
7.77
7.64
7.52
7.26
7.25
6.83
6.82
2.50 DMSO
0.98
1.04
4.31
2.10
3.32
1.05
1.00
f1 (ppm)

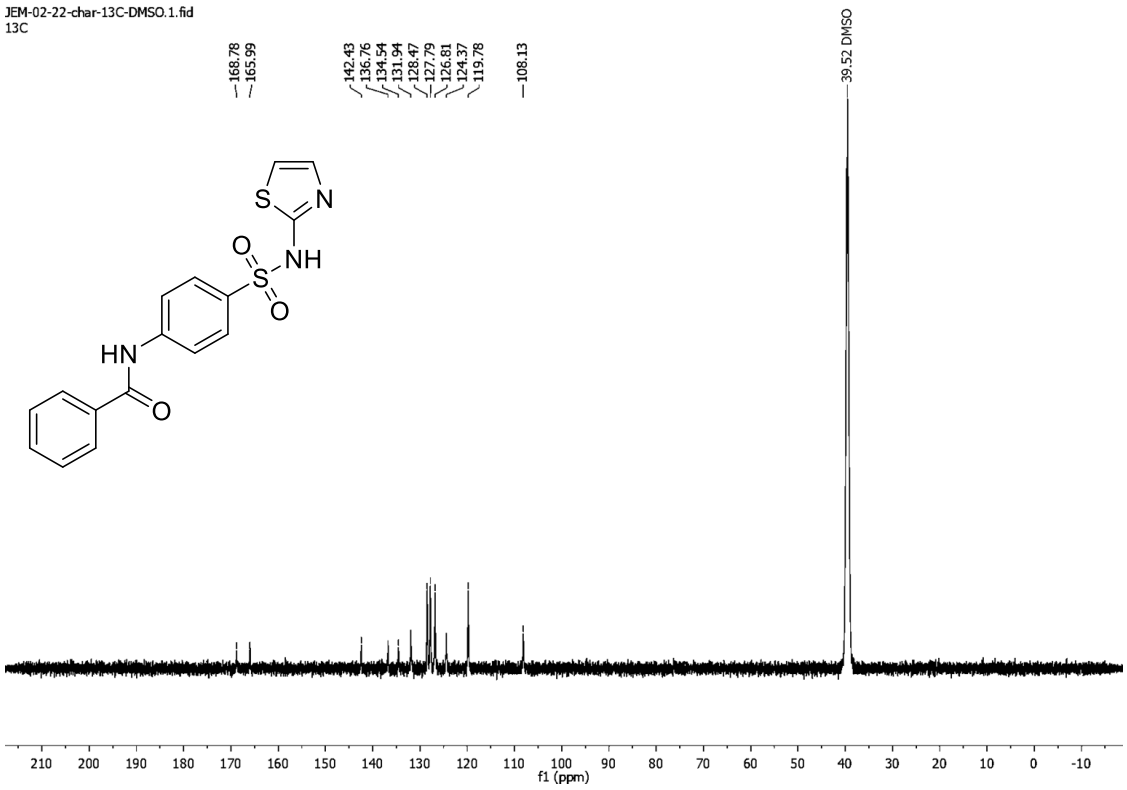
JEM-02-22-char-13C-DMSO.1.fid
13C
168.78
165.99
142.43
136.76
134.54
131.94
128.47
127.79
126.81
124.37
119.78
108.13
39.52 DMSO
f1 (ppm)

16 – spectral data corresponds to literature reference

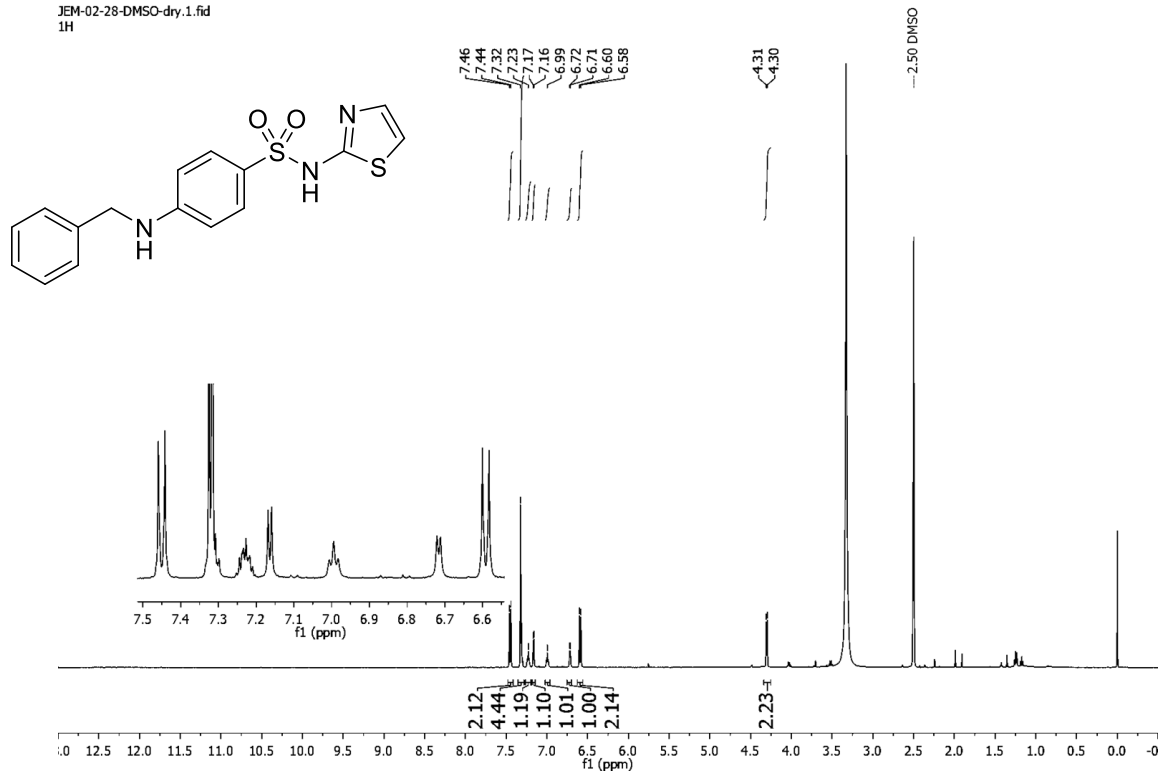

17

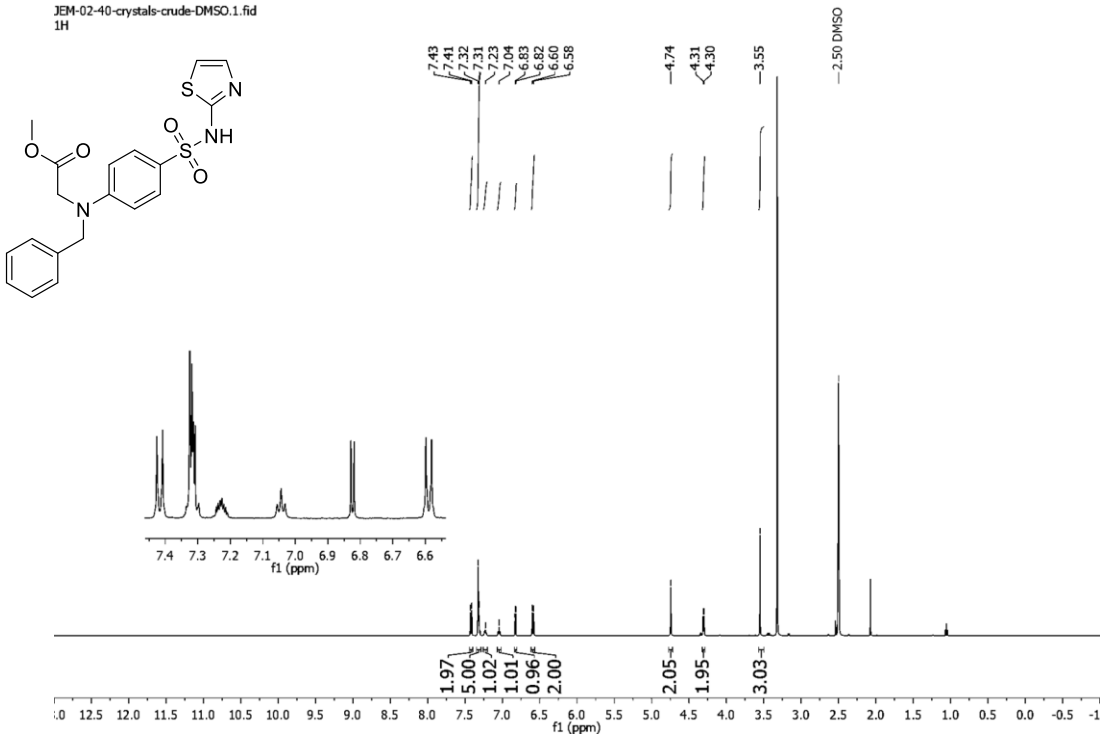
JEM-02-40-crystals-crude-DMSO.1.fid
1H
7.43
7.41
7.32
7.31
7.23
7.04
6.83
6.82
6.60
6.58
4.74
4.31
4.30
3.55
2.50 DMSO
1.97
5.00
1.02
1.01
0.96
2.00
2.05
1.95
3.03
f1 (ppm)

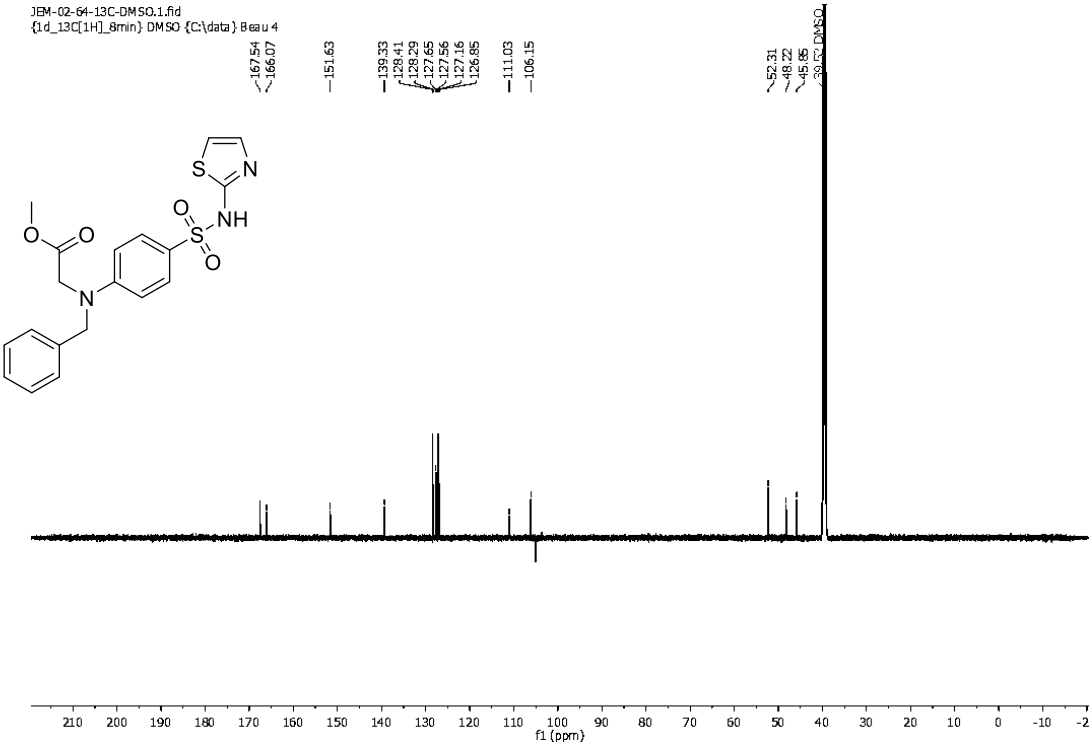
JEM-02-64-13C-DMSO.1.fid
{1d_13C{1H}_8min} DMSO {C:\data} Beau 4
167.54
166.07
151.63
139.33
128.41
128.29
127.65
127.56
127.16
126.85
111.03
106.15
52.31
48.22
45.85
39.52 DMSO
f1 (ppm)

18a

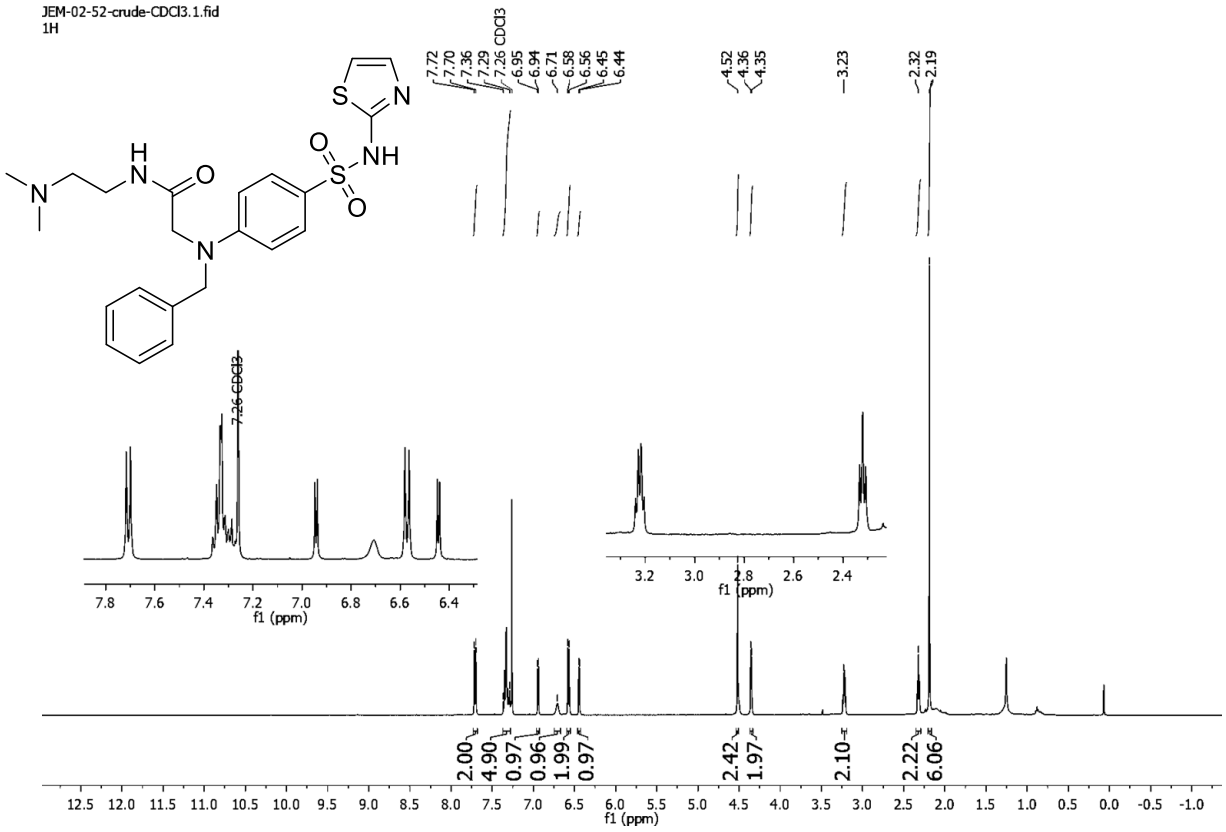
JEM-02-52-crude-CDCl3.1.fid
1H
7.72
7.70
7.36
7.29
7.26 CDCl3
6.95
6.94
6.71
6.58
6.56
6.45
6.44
4.52
4.36
4.35
3.23
2.32
2.19
2.00
4.90
0.97
0.96
1.99
0.97
2.42
1.97
2.10
2.22
6.06
f1 (ppm)

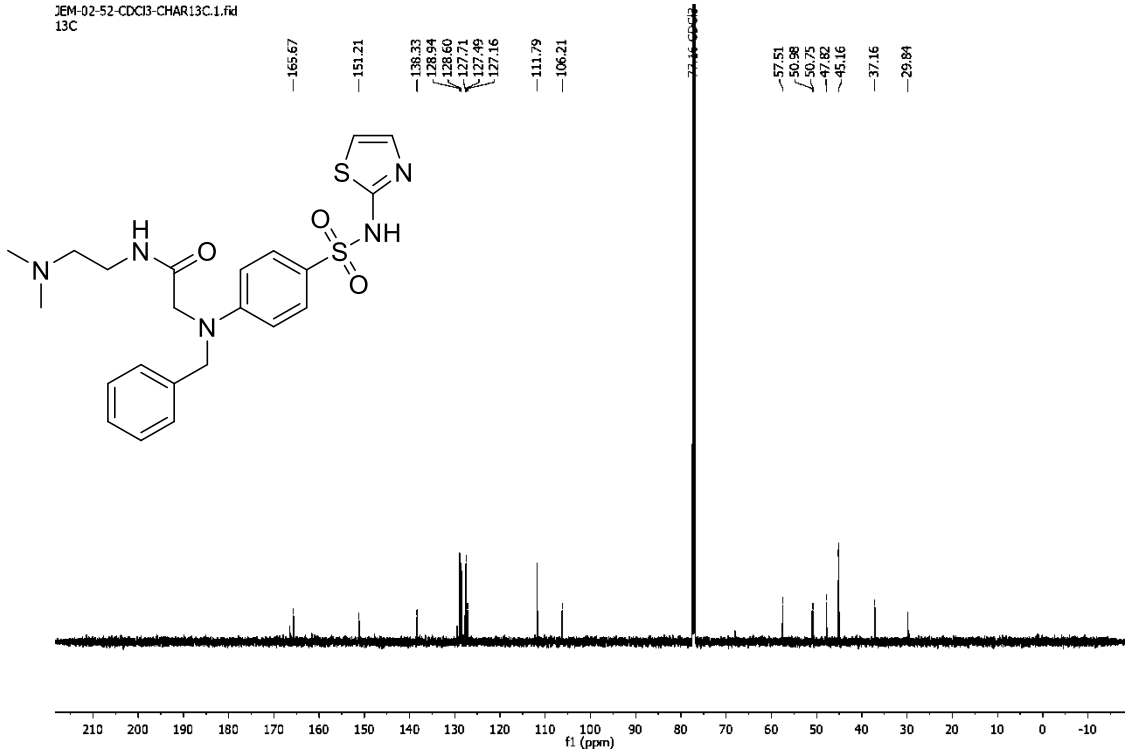
JEM-02-52-CDCl3-CHAR13C.1.fid
13C
165.67
151.21
138.33
128.94
128.60
127.71
127.49
127.16
111.79
106.21
77.16 CDCl3
57.51
50.98
50.75
47.82
45.16
37.16
29.84
f1 (ppm)

18b

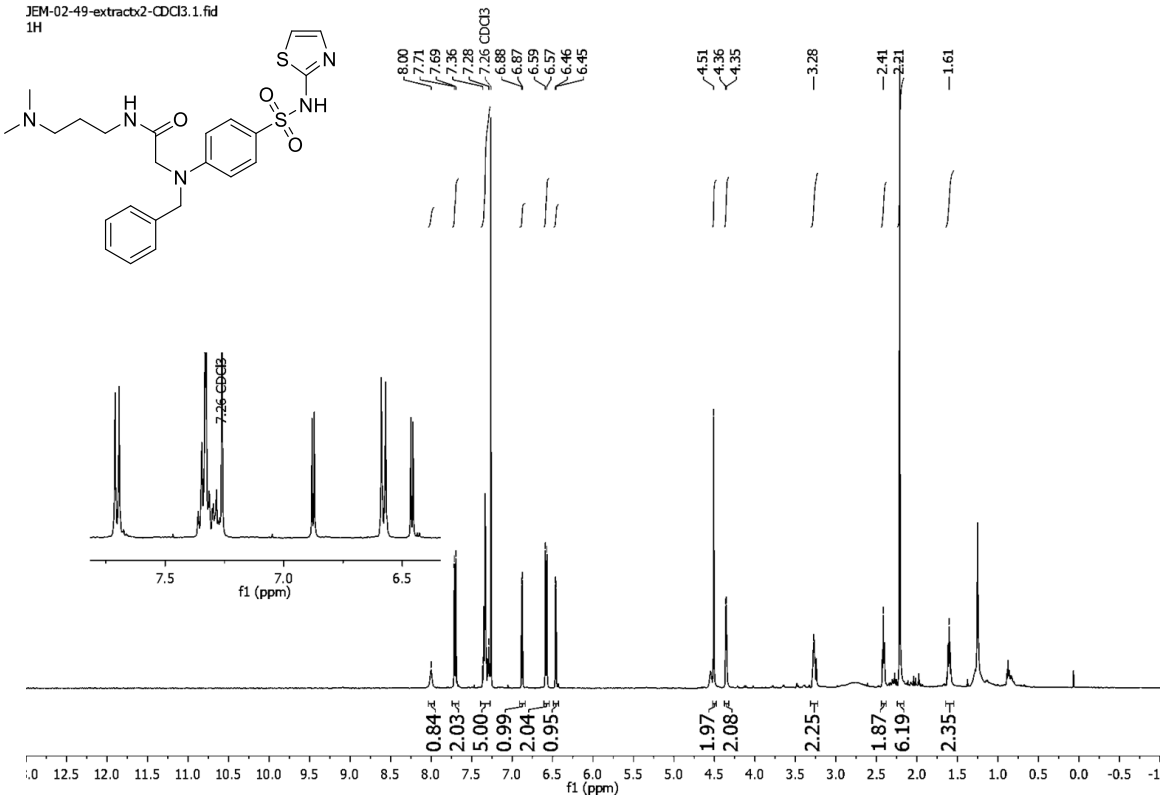
JEM-02-49-extractx2-CDCl3.1.fid
1H
8.00
7.71
7.69
7.36
7.28
7.26 CDCl3
6.88
6.87
6.59
6.57
6.46
6.45
4.51
4.36
4.35
3.28
2.41
2.21
1.61
0.84
2.03
5.00
0.99
2.04
0.95
1.97
2.08
2.25
1.87
6.19
2.35
f1 (ppm)

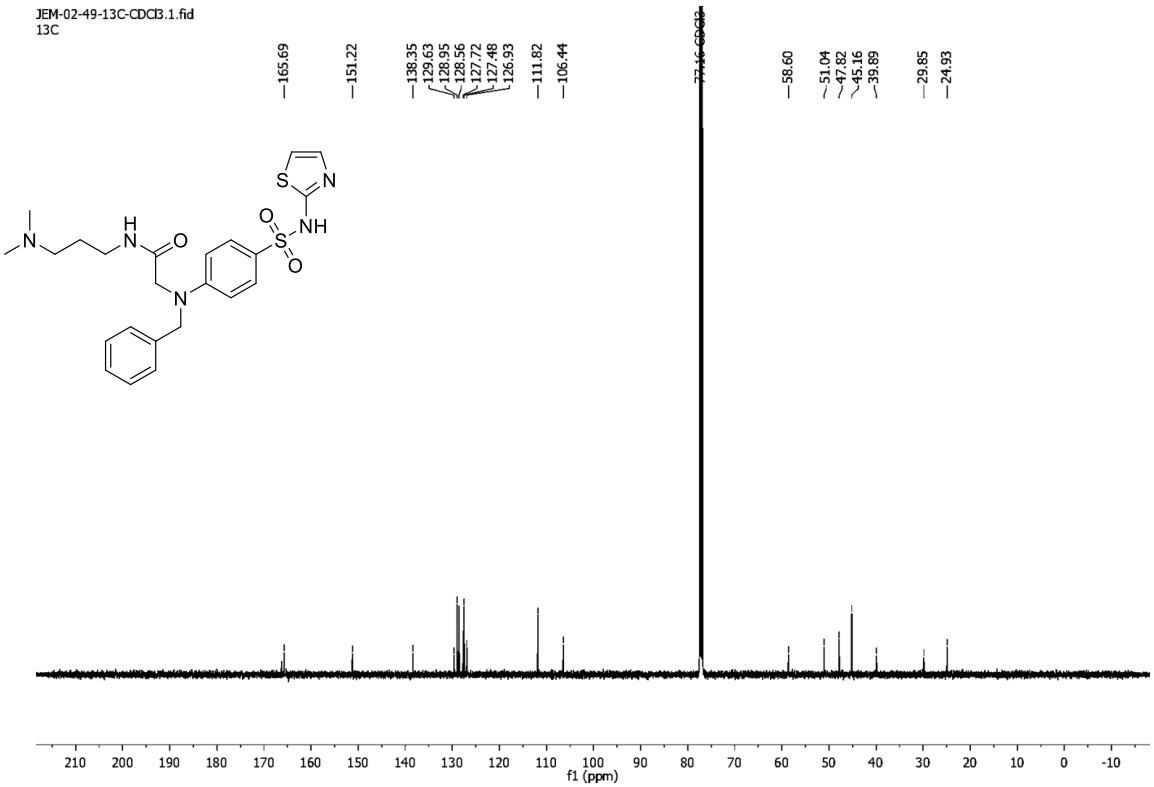
JEM-02-49-13C-CDCl3.1.fid
13C
165.69
151.22
138.35
129.63
128.95
128.56
127.72
127.48
126.93
111.82
106.44
77.16 CDCl3
58.60
51.04
47.82
45.16
39.89
29.85
24.93
f1 (ppm)

23a

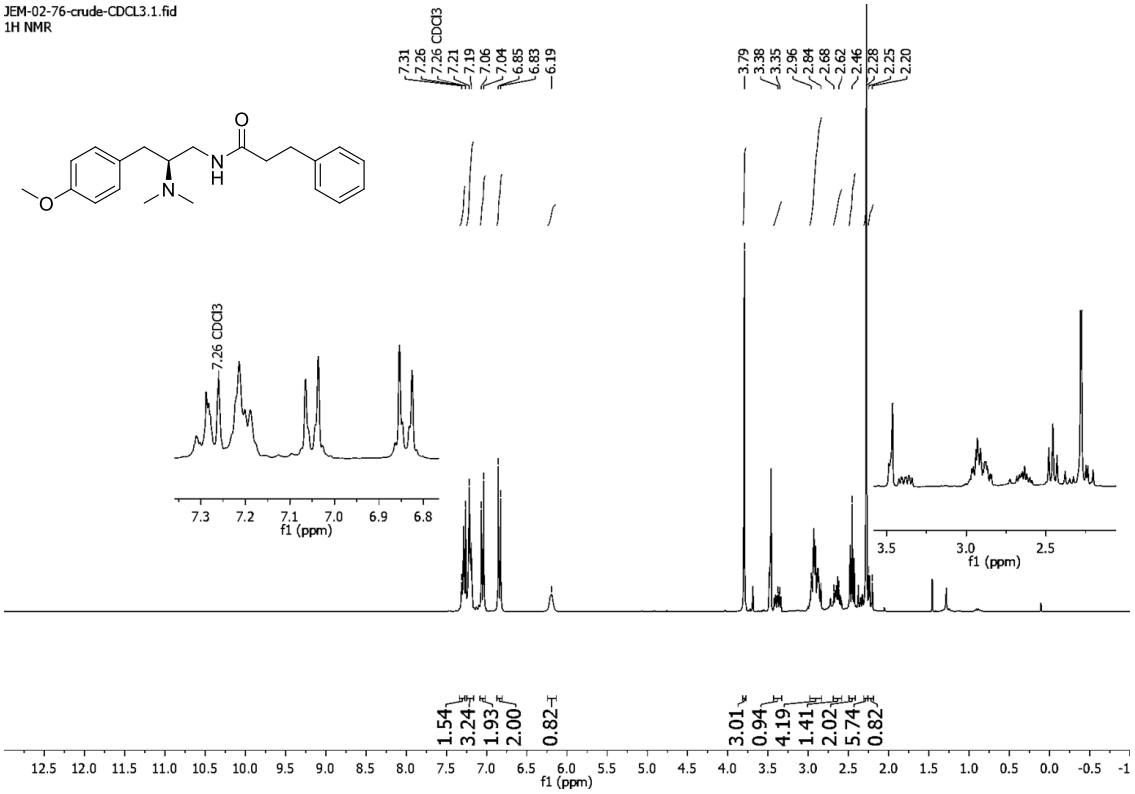
JEM-02-76-crude-CDCL3.1.fid
1H NMR
7.31
7.26
7.26 CDCl3
7.21
7.19
7.06
7.04
6.85
6.83
6.19
3.79
3.38
3.35
2.96
2.84
2.68
2.62
2.46
2.28
2.25
2.20
1.54
3.24
1.93
2.00
0.82
3.01
0.94
4.19
1.41
2.02
5.74
0.82
f1 (ppm)

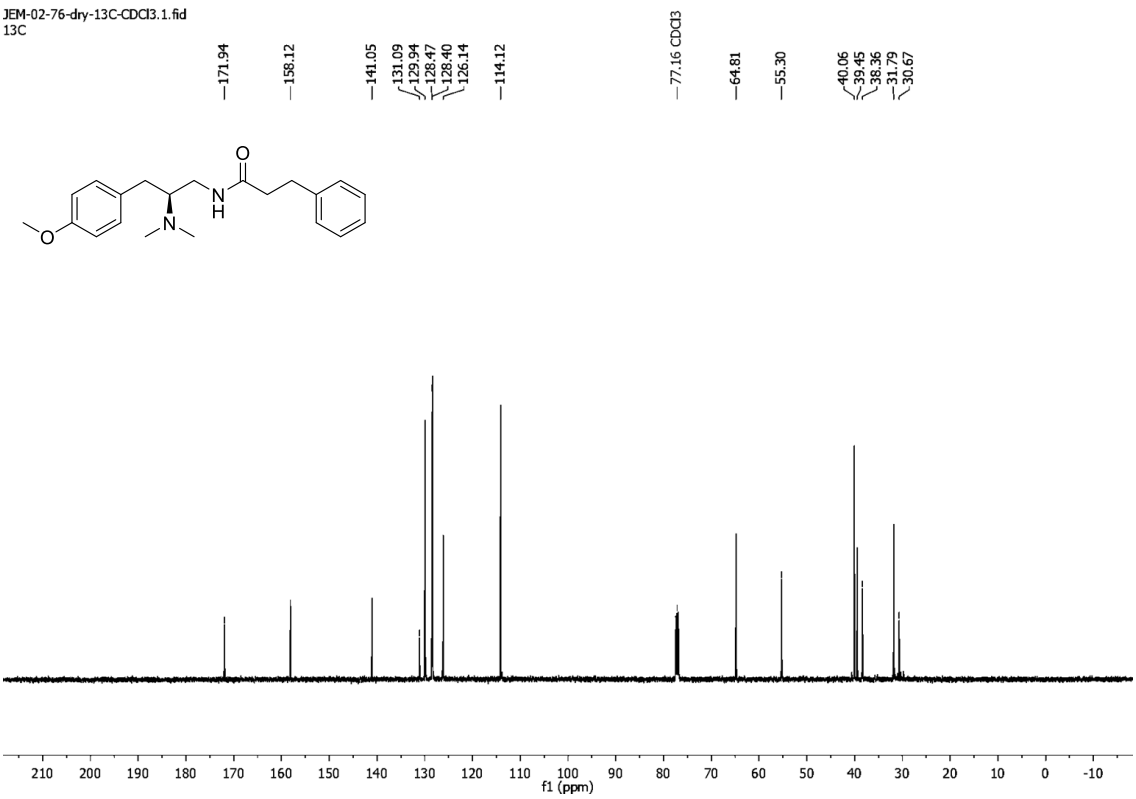
JEM-02-76-dry-13C-CDCl3.1.fid
13C
171.94
158.12
141.05
131.09
129.94
128.47
128.40
126.14
114.12
77.16 CDCl3
64.81
55.30
40.06
39.45
38.36
31.79
30.67
f1 (ppm)

24a

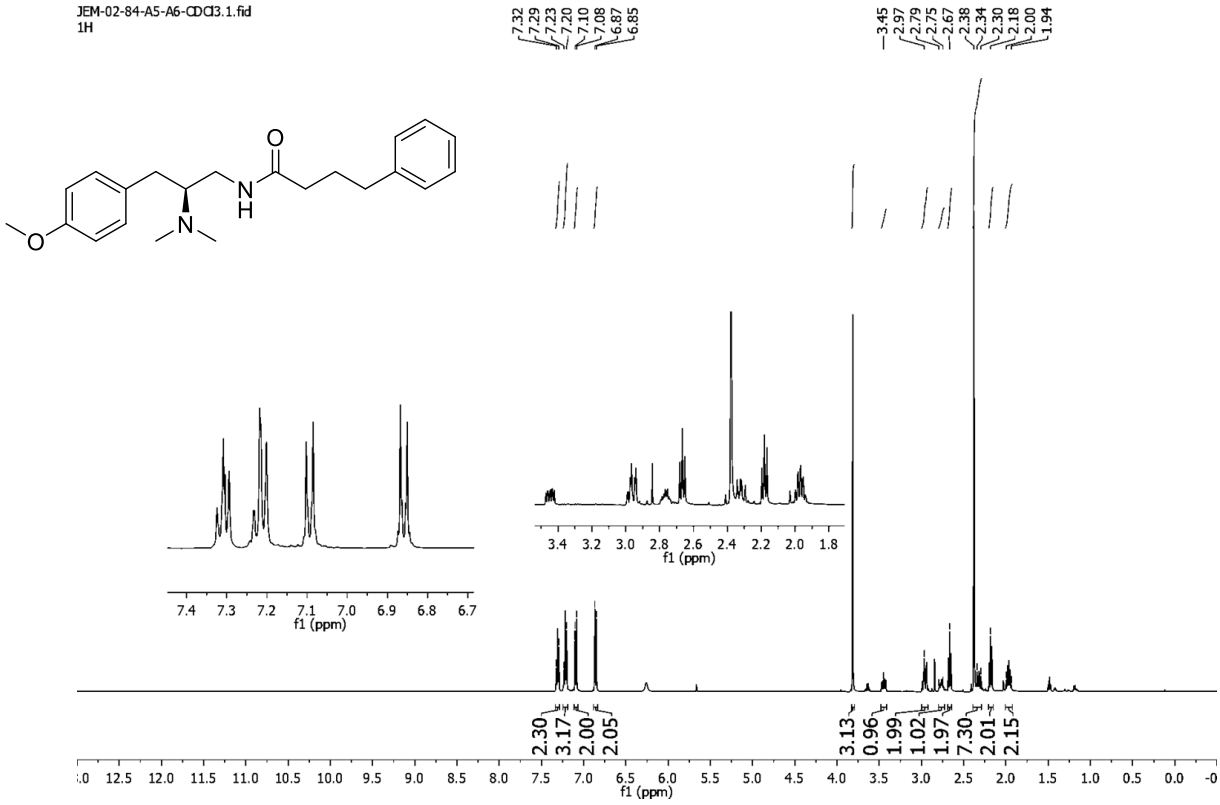
JEM-02-84-A5-A6-CDCl3.1.fid
1H
7.32
7.29
7.23
7.20
7.10
7.08
6.87
6.85
3.45
2.97
2.79
2.75
2.67
2.38
2.34
2.30
2.18
2.00
1.94
O
N
H
O
N
2.30
3.17
2.00
2.05
3.13
0.96
1.99
1.02
1.97
7.30
2.01
2.15
f1 (ppm)

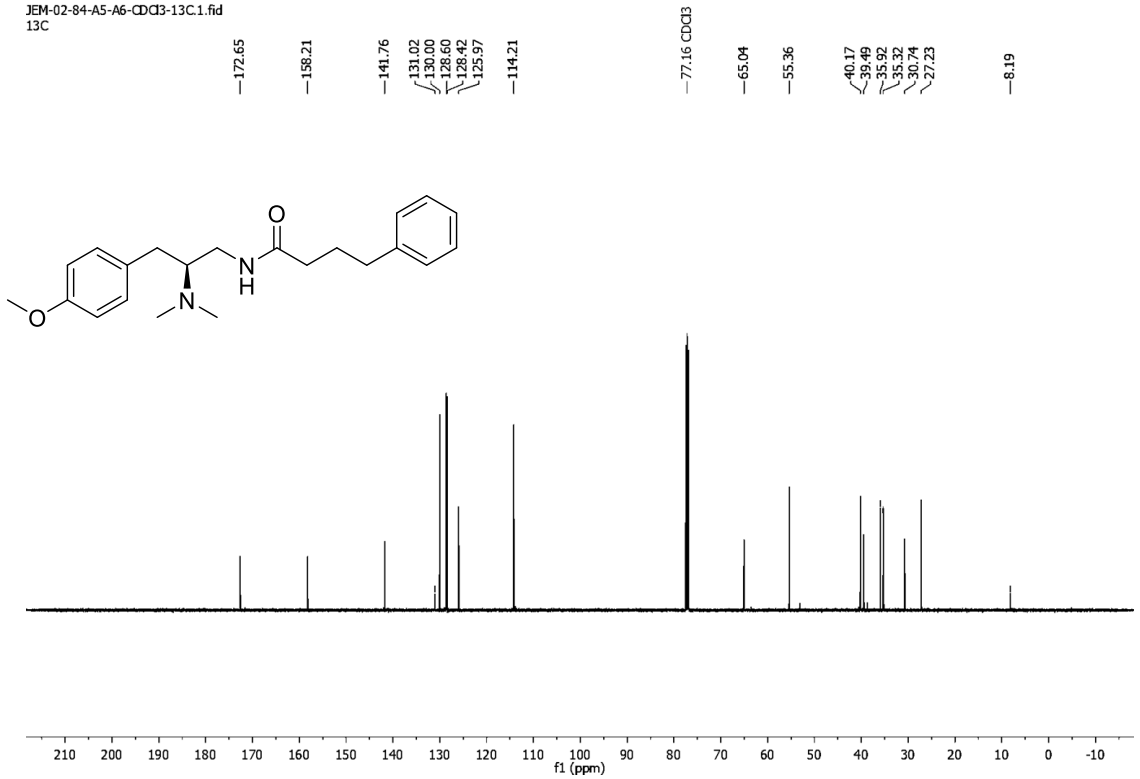
JEM-02-84-A5-A6-CDCl3-13C.1.fid
13C
172.65
158.21
141.76
131.02
130.00
128.60
128.42
125.97
114.21
77.16 CDCl3
65.04
55.36
40.17
39.49
35.92
35.32
30.74
27.23
8.19
O
N
H
O
N
f1 (ppm)

24b

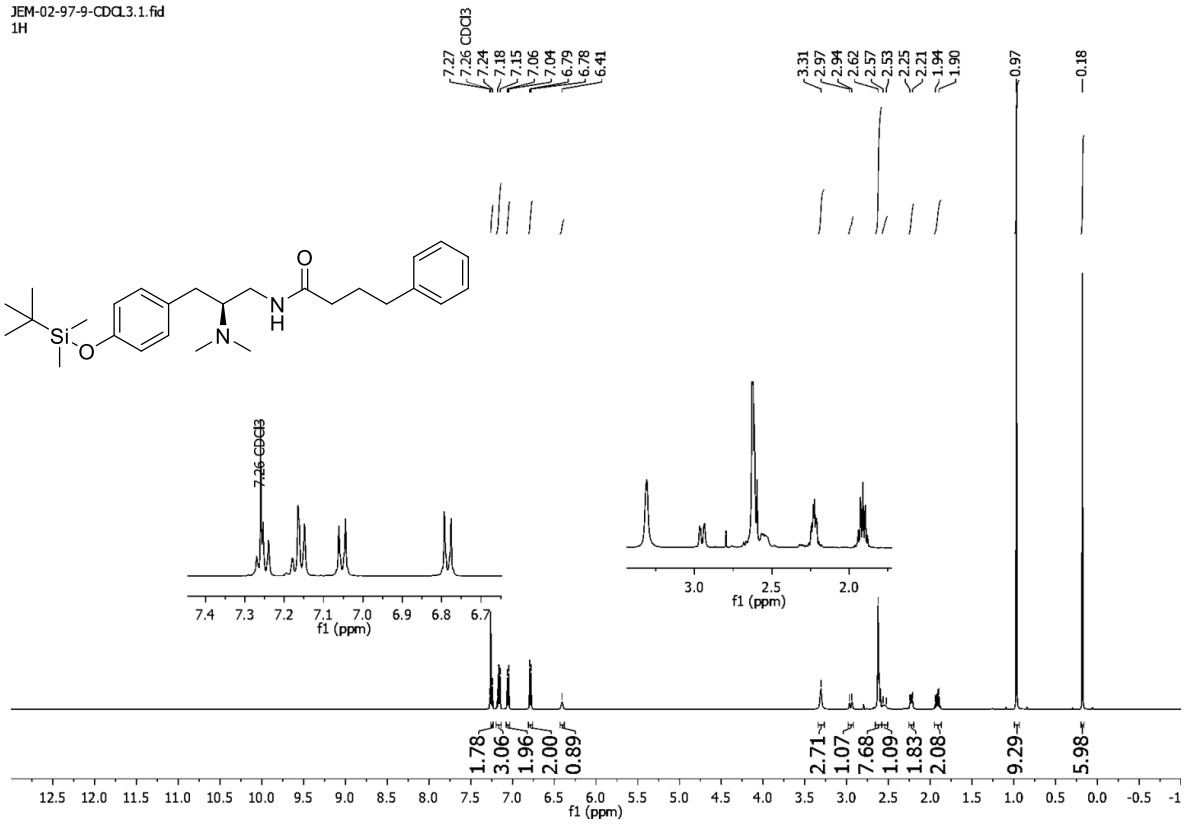
JEM-02-97-9-CDCL3.1.fid
1H
7.27
7.26 CDCl3
7.24
7.18
7.15
7.06
7.04
6.79
6.78
6.41
3.31
2.97
2.94
2.62
2.57
2.53
2.25
2.21
1.94
1.90
0.97
0.18
1.78
3.06
1.96
2.00
0.89
2.71
1.07
7.68
1.09
1.83
2.08
9.29
5.98
f1 (ppm)

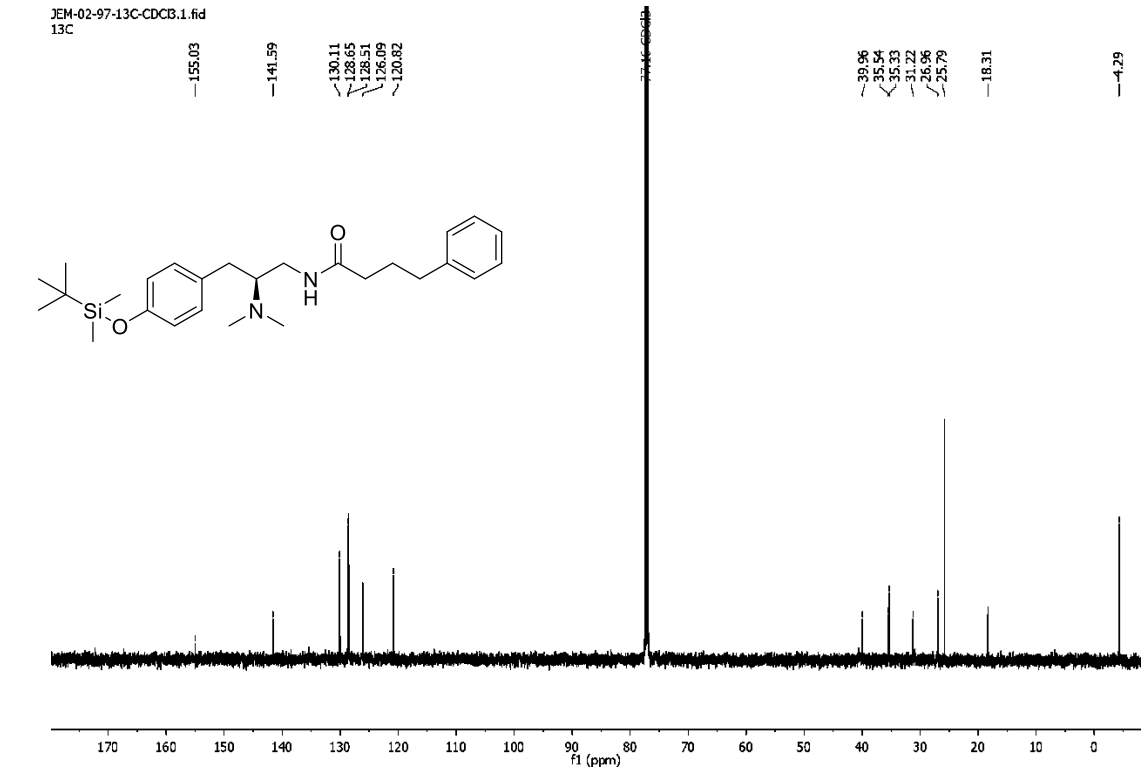
JEM-02-97-13C-CDCl3.1.fid
13C
155.03
141.59
130.11
128.65
128.51
126.09
120.82
77.46 CDCl3
39.96
35.54
35.33
31.22
26.96
25.79
18.31
-4.29
f1 (ppm)